Exploring skeletal asymmetry and indicators of developmental stress in a South African sample

Submitted by:

Miksha Harripershad

A thesis presented in publication format, submitted to the Department of Anatomy, School of Medicine, Faculty of Health Sciences, University of Pretoria, in fulfilment of the requirements for the degree.

of

MSc in Anatomy

November 2022

Supervisor: Ms. L Liebenberg

Co-supervisors: Dr. C. E.G Theye & Dr. A.F Ridel

DECLARATION

I, Miksha Harripershad, declare that this dissertation is my own work. It is being submitted for the degree of MSc in Anatomy at the University of Pretoria. It has not been submitted before for any other degree or examination at this or any other institution.

Sign: _____

30th of November 2022

Thesis supervisor

Ms. L Liebenberg
Lecturer
Forensic Anthropology Research Centre
Department of Anatomy
Faculty of Health Science
University of Pretoria

Thesis co-supervisors

Dr. C.E.G Theye
Researcher
Forensic Anthropology Research Centre
Department of Anatomy
Faculty of Health Sciences
University of Pretoria

Dr. A.F Ridel
Researcher & Trainer
Forensic Anthropology Research Centre
Department of Anatomy
Faculty of Health Sciences
University of Pretoria

UNIVERSITEIT VAN PRETORIA
UNIVERSITY OF PRETORIA
YUNIBESITHI YA PRETORIA

Faculty of Health Sciences

Institution: The Research Ethics Committee, Faculty Health Sciences, University of Pretoria complies with ICH-GCP guidelines and has US Federal wide Assurance.
- FWA 00002567, Approved dd 18 March 2022 and Expires 18 March 2027.
- IORG #: IORG0001762 OMB No. 0990-0278 Approved for use through August 31, 2023.

Faculty of Health Sciences **Research Ethics Committee**

15 June 2022

Approval Certificate
Annual Renewal

Dear Miss M Harripershad,

Ethics Reference No.: 386/2021 – Line 1
Title: Exploring skeletal asymmetry and indicators of developmental stress in a South African sample

The **Annual Renewal** as supported by documents received between 2022-05-18 and 2022-06-15 for your research, was approved by the Faculty of Health Sciences Research Ethics Committee on 2022-06-15 as resolved by its quorate meeting.

Please note the following about your ethics approval:
- Renewal of ethics approval is valid for 1 year, subsequent annual renewal will become due on 2023-06-15.
- Please remember to use your protocol number (386/2021) on any documents or correspondence with the Research Ethics Committee regarding your research.
- Please note that the Research Ethics Committee may ask further questions, seek additional information, require further modification, monitor the conduct of your research, or suspend or withdraw ethics approval.

Ethics approval is subject to the following:
- The ethics approval is conditional on the research being conducted as stipulated by the details of all documents submitted to the Committee. In the event that a further need arises to change who the investigators are, the methods or any other aspect, such changes must be submitted as an Amendment for approval by the Committee.

We wish you the best with your research.

Yours sincerely

On behalf of the FHS REC, Dr R Sommers
MBChB, MMed (Int), MPharmMed, PhD
***Deputy Chairperson** of the Faculty of Health Sciences Research Ethics Committee, University of Pretoria*

The Faculty of Health Sciences Research Ethics Committee complies with the SA National Act 61 of 2003 as it pertains to health research and the United States Code of Federal Regulations Title 45 and 46. This committee abides by the ethical norms and principles for research, established by the Declaration of Helsinki, the South African Medical Research Council Guidelines as well as the Guidelines for Ethical Research: Principles Structures and Processes, Second Edition 2015 (Department of Health)

Research Ethics Committee
Room 4-60, Level 4, Tswelopele Building
University of Pretoria, Private Bag x323
Gezina 0031, South Africa
Tel +27 (0)12 356 3084
Email: deepeka.behari@up.ac.za
www.up.ac.za

Fakulteit Gesondheidswetenskappe
Lefapha la Disaense tša Maphelo

SUMMARY

Biological anthropologists have shown great interest in understanding health and disease and its correlation to skeletal asymmetry. Fluctuating asymmetry, which is defined as the random deviation from perfect symmetry resulting in inequality in size or shape of bilateral traits, is often used to understand this correlation. Literature has shown that fluctuating asymmetry results from developmental instabilities and could be indicative of developmental stressors and an individual's quality of life. Skeletal asymmetry and its correlation to different developmental stressors provide invaluable information regarding the interpretation of skeletal variation often observed among individuals. The understanding of human skeletal variation has many applications, ranging from forensic skeletal identification to facial surgery. While traditional methods for studying facial and dental asymmetry have been used in the past, the methods can be methodologically challenging, and not always practical in clinical settings. As such, virtual biological anthropology has become an increasingly popular alternative. Among the imaging modalities, micro-focus X-ray computed tomography (micro-XCT) is often considered as the gold standard, because of its non-invasive and non-destructive properties, as well as its remarkably high resolution and its consistency compared to other micro-XCT systems. Micro-XCT imaging has thus proven to be extremely useful for better evaluation of facial structures, with detailed images that can assist in identifying and quantifying facial asymmetry, especially when employed in conjunction with geometric morphometrics. Therefore, this study aimed to assess facial asymmetry in a South African population using micro-XCT and further explore the link between asymmetry and developmental stress. One hundred and fifteen individuals (59 black South Africans and 56 white South Africans, with 57 females and 58 males) and their associated micro-XCT scans, sourced from the Pretoria Bone Collection (University of Pretoria) were analysed to evaluate facial asymmetry. Anatomical landmarks were employed to take a series of cranial measurements and collect 3D coordinate data for geometric morphometric analysis. The measurements and extraction of 3D coordinate data were performed on 3D models virtually extracted from micro-XCT scans of crania of the same individual. Once collected, fluctuating asymmetry indices were calculated. The entire skeleton of the individuals was assessed for pathological lesions linked to nutritional disease and to assess the overall link to developmental stress of the individuals. The location and number of lesions was recorded for each individual.

Statistical analyses were employed to assess intra- and inter-observer reliability for landmarks, measurements, and pathology analysis; to examine any significant differences between the left and right distances and shapes for measurements and geometric morphometric analysis, respectively; and finally, to evaluate the correlation between the presence of pathological lesions and the degree of asymmetry expressed in an individual. This study showed that the orbits, nasion and temporal regions expressed a high magnitude of asymmetry, particularly in black South African females. However, no link was found between asymmetry and signs of developmental stress. Thus, more research can be done to understand how, and when developmental stressors may influence skeletal asymmetry.

Key words: Fluctuating asymmetry; Pathological lesions; Inter-landmark distances; Shape variation; Geometric morphometrics; Craniometric landmarks; Micro-XCT; Correlations.

ACKNOWLEDGMENTS

This masters research provided an immeasurable learning experience and an opportunity for personal growth in the field of biological anthropology and would have not been possible without the help of various institutions and individuals. Immense appreciation and gratitude for their benevolence, assistance and support are extended to the following people, who have contributed to the achievement of this master's dissertation. I would like to express my utmost gratitude to Ms. Leandi Liebenberg for intrusting me with this project and her positive, timely guidance during the last two years. Her critical analysis and reviews, patience and availability allowed for this manuscript to be what is today. Thank you for managing my stress in these last two years and providing me with this amazing opportunity. I would like to express my deepest appreciation to Dr. Alison Ridel for her continued support, motivation and invested time during this research project. Her invaluable scientific knowledge and statistical expertise has greatly contributed to the success of this project and strengthened my scientific knowledge. A debt of gratitude is owed to Dr. Charlotte Theye for her tireless efforts, kindness and insightful remarks throughout the last two years which has led to the success of this dissertation. Thank for all your help and providing with me with an abundance of skills that I will carry with me throughout my scientific career. I am extremely grateful to Prof Ericka L'Abbé for always being welcoming and supportive and providing me with countless opportunities within the Forensic Anthropology Research centre and intrusting me to work in Bakeng se Afrika and Dirisana+. I would like to acknowledge the University of Pretoria for funding this research degree. I also wish to express many thanks to Gabi, Okuhle and Alieske for their willingness to help, availability for all my questions and providing me with support when needed. A special thank you goes out to Pearl Bothma, for her unconditional support and friendship that helped me through the last 2 years. A big thanks goes out to Leshan Pillay, for his continued motivation, support, and encouragement. Thank you for being my sounding board and having endless patience when I needed it the most. Thank you to my entire family , this work would have not been possible without your full support and encouragement. Lastly, an infinite amount of thanks my mum and dad, without whom none of this would be possible. Thank you for always believing in me.

TABLE OF CONTENTS

LIST OF FIGURES

LIST OF TABLES

Appendix A

Chapter 1 - INTRODUCTION

1.1. Problem statement

Skeletal asymmetry is defined as inequality in the size and shape of bilateral anatomical structures (Graham and Özener, 2016). Anthropological literature identifies three categories of asymmetry, namely directional asymmetry, antisymmetry, and fluctuating asymmetry. Fluctuating asymmetry refers to the random deviation from perfect symmetry with an inequality in size or shape of bilateral (left and right sided) traits (Graham and Özener, 2016). While directional asymmetry is the constant growth of one side of a bilateral trait, with larger dimensions expressed on the dominant side. As such, right-bias is frequently observed in the general population (right side traits larger than left side traits) due to pattern limb dominance, or handedness (Hagg et al., 2017). Similarly, antisymmetry is defined as one side being more developed in bilateral traits. Antisymmetry, unlike directional asymmetry, is random and not caused by pattern limb dominance (Hagg et., 2017).

Directional asymmetry is a popular research topic among anthropologists as it is easily quantifiable; yet fluctuating asymmetry tends to be overlooked, especially in modern human samples (Latimer and Lowrance, 1965; Hiramoto, 1993; Cuk et al., 2001; Auerbach and Ruff, 2006; Kanchan et al., 2008). Fluctuating asymmetry is suggested to be the result of developmental instability and can potentially be used as an indicator of developmental stress (Graham and Özener, 2016). Therefore, biological anthropologists are interested in understanding developmental stressors(environmental and genetic) and its correlation to skeletal asymmetry. Stressors such as infections and nutritional deficiencies may produce a bony response resulting in specific pathological lesions on the skeleton. Non-specific signs of disease, such as cribra orbitalia, porotic hyperostosis and enamel hypoplasia, produce such bony responses and are commonly linked to poor and stressful living conditions. However, such pathological lesions can only be identified if the process of the disease or pathology is understood (Ortner, 2019).

The main focus of this study is fluctuating asymmetry: therefore, unless specified otherwise the term asymmetry can be assumed to b referring to fluctuating asymmetry. By understanding skeletal asymmetry and the roles played by different stressors (environmental and genetic), anthropologists are able to better interpret skeletal

variation observed among individuals (De Coster et al., 2013). The assessment of human skeletal variation has many applications, ranging from forensic skeletal identification to facial surgery and medical implants. For instance, the understanding of asymmetry is required in forensic anthropology as it may potentially influence estimates of the biological profile. In constructing the biological profile, a series of measurements are taken, and various morphological traits are scored, which can assist in estimating ancestry, sex, and stature. If asymmetry is not accounted for, an individual can easily be misclassified (Cole et al., 2020). For instance, a male may have more robust postcranial elements (such as the humerus, ulna, femur, or tibia) on the right side as opposed to the left side. Thus, if only the left skeletal elements, which may be more gracile, were used to estimate the biological profile, there is a greater probability of misclassifying this male individual as female. Multiple studies have shown that limb asymmetry may cause difficulty in forensic and bioarchaeological assessment of the biological profile, particularly when assessing stature and age estimates. Asymmetry may also cause difficulty when trying to identify the number of individuals in comingled remains (Zivanović, 1983; Kanchan et al., 2008; Krishan et al., 2010; Corron and Stull, 2017; Nandi et al., 2018). Cole et al. (2020) also noted that both cranial and pelvic asymmetry can have implications on sex estimation and that a better understanding of the magnitude of asymmetry expressed by an individual is imperative for accurate sex estimates. Knowledge of facial asymmetry is also required in the medical field, as complications may arise when placing facial or dental implants (Srivastava et al., 2018). For instance, Kim (2011) reported that mental nerve injuries can occur due to misplacement of dental implants, as this nerve often arises from asymmetric foramina. As such, when implants are planned, clinicians need to consider the location of the mental foramen, the anterior loop of the nerve and the location of the inferior alveolar nerve on both sides (Kim, 2011). Therefore, a good grasp on the knowledge of craniofacial asymmetry in the South African population and in individuals can be beneficial to medical professionals.

For this reason, the present study focuses on facial asymmetry. Unlike postcranial elements, the cranium lacks a pattern of one-sided dominance. Thus, the cranium is minimally affected by directional asymmetry and provide a better gauge of fluctuating asymmetry in South African individuals.

Past research on facial asymmetry, specifically in odontology, has focused on utilising physical measurements (following traditional methods with calipers) or two-dimensional (2D) posteroanterior cephalometric images (Letzer and Kronman, 1967; Shah and Joshi, 1978; Cohen, 2005; de Moraes et al., 2011). However, many limitations are associated with these methodologies. Traditional methods can often be time consuming, based on small samples, requires the handling and contamination of skeletal material and may not be practical in a clinical setting for medical professionals. The use of digital 2D cephalometric images is often compromised due to the difficulty in identifying and placing anatomical landmarks (Cohen, 2005; de Moraes et al., 2011). Consequently, literature (Cohen, 2005; de Moraes et al., 2011) has found low agreements between measurements taken on 2D digital images and physical measurements. This poor agreement is due to the fact that cephalometric radiograph images are often distorted, magnified, and can have erroneous projections due to misalignment of the cephalostat (de Moraes et al., 2011). This limitation was further confirmed in a study conducted by de Moraes et al. (2011) when evaluating craniofacial asymmetry comparing cone-beam computed tomography (CBCT) and digital cephalometric images.

Virtual biological anthropology has become widely employed in research such as forensic anthropology, dental anthropology, and palaeoanthropology. Three-dimensional imaging modalities such as computed tomography (CT), cone-beam computed tomography (CBCT), and 3D surface imaging (3dMD) are frequently used in research (Friess, 2012; Ridel et al., 2018; Profico et al., 2019; Theye, 2022). These imaging modalities eliminate the need for handling or damaging skeletal remains and provide access to large virtual samples. Another scanning modality, the micro-focus X-ray computed tomography (micro-XCT), is often used in research, as it is considered as the gold standard compared to all other imaging technologies (Olejniczak et al., 2007; Grünheid et al., 2014; Andronowski et al., 2018). This is in part due to the fact that micro-XCT imaging not only provides very high-resolution images but is also non-destructive and non-invasive in nature (Suwa and Kono, 2005; Marciano et al., 2012). Furthermore, it produces approximately the same measurements when employing different micro-XCT systems with all systems being calibrated in the same manner, unlike other imaging systems such as CBCT's (Olejniczak et al., 2007). As such, micro-XCT imaging has become useful for the reconstruction of the cranium allowing for better visualization of facial structures, is highly effective in providing detailed images

which can assist in identifying facial asymmetry and providing an accurate and concise ways to take facial measurements. Multiple studies (de Moraes et al., 2011; Akhil et al., 2015; Klingenberg, 2015) have employed the use of 3D imaging modalities to study facial asymmetry and have found near perfect correlations with measurements taken on 3D images and physical measurements. However, only a few studies have focused on the use of micro-XCT imaging for the analysis of fluctuating asymmetry and have also employed the use of geometric morphometrics (Schlager, 2013; Klingenberg, 2015; Benítez et al., 2020).

Geometric morphometrics focuses on biological shape analysis using Cartesian coordinates (x, y, z) of landmarks placed on a 3D model. The extracted resultant Procrustes shape coordinates can now be used for statistical analysis. As such, geometric morphometrics is an approach frequently employed in the assessment of fluctuating asymmetry (Benítez et al., 2020). This method is extremely useful as it allows to detect very subtle asymmetrical differences, is precise and has low measurement error. Unlike the traditional measurements employed to study fluctuating asymmetry, data obtained by geometric morphometrics are highly sensitive to genetic and environmental stressors that influence asymmetry and provides a more complex and detailed way of examining asymmetry (Benítez et al., 2020).

This present study thus evaluates facial asymmetry thanks to a series of measurements, and anatomical landmarks taken and placed on the cranium, and virtually extracted from micro-XCT scans. Additionally, this research project specifically assesses the possible relationship between facial asymmetry and signs of developmental stress on the skeleton, such as cribra orbitalia and enamel hypoplasia to name a few. The results of this study may give us a better understanding of the functional complications that may arise due to facial and dental asymmetry and help the medical and forensic professionals be more conscious of the variation when working on the biological profile or on medical applications such as implants. The results will provide an understanding of skeletal variation observed in black and white South African populations and provide us with information on potential correlations between developmental stressors (brought on by environmental or genetic conditions) and fluctuating asymmetry.

1.2. Scope of the dissertation

The aim of this dissertation is to assess craniofacial asymmetry in a South African population using micro-XCT and to further explore the possible link between developmental stressors and asymmetry. The first objective is to testf the repeatability, and reliability of the collection of craniofacial measurements and shape data using micro-XCT scans. The second objective is to explore the presence of craniofacial asymmetry by employing inter-landmark distances and shape analysis. The last objective is to find the statistical relationships between fluctuating asymmetry and factors such as sex, ancestry, as well as with different skeletal signs of disease.

The specific objectives of this research are the following:

- To obtain a series of craniofacial inter-landmark distances and shape data from the cranium using micro-XCT scans:
    - To place standard anatomical landmarks on the crania, calculate inter-landmarks linear distances, and perform shape analysis using the 3D coordinate data.
- To explore the presence and magnitude of facial asymmetry from inter-landmark distances and shape analysis.
- To explore the presence and magnitude of asymmetry between population groups and sexes by conducting statistical analysis.
- To examine each skeleton for signs of visible developmental stress such as cribra orbitalia, porotic hyperostosis, periostitis, and enamel hypoplasia using diagnostic aids and the frequency and correlation of these pathologies in the sample.
- To assess if there is a correlation between asymmetry and skeletal signs of stress by conducting statistical analysis.

Chapter 2 - LITERATURE REVIEW

2.1. Population asymmetries

Organisms are considered perfectly symmetrical when they are in constant homeostasis with their internal environment and the external environment that surrounds them (Hagg et al., 2017). Homeostasis is controlled by self-regulating mechanisms intended to maintain developmental stability, which may produce the ideal phenotype resulting in perfect symmetry (Hagg et al., 2017). Therefore, if an organism undergoes genetic and/or environmental stress, the resulting response may lead to inconsistencies in growth and development and thus in the expression of asymmetry (Hagg et al., 2017).

In the literature, three categories of asymmetry have been identified. These are: (1) fluctuating asymmetry, (2) directional asymmetry, and (3) antisymmetry, and are illustrated in Figure 2.1.

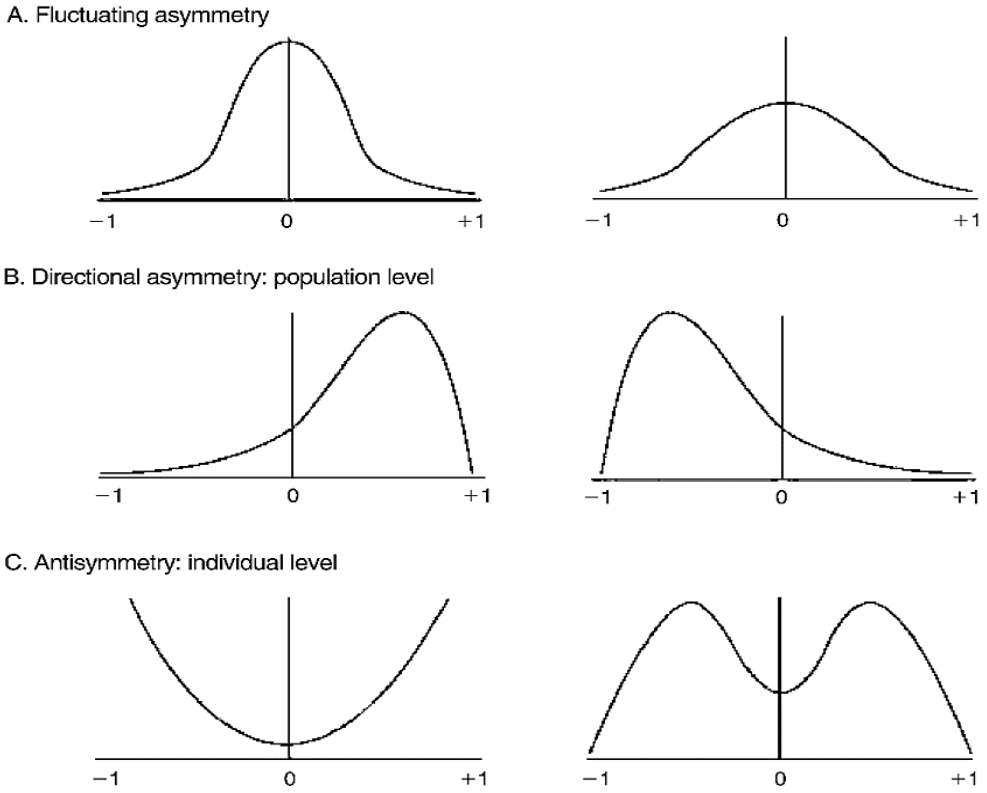

Figure 2.1 - *Frequency distributions showing examples of data variation for A) fluctuating asymmetry, B) directional asymmetry and C) antisymmetry (adapted from Palmer (1996) and Møller and Swaddle (1997))*

Fluctuating asymmetry is defined as the random deviation from perfect symmetry with an inequality in the size or shape of bilateral (left and right sided) traits (Franks and Cabo, 2014; Graham and Özener, 2016) (Figure 2.1A). However, fluctuating asymmetry does not favour one side but rather results in random differences between left and right sides of a trait (Van Valen, 1962; Palmer, 1996). This is usually as a result of developmental instability, such as genetic and environmental stressors which can be used as an indicator for an individual's health and lifestyle (Graham and Özener, 2016). Fluctuating asymmetry is commonly seen on the cranium, dentition, dermatoglyphics and long bones because these bones tend to be affected by developmental instabilities during childhood (Graham and Özener, 2016; DeLeon, 2018). Anthropological measurements can help identify and quantify these slight variations. However, genetic, and environmental disruptions have an additive effect, as such multiple disruptions can lead to a greater magnitude of asymmetry being observed. The variation can be evaluated by the difference between right and left sides with a mean distribution around zero (Graham and Özener, 2016).

Directional asymmetry is a constant growth or enlargement to one side of a bilateral trait, to such an extent that it is common amongst the majority of the population, with the larger dimensions on the dominant side. Right-bias is frequently seen in the general population (right side traits larger than left side traits) (Graham and Özener, 2016). The development of directional asymmetry is in part due to a small portion of genetics rather than just developmental stress (Hagg et al., 2017) (Figure 2.1B). Directional asymmetry can be influenced by behavioural actions such as handedness (dominant limb usage), which is directly linked to the locomotive behaviour during childhood. As such, right-hand dominance is common in majority of the population because of the constant use of one side over the other, resulting in asymmetry. Therefore, even though directional asymmetry can be used as an indicator for developmental instability, it is not entirely accurate (Hagg et al., 2017). Directional loading affects skeletal proportions in directional asymmetry due to a constant stimulus being placed upon one side of the musculoskeletal system. The mean distribution between the right and left sides are not equal to zero due to the unequal right and left side development (Graham and Özener, 2016).

Similar to directional asymmetry, antisymmetry refers to one side being more developed in bilateral traits; however, the concept differs, as antisymmetry tends to be random while directional asymmetry (handedness) follows a pattern of limb dominance (usually right-hand bias) (Hagg et al., 2017) (Figure 2.1C). Thus, the distribution of antisymmetric bilateral trait development within a population will be variable. Half of the population will exhibit right side dominance while the other half will exhibit left side dominance (Palmer, 1996). The distribution of the mean of antisymmetry is bimodal and the mean is close to or equal to zero (Graham and Özener, 2016). This means that there will be an even distribution of dominant right side or left side trait expression in a population. An example of antisymmetry discussed by Graham and Özener (2016) pertain to lobster claws in a specific population, in which 50% of the individuals had larger right claws and 50% had larger left claws, while only a few had equal sized ones (Graham and Özener, 2016). An example of antisymmetry among humans is the size asymmetry of female breasts. The asymmetry in breast size is influenced by the inconsistencies in menstrual cycles and human variation in the female population. As such, some women will have bigger right breasts while others will have bigger left breasts, and a few women will have perfectly symmetrical breasts (Manning et al., 1997; Graham and Özener, 2016). However, antisymmetry on skeletal remains has not been well-documented and further research is still needed to understand the effects of antisymmetry on the skeleton.

Multiple anthropological studies have focused on fluctuating asymmetry and its correlation to skeletal asymmetry (DeLeon, 2007; Graham and Özener, 2016; Hagg et al., 2017). However, two issues, such as directional asymmetry and bone remodelling on traits, need to be acknowledged and subsequently removed from studies assessing asymmetry to evaluate developmental instabilities and its association to symmetry effectively (Graham and Özener, 2016). Multiple skeletal elements are influenced by fluctuating asymmetry due to developmental stressors. The term developmental stressors are often used in biological anthropology and refers to the event that results in physiological change caused by strain placed upon an individual brought about by environmental and genetic conditions during stages of growth. However, compared to the skull, postcranial elements tend to exhibit greater degrees of directional asymmetry due to patterns of limb dominance. Indeed, the cranium and teeth lack patterns of one-sided dominance as it is difficult to use one

side of the face more than the other. As a result, the cranium and teeth are minimally affected by directional asymmetry and provide a better gauge of fluctuating asymmetry in the individual. This study is therefore focusing on facial asymmetry.

2.1.1 Facial asymmetry

Facial asymmetry can arise due to environmental stressors, functional factors, and congenital defects. Variants in how facial asymmetries occur are difficult to detect and not easily observable (Cheong and Lo, 2011). Fluctuating asymmetry acting on facial traits are highly common and mostly undetectable, but even the slightest inconsistencies may result in facial unattractiveness (Cheong and Lo, 2011). Many studies have focused on facial asymmetry and the link to mate choice (Gangestad et al., 1994; Simmons et al., 2004; Wade, 2010; Graham and Özener, 2016). While most of the literature looked at facial attractiveness, only a few have investigated facial asymmetry and its implications in forensic and medical fields (Cheong and Lo, 2011).

Bilateral traits or anatomical landmarks, such as dacryon, the horizontal plates of the palatines, or pterions, are all suggested to be more sensitive to stress and therefore show a greater degree of facial asymmetry (Hagg et al., 2017). Storm and Knusel (2005) examined 17 cranial and mandibular traits from two Medieval English populations to determine which traits had the greatest magnitude of asymmetry. The results showed that the mastoid breadth and height, orbital breadth, bregma-porion height and mandibular ramus height were the most asymmetrical traits, while the orbital height, zygomatic height and mandibular ramus breadth showed the least asymmetry. Similarly, Gawlikowaka et al. (2007) and DeLeon (2007) observed that in modern populations, fluctuating asymmetry was mostly observed in the cranial vault and base, with low levels of asymmetry noted in the facial region. Therefore, according to literature there is evidence that the cranium and height of the mandibular ramus demonstrate more asymmetry than the facial region and breadth of the mandibular ramus (Hagg et al., 2017).

2.1.2 Dental asymmetry

Dental asymmetry may be caused by several types of factors, such as habits (like thumb or dummy sucking), congenital absence of a tooth or premature tooth loss, or

lack of precision in genetic expression (Anison et al., 2015). Environmental and genetic stressors acting on teeth can cause differences between the right and left mesio-distal diameters in specific tooth groups (incisors, canines, premolars, and molars) (Anison et al., 2015). Greater degrees of asymmetry have been noted on the posterior teeth as well as on both the dental arches (maxilla and mandible) (Anison et al., 2015).

Since teeth are minimally affected by the environment, as opposed to the rest of the skeleton, paleoanthropologists, biological anthropologists, and forensic anthropologists may reliably conduct studies on dental asymmetry. Dental studies are usually based on caliper measurements performed on actual teeth from skeletal remains (Graham and Özener, 2016). To assess symmetry, the most commonly taken measurements are the buccolingual and mesiodistal diameters. Multiple studies found that maxillary teeth tend to exhibit a much higher degree of fluctuating asymmetry than mandibular teeth, with mesiodistal measurements showing more asymmetry compared to buccolingual measurements (Harris and Nweeia, 1980; Townsend and Brown, 1980; Hoover, 2007; Hagg et al., 2017). Literature recommends that dental asymmetry should be assessed within categories of tooth (e.g., incisor, canine etc.) with little positive size scaling (Graham and Özener, 2016). Positive size scaling in fluctuating asymmetry refers to the degree of asymmetry increasing with tooth size (e.g., molars will express a higher degree of asymmetry than incisors, because they are larger) due to active growth or dental defects. However, majority of dental studies, such as those by Sciulli (2002) and Barrett et al. (2012) corrected for size scaling (without justifying the correction) and compared different categories of teeth which resulted in the studies being highly flawed (Graham and Özener, 2016). Lastly, recent publications have since explored the use of geometric morphometrics to study shape differences for asymmetry in dentition. Varner (2015) examined dental arch shape and symmetry differences using geometric morphometrics for deciduous and permanent dentition. The results of this study showed that geometric morphometrics provided invaluable information on dental arch shape differences for primary dentition, which may be useful for detection and treatment of malocclusion early in childhood (Varner, 2015). Hagg et al., (2017) noted that fluctuating asymmetry observed on teeth tend to be less variable than that observed on the skeletal elements. Therefore, dentition is an ideal element for the analysis of fluctuating asymmetry.

2.2 Demographic profiles and fluctuating asymmetry

2.2.1 Sex differences

The literature seems to be inconsistent in describing fluctuating asymmetry between the sexes, which may differ with regards to the population being studied as well as the skeletal elements used (Graham and Özener, 2016). Females are thought to be more resistant to stressors, such as those caused by genetics or the environment, because they have two X-chromosomes (Graham and Özener, 2016). Thus, females are considered to be more “stable,” and males are predicted to express a higher degree of asymmetry than females. This is due to XX-chromosomes being able to buffer recessive alleles, while the single X chromosome in the male genotype cannot (Graham and Özener, 2016). However, if there is random inactivation of an X-chromosome in females, this will produce a heterozygous locus around the X-chromosome which can result in instability, and in turn increase the likelihood of asymmetry in some traits (Graham and Özener, 2016). Additionally, females are also considered to have a ”maternal buffering system” which is a physiological response to physical stress. When a female is pregnant, the buffering system will work to protect (or buffer) the infant, so that the infant is able to experience sufficient *in utero* growth and develop sufficiently, while the mother is able to absorb all environmental stressors that may otherwise be applied to the infant. Essentially, the mother’s body will bear the burden of environmental stress, while protecting the growing foetus, so as not to withhold any essential nutrients. However, if the mother herself experienced stressful conditions while developing, her buffering system will not be as efficient. Thus, when she is pregnant and experiences stressful conditions, the infant will be extremely sensitive to environmental stressors; therefore, increasing developmental instability in the child (Reck et al., 2016; Howell et al., 2017). In this way, the generational effects of poverty and poor living conditions can be seen.

Sex hormones have been noted to play a crucial role in the development of facial asymmetries. As discussed by Graham and Özener (2016), high levels of testosterone can result in a weakened immune system, causing males to be more susceptible to disease and environmental stressors. This theory is supported by Fink et al. (2004),

who found an association between facial asymmetry in males and prenatal testosterone. High levels of testosterone may therefore increase the expression of fluctuating asymmetry (Graham and Özener, 2016).

Kujanova et al. (2008) observed that females showed a higher level of fluctuating asymmetry in postcranial elements in medieval populations, while in modern populations, males displayed a greater degree of asymmetry in postcranial traits. In a modern living Turkish sample, Özener and Fink (2010) did not find asymmetrical sex differences among individuals living under good conditions (i.e., higher socio-economic status), while when living in poor conditions, males showed greater levels of asymmetry than females. Weisensee (2013) studied fluctuating asymmetry in a modern Portuguese sample and the results highlighted that, in the craniofacial region, males had a higher degree of fluctuating asymmetry compared to the females, even if no significant differences were detected. Similarly, in a study conducted by Simmons et al. (2004), in an unspecified mixed-ethnic sample, males were found to be generally more asymmetric in the facial region than females. Numerous studies on dentition have found that males have a high number of asymmetrical teeth compared to females, but once again, the results were not statistically significant (Townsend and Brown, 1980; Saunders and Mayhall, 1982; Hallgrimsson, 1999; Hoover, 2007). However, multiple other studies demonstrated contradictory results. Such studies found there were no significant sex differences for fluctuating asymmetry when evaluating the crania, mandible, dentition, and postcranial bones (such as long bones, metacarpals, and metatarsals) (Perzigian, 1977; Townsend and Garcia-Godoy, 1984; Costa, 1986; Hallgrimsson, 1999), while Harris and Neewia (1980) found that, for mesiodistal dental measurements, females showed a higher degree of asymmetry than males. Gautelli-Steinberg et al. (2006) noted that for mandibular canine buccolingual measurements, females showed high levels of fluctuating asymmetry, while for maxillary premolar buccolingual measurements, males had a higher degree of asymmetry compared to females.

The myriad of contradictory results noted in the literature indicates that more research is needed to better understand to which extent asymmetry differs between sexes, especially in the South African population.

2.2.2 Population differences

Little research has been conducted with regards to asymmetry and different population groups. Since different population groups experience different stressors or no stressors at all, this can be extremely helpful when studying the extent and correlation of fluctuating asymmetry to developmental instabilities. For example, Kieser et al. (1986) compared levels of asymmetry between a European population without stress and a pre-literate Paraguayan Lengua Indian population. The European population was considered being without stress as they lived in a relatively resource-rich environment, with little nutritional deficits. Skeletal remains from this population show few markers associated with nutritional deficiencies or diseases. The results showed significant asymmetrical differences between populations for mesiodistal diameters, with more asymmetry in the Paraguayan Lengua Indian population. However, there was no significant asymmetrical differences between sexes. This study concluded that if a population is subjected to an increase in dietary stress and disease, developmental instability would increase drastically, which would lead to an increase in the expression of asymmetry in the population (Kieser et al., 1986). In another study, Kieser and Groeneveld (1988) compared dental asymmetry between three populations, namely black and white South Africans (living in the same area) and Paraguayan Lengua Indians. The results showed that among all three groups, black South Africans showed the highest degree of asymmetry (Kieser and Groeneveld, 1988). Furthermore, it was noted that due to socio-economic constraints applied to the black South African population, resulting from population history stressors (e.g., apartheid, poverty), the level of dental asymmetry was much higher in this population as opposed to the white South African individuals (Kieser and Groeneveld, 1988). This great degree of asymmetry in the South African population was attributed to the potentially high prevalence of disease and malnutrition in this population group during apartheid. This study showed that the common cause of childhood death in white South Africans were most likely due to accidents, sudden infant death syndrome or different types of cancers, while the most common causes of childhood death in black South Africans were due to poor nutrition or infections such as tuberculosis, pneumonia, and infectious diarrhoea (Kieser and Groeneveld, 1988). Importantly, even though the Paraguayan Lengua Indians had a similar profile of developmental instabilities as the black South African population, the level of asymmetry in the black South African

population was still much higher (Kieser and Groeneveld, 1988). The authors concluded that the magnitude of fluctuating asymmetry is dependent on the nature of the stress, its severity and if the individual is able to buffer the stressors being placed upon them (Kieser and Groeneveld, 1988).

Sajid et al. (2018) assessed facial asymmetry in African, Asian, Hispanic, Europeans and other ethnic groups not specified in the article. Compared to the European population, all the other ethnic groups showed a greater magnitude of asymmetry (Sajid et al., 2018). More specifically, facial asymmetry in Africans and the non-specified other ethnic groups was the most distinct, followed by Asians, Hispanics, and finally European groups (Sajid et al., 2018). However, looking at the asymmetry of the hard tissue of the nose, Schlager (2013) found that, compared to the Chinese population, the European population had considerably more variation and a statistically significant higher degree of fluctuating asymmetry. Such information on asymmetry was extremely useful and important to consider before the reconstruction of the soft tissue of the nose for facial approximation purposes, specifically in the European population studied (Schlager, 2013).

Research on asymmetrical population differences is greatly needed, not only to better comprehend the understanding of population history and instability but as well as to assist the medical and forensic field in facial reconstruction and identification, respectively.

2.2.3 Age differences

Multiple studies have evaluated fluctuating asymmetry and its correlation to age. Several authors have looked at the extent of asymmetry on adults and subadults separately (Wilson and Manning, 1996; Kujanová et al., 2008; Bigoni et al., 2013), while others did comparative studies on the asymmetrical differences between subadults and adults (Saunders and Mayhall, 1982; Hallgrimsson, 1999; Guatelli-Steinberg et al., 2006; Storm, 2009). Wilson and Manning (1996) assessed facial measurements of 680 individuals aged between two and eighteen years. The results of the study indicated that asymmetry decreased with age. Between the ages of two- and eleven-years, asymmetry seemingly decreased; then spiked at thirteen years in males, and fourteen in females. After age fifteen however, fluctuating asymmetry was

reduced and remained constant until the age of eighteen (Wilson and Manning, 1996). Similarly, Rossi et al. (2003) and Storm (2009) found that levels of fluctuating asymmetry decreased from subadults to adults. However, it was also noted that asymmetry tended to increase from late childhood to adolescence and as age increased in adulthood (Storm, 2009). Hallgrimsson (1999) studied both cranial and post cranial elements in subadults and adults. Interestingly, it was found that fluctuating asymmetry continued to increase with age in cranial elements even after 20 years of age; however, the degree of asymmetry in post cranial elements increased until the age of 20 and not after (Hallgrimsson, 1999).

On the other hand, Rossi et al. (2003) noted that some craniofacial measurements (such as the measurement from the infraorbital foramen to the anterior nasal spine (IOF), the measurement from the greater palatine foramen to the posterior nasal spine (GPF) and the measurement from the spinous foramen to the basion (SF)) did not display any correlations between age and fluctuating asymmetry. Hallgrimsson (1999) noted that in dentition, age and fluctuating asymmetry were not associated. However, Saunders and Mayhall (1982) noted that permanent teeth were more asymmetrical as opposed to deciduous teeth, but Guatelli-Steinberg et al. (2006) found that there were no statistical asymmetrical differences between deciduous and permanent teeth, as only three teeth had greater differences, with two of the teeth having a higher degree of asymmetry in deciduous teeth. More research is still needed to understand the correlation of age and fluctuating asymmetry. However, due to the broad nature of this study, age will not be further explored.

2.3 Developmental stress and the effect on adult health

Childhood developmental stress usually arises from congenital defects, living in poverty, having nutritional defects and increased susceptibility to disease. Reasons for congenital defects may be due to genetics, drug exposure or infections during pregnancy, and low socio-economic status experienced by the mother (Thompson, 2014). Coolidge (2015) noted that children born or raised in conditions of low socio-economic status have shown to have a higher likelihood of dying from diseases such as asthma, congenital abnormalities, certain cancers, injuries, flu, and pneumonia than those from high socio-economic status. Furthermore, children living in low socio-economic families are in more frequent need of hospitalization due to the susceptibility

to disease. Coolidge (2015) found that significant childhood stress usually resulted in a higher susceptibility to develop more health problems throughout the person's lifetime. Similarly, it was stated that a higher degree of fluctuating asymmetry was seen in populations with lower-socio-economic status, if foetal development occurred while the mother lived in a polluted environment, underwent physiological stress, contracted an infectious disease, or had severe nutritional deficits (Harris and Nweeia, 1980; Livshits et al., 1988; Gawlikowska et al., 2007; Storm, 2009). Therefore, fluctuating asymmetry can be used to study the appearance and cause of congenital defects that arise during ontogeny and continue to affect adult health (Livshits et al., 1988). Coolidge (2015) stated that there is increasing evidence that adult susceptibility to bad health is most likely linked to childhood health. Thus, some pathological responses on bone associated with childhood stress may remain in adulthood and therefore can be used to examine its link to skeletal asymmetry.

In South Africa, apartheid has contributed largely to disparities in economic status between individuals within the country. Between 1948 and 1994, apartheid was a system of institutionalised racial segregation which created a wealth and power imbalance among the racial groups (particularly in favour of white South Africans compared to black and coloured South Africans) (Linford, 2011). As a result of apartheid, access to high-level jobs, education, and urban areas were limited for people of colour, leaving many black and coloured South Africans poorly educated and possibly without jobs to improve their living conditions (Linford, 2017; Fogel, 2019). Presently, the economic effects of apartheid are still prevalent in South Africa even after the end of apartheid in the early 1990's. Many children and adults of colour in South Africa are thus experiencing multidimensional (poor health, lack of education and inadequate living standard) generational poverty due to the lasting effects of the apartheid regime. As a result, numerous children and adults have inadequate access to health care and are highly susceptible to disease and the development of pathological lesions (Daniel, 2020; Stoddard, 2022).

2.4 Pathological lesions

Pathological lesions can appear on the skeleton and occur as a result of stress. Stressors like infections and nutritional deficiencies can produce a bony response on the skeleton, which can then be used as an indicator to assess the developmental

stressors experienced by a population (Hagg et al., 2017; Ortner, 2019). Usually, when bone undergoes a type of stress, a bony response is produced, thanks to the osteoblast and osteoclast activity. Bone is then resorbed and starts to form again and is replaced with new bone cells, which is a continuous process in healthy bone. However, if a disease or infection interrupts this process, bone formation is disrupted (Ortner, 2019). This disruption leads to the formation of specific lesions in response to the type of disease or stressor. In order to give a possible diagnosis of the type of pathology, an understanding of how the lesions were formed and the main process of the disease is needed (Hagg et al., 2017; Ortner, 2019). As described in detail below, this study will focus on pathologies caused by infectious and nutritional diseases, such as cribra orbitalia, porotic hyperostosis, enamel hypoplasia and periostitis.

2.4.1 Cribra orbitalia

Cribra orbitalia presents as porosities or pitting paired with a thickening of the roof of the orbits (Zariſa et al., 2016). The lesions tend to be more severe and active in children, and as such the condition has typically been associated with nutritional stress during childhood. In adults, the condition is noted less frequently, and when present, the lesions tend to be healed with less severe expressions of pitting (Ortner, 2019). More recent literature discusses a proposed aetiology of anaemia-induced marrow hypertrophy resulting from haemolytic and/or megaloblastic anaemia as a cause for cribra orbitalia to develop (Walker et al., 2009; Hagg et al., 2017; Ortner, 2019). Haemolytic anaemias, such as thalassemia or sickle cell anaemia, have shown to be caused when red blood cells are destroyed prematurely producing the expression of osseous haemopoietic marrow expansion (Walker et al., 2009). On the other hand, megaloblastic anaemia has shown to be acquired in infants through nursing, due to the combination of the mother being extremely deficient in vitamin B12 and experiencing poor living conditions (low SES), resulting in the infant developing the deficiency from birth. Vitamin B12 deficiencies from childhood produce active, expansive pitting on the roof of the orbits (Walker et al., 2009). Lastly, Walker et al. (2009) noted that another probable cause for cribra orbitalia may be due to subperiosteal bleeding that occurs with a deficiency for both vitamin B12 and vitamin C. Hence, individuals that have suffered or are suffering from scurvy often have a vitamin C deficiency, which can cause a decrease in collagen synthesis and

susceptibility to infectious disease and haemorrhage and often exhibit pitting on the lateral sides of the orbit roofs.

2.4.2 Porotic Hyperostosis

Porotic hyperostosis manifests in the same way as cribra orbitalia but on the parietal and occipital bones and therefore, may be directly correlated. This pathological lesion usually occurs by marrow hypertrophy between the inner and outer skull tables (Rinaldo, 2018). A possible differential diagnosis for porotic hyperostosis may be a chronic scalp infection, scurvy, or anaemia. During anaemic conditions, the body starts to become starved of oxygen, and this type of hypoxic state will trigger an increased production of red blood cells which stimulates haemopoietic marrow red blood cell production (Salvadei et al., 2001). This results in enlargement of the diploë through the outer table of the cranial vault with porosities or pitting on the cranial vault. In severe cases, this may even cause exposure of the underlying trabecular bone. The porotic lesions are seen with massive marrow hypertrophy that can only be produced by high levels of erythropoiesis such as haemolytic and megaloblastic anaemia (Walker et al., 1997). Haemolytic and megaloblastic anaemia increases the production of red blood cells but then causes their premature death. If the number of dead red blood cells exceeds the number of red blood cells produced, this will stimulate the bone marrow expansions (Walker et al., 1997). In a study conducted by Walker et al. (2009), the majority of active lesions were noted in the skeletons of children in the archaeological sample while healed lesions are typically noted in older adults. Therefore, the appearance of porotic hyperostosis is most likely a reflection of childhood anaemia. This can be supported by bioarchaeological data as well as modern clinical data that have shown that children have much lower capacity to support elevated levels of red blood cell production, which increases the likelihood of porotic hyperostosis being frequently seen in children (Walker et al., 1997).

2.4.3 Periostitis

Periostitis occurs because of the inflammation or lifting at an infected area under the periosteum (Ortner, 2019). The periosteum is the membranous soft tissue layer that encapsulates the bone and stimulates circumferential growth of bones during the physiological growth of subadults, as well as remodelling in response to stress or

strain in adults (Waldron, 2009). Bone reacts to pathological responses related to the periosteum by continuously depositing bone at sites of infection and inflammation. These subperiosteal bone reactions, mostly exhibited on long bones, are highly variable, as they can be unilateral, bilateral, or diffuse (Waldron, 2009). Active lesions are attached loosely to the cortical bone with signs of newly formed bone having a loose and irregularly striated appearance. To identify periostitis, the area of the active lesions displays striations, pits, and porous bone with well-defined margins (Ortner, 2019). When the lesions start to heal, the bone will begin to remodel from primary woven bone to secondary cortical bone which appears smoother with some residual pitting or striations (Ortner, 2019). While commonly attributed to infection, periostitis is considered a non-specific sign of disease as it may also be the result of trauma, bacterial infections, neoplasms, scurvy, chronic distribution of drugs into the periosteum using a needle and venous insufficiency (which can occur frequently in individuals of low SES) (Waldron, 2003; Hagg et al., 2017).

2.4.4 Enamel Hypoplasia

Enamel tends to carry vital information on the history of childhood stress with lasting signs in adulthood seen as enamel hypoplasia. Enamel is the smooth, thin hard outer layer covering the tooth crown. Amelogenesis occurs at four stages to form enamel (Smith et al., 2017) and these four stages include the use of ameloblasts, ameloblastin, amelogenin and enamelin which are secreted by enamel crystals. Ameloblasts are single cells that develop the enamel, and they differentiate, mature, and orientate themselves into bundles forming prisms with cross-striations known as striae of Retzius. Therefore, ameloblast activity and enamel matrix will form stable and mature mineralised enamel on the crown surface (Smith et al., 2017). Defects in enamel formation will result in imperfect formation of enamel with pits, furrows, grooves, and lines with uneven thickness distribution on the enamel layer (Hagg et al., 2017; Alblas, 2019; Ortner, 2019). Many factors may cause this disruption in enamel formation such as infections, poor nutrition, trauma during birth, low weight at birth and a genetic predisposition. Other causes may be low levels of calcium, hypovitaminosis D, gestational diabetes, defects in growth hormone concentrations, anaemia, jaundice, pneumonia, influenza, or metabolic disorders (Waldron, 2003). However, the most common causes for enamel hypoplasia noted by Hagg et al. (2017) were severe

malnutrition or premature births. Enamel hypoplasia can start in the second trimester of pregnancy up to the age of age and will continue to remain into adulthood as the enamel cannot repair itself once its formation has been disrupted (Goodman and Rose, 1990; Brook, 2009; Schuurs, 2013). Enamel hypoplasia can therefore be seen on both permanent and deciduous teeth. Furthermore, anterior teeth generally exhibit higher levels of enamel hypoplasia than posterior teeth with mandibular canines being mainly affected in adult populations (Wright, 1997). As such, enamel hypoplasia can be an indicator for developmental stress due to its link to infection or nutritional deficiencies and its persistence into adulthood.

2.5 3D imaging methods

2.5.1 Micro-focus X-ray computed tomography imaging (micro-XCT)

For bone and dental analyses, micro-XCT imaging is frequently considered the gold standard against all other modalities, because of its relatively high resolution and its non-destructive and non-invasive nature (Olejniczak et al., 2007). Furthermore, a study conducted by Olejniczak et al. (2007) evaluated the compatibility of different microtomographic imaging systems and found that not only were all four different micro-CT imaging systems comparable and produced similar results, but the study also supported the claim that micro-XCT imaging is highly consistent and accurate. Three-dimensional imaging methods have become frequently used in various fields, like biological anthropology, or dentistry, as it allows for precise and accurate reconstructions of skeletal and dental structures. Micro-XCT imaging has assisted in taking measurements in a more precise manner on an anatomical structure. This has helped reduce distortion and magnification of anatomical structures that was a huge disadvantage when using standard radiographical methods (Akhil et al., 2015).

As noted by Akhil et al. (2015), 3D imaging can be highly effective in providing accurate and detailed results, that can assist in identifying and treating facial asymmetry. It can also allow for better visualizations and analysis of facial structures and provide a more concise way to take facial measurements in order to assess left and right differences (Akhil et al., 2015). Studies assessing fluctuating asymmetry, have often employed geometric morphometrics methods in 3D imaging to assess

magnitudes of facial asymmetry (Schlager, 2013; Klingenberg, 2015; Benítez et al., 2020).

2.5.2 Geometric morphometrics

Geometric morphometrics is a method that focuses on biological shape analysis using Cartesian coordinates (x, y, z) of anatomical landmarks. Once the shape of the landmarks has been extracted from its position, size and orientation, a resulting Procrustes shape coordinate can be employed for statistical analysis (Slice, 2007; Mitteroecker and Gunz, 2009).

Anatomical landmarks are homologous points that are in the same location on every individual in a data set. These homologous points can be utilised to take measurements of angles, distances (Schlager, 2013), or to analyse biological shapes. These landmarks are placed on three dimensional or two-dimensional images using an imaging software (Schlager, 2013), and can be placed automatically or manually (Ridel, 2020a). There are two different categories and three types of landmarks. Landmarks can be craniometric or capulometric and can be either Type I (points where sutures intersect e.g., bregma), Type II (points on maximum curvatures e.g., condylion) or Type III (points where a line must be drawn to connect sutures e.g., alveolon) (Schlager, 2013). Many studies have employed 3D anatomical landmarks and found them to be accurate and precise (Cavalcanti et al., 2004; Gribel et al., 2011; Schlager, 2013).

Geometric morphometric methods detect even the slightest size and shape differences (Goodall, 1991; Benítez et al., 2020) and has become frequently used and proven extremely useful and accurate. For instance, geometric morphometrics is often used in forensic anthropology with regards to sex and ancestry estimations, with high accuracy levels (Franklin et al., 2012; Schlager, 2013). Furthermore, geometric morphometrics have become a popular method for the assessment of fluctuating asymmetry due to its precision and low measurement error (Benítez et al., 2020). This tool allows for the detection of subtle asymmetrical differences and variations (Benítez et al., 2020). Benítez et al. (2020) noted that the use of geometric morphometrics is more sensitive to environmental and genetic stress that cause asymmetrical size and shape differences than the traditional approach in assessing asymmetry (Figure 2.2).

Similarly, Klingenberg (2015) noted that, unlike the traditional linear measurements usually used to assess asymmetry, multivariate shape analysis offers a more complex and detailed method, particularly when examining asymmetry. Schlager (2013) employed geometric morphometrics in a study focusing on predicting nasal soft tissue shape, in which the author examined the correlation of asymmetry with hard and soft tissue between populations. The results highlighted that the magnitude of asymmetry was stronger in the European sample compared to a Chinese sample, but the degree of directional asymmetry expressed by both populations were similar, with comparable findings on sexual dimorphism. In this study, geometric morphometrics provided valuable insight on the degree of asymmetry expressed on the nose between populations and sexes (Schlager, 2013).

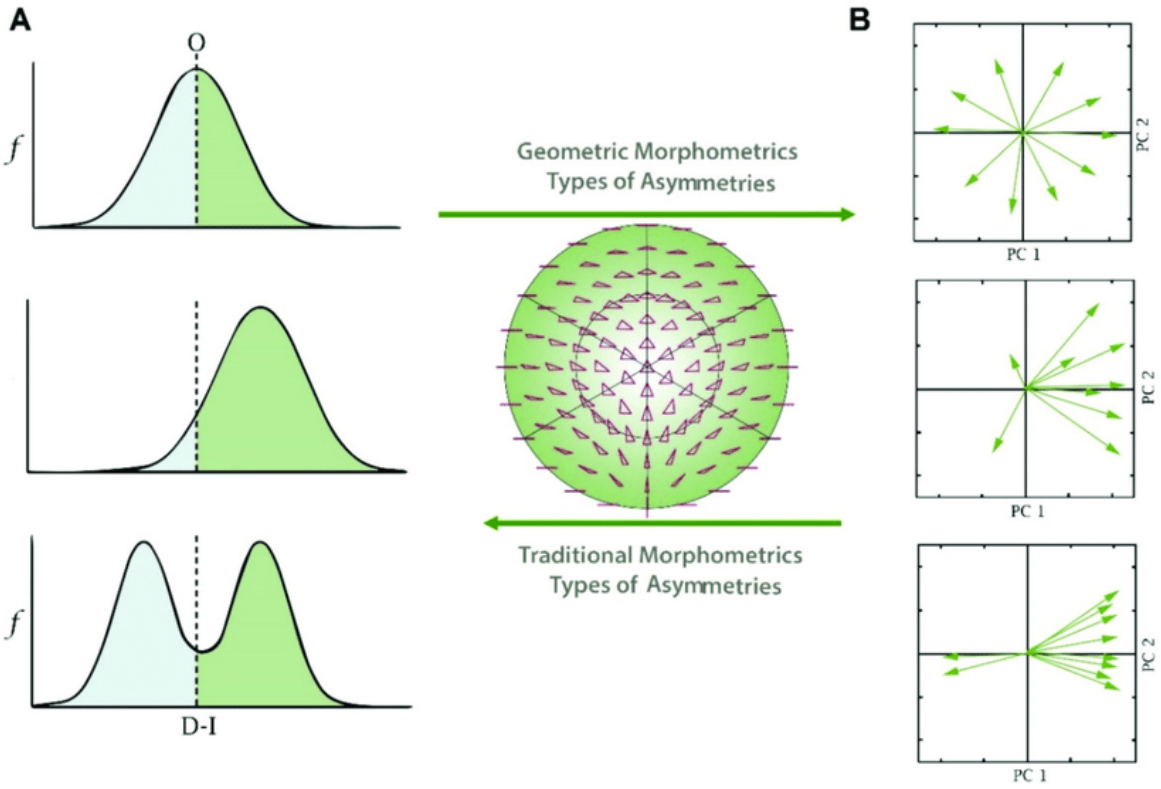

Figure 2.2 *- The translation of different types of asymmetries into a geometric morphometric paradigm (adapted from Benítez et al., 2020) A – represents the 3 categories of asymmetry , B – represents the GMM PC distribution for each type of asymmetry*

Chapter 3 - INTRODUCTORY MATERIALS AND METHODS

3.1. Materials

The sample consisted of 115 crania from adult individuals (mean age: 53 ± 16 years), and their associated postcranial remains sourced from the Pretoria Bone Collection (PBC) (L'Abbé et al., 2005; L'Abbé et al., 2021), housed in the Department of Anatomy, University of Pretoria, South Africa (see Table 3.1). As demographic parameters have been included in this study, information regarding sex and ancestry have been recorded. Only adults were analysed, and age was not investigated as it was beyond the scope of this study. Only well-preserved skulls with absence of trauma, bone alterations and absence of metal restorations were selected. The PBC is a fairly modern sample consisting of South African individuals born between 1863 to 1996 and is a good indicator of modern human variation seen amongst the South African populations (L'Abbé et al., 2005; L'Abbé et al., 2021). The skeletons are of known sex and population affinity and were obtained from cadavers that are composed of unclaimed and donated bodies acquired by the University of Pretoria (L'Abbé et al., 2005; Krüger et al., 2015; Liebenberg et al., 2019). Two sets of data were collected from each individual. Firstly, micro-XCT scans of the cranium were utilised to place anatomical landmarks and thus obtain left and right measurements, as well as conduct shape analysis from bilateral traits. Micro-XCT allows for optimal visualisation of facial structures and is a more concise methodology to take measurements accurately without damaging skeletal material. Secondly, the entire skeleton was assessed for pathological signs of stress typically linked to non-specific signs of disease and nutritional diseases. It was important to examine the whole skeleton to ensure that all pathological signs of stress are observed closely and recorded.

The crania analysed in this study were previously micro-XCT scanned for other projects (Approval Ethics Certificate references: 340/2015, 35/2016 and 57/2017) at the South African Nuclear Energy Corporation (Necsa). Scanning was performed using a Nikon XT H 255L industrial computed tomography system (Nikon Metrology) (Hoffman and De Beer, 2012). During the scanning process, the specimen was placed into the micro-XCT and was then rotated over 360 degrees while the X-ray source

beamed. Two-dimensional radiographic projection images were thus generated, which were then reconstructed into a 3D volume. Ethical approval to conduct this research was obtained by the University of Pretoria Ethical committee (Ethics reference: 386/2021).

Table 3.1 *- Study sample distribution*

	black South Africans	**white South Africans**	**Total**
Females	30	27	57
Males	29	29	58
Total	59	56	115

3.2. Methods

Firstly, the micro-XCT scans had to be segmented (i.e., virtual extraction of the region of interest) using the semi-automatic watershed method available in Avizo 2019 (ThermoFisher Scientific Inc.), a 3D imaging software. The segmentation allows the generation of accurate 3D models than can be used in the subsequent analysing steps. All the 3D models were re-oriented and aligned according to a similar reference plane: the Frankfort plane. The orientation was performed by placing four anatomical standard landmarks: the right and left porion, and the right and left orbitale. Once all crania were in a standard position, 34 craniometric landmarks were manually placed (see Table 3.2 for definitions and Figure 3.1). Asymmetry was evaluated from the landmarks by calculating inter-landmark distances (refer to Table 3.3 for details on the inter-landmark distances) as well as analysing shapes using geometric morphometric methods.

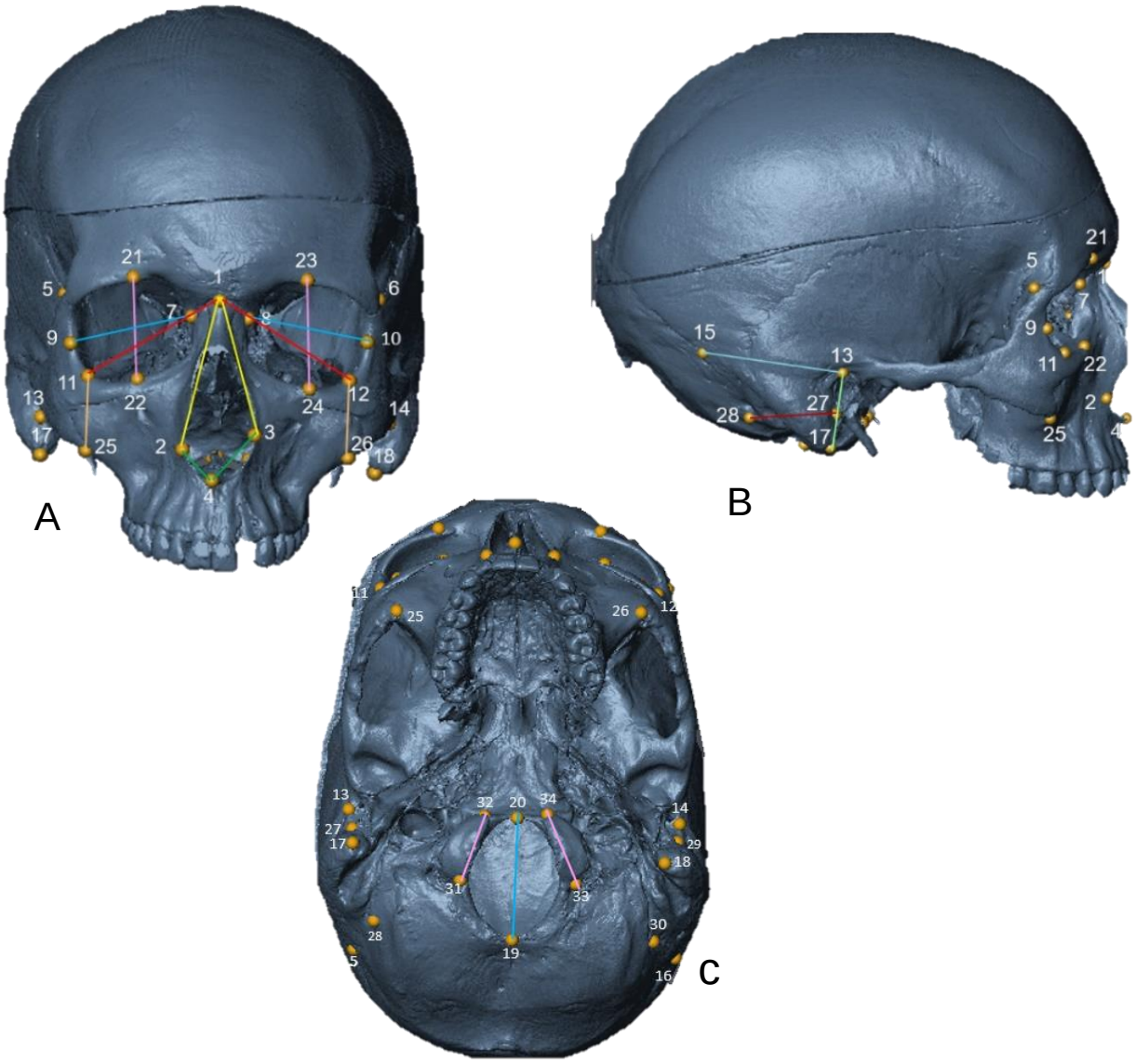

Figure 3.1 *- Landmarks (1 – 34) placed on the cranium (cf. Table 3.2 for definitions). A: Frontal view; B: Lateral view; C: Inferior view*

Table 3.2 *- Craniometric landmarks placed on each cranium (adapted from Caple and Stephan, 2016; Langley et al., 2016; Ridel, 2019)*

Nr.	Name		Abr.	Definition
1	Nasion	Midline	N	Located on the frontal bone, at the intersection of the nasal bone and frontal bone.
2,3	Alare	Bilateral	Al	Most lateral points on the nasal aperture.
4	Nasospinale	Midline	Ns	Located at the midpoint of a line connecting the lowest points of the inferior margin of the nasal aperture.
5, 6	Frontomalaretemporale	Bilateral	Fmt	Most laterally positioned point on the frontomalare suture.
7, 8	Dacryon	Bilateral	D	Intersection of the lacrimomaxillary suture and the frontal bone. If the suture cannot be seen, it is aligned with lacrimal fossa.
9, 10	Ectoconchion	Bilateral	Ec	Located on the lateral margin of the orbits, such that when a straight line is drawn from dacryon to the lateral margin, the line runs parallel to the supraorbital margin and bisects the orbit into two.

11, 12	Orbitale	Bilateral	Or	Most inferior point on the lower orbital rim.
13, 14	Porion	Bilateral	Po	Located at the most superior point along the upper margin of the external acoustic meatus.
15, 16	Asterion	Bilateral	Ast	Located on the occipital bone where sutures intersect, between temporal, occipital, and parietal bones.
17, 18	Mastoidale	Bilateral	Ms	Most inferior point on the tip of the mastoid process.
19	Opisthion	Midline	O	The most inferior point at the posterior margin of the foramen magnum, on the midsagittal plane.
20	Basion	Midline	Ba	Located at the midpoint of the ridge forming the anterior border of foramen magnum.
21, 23	Superior Orbital	Bilateral	So	Located on the superior orbital margin perpendicular to orbital breadth.
22, 24	Inferior Orbital	Bilateral	Io	Located on the inferior orbital margin perpendicular to orbital breadth.
25, 26	Zygomatic	Bilateral	Z	Located superiorly on the Inferior border of the zygoma.
27, 29	Posterior External Meatus	Bilateral	Pem	Located on the posterior border of the of the external meatus.

28, 30	Posterior Mastoid	Bilateral	Pm	Located on the most anterior point on the Posterior margin of the mastoid.
31, 33	Posterior Occipital Condyle	Bilateral	Poc	Located on the most posterior point on the occipital condyle.
32, 34	Anterior Occipital Condyle	Bilateral	Aoc	Located on the most anterior point on the occipital condyle.

Table 3.3 *- Inter-landmark distances calculated from the craniometric landmarks (adapted from Hagg et al., 2017). Refer to Table 2 for landmark definitions*

Nr.	Name	Abr.	Definition
1	Orbital breadth	OBB	Lateral distance from the dacryon (D) to ectoconchion (Ec).
2	Orbital height	OBH	Direct distance between the superior (So) and inferior (Io) orbital margins perpendicular to the orbital breadth.
3	Diagonal orbital breadth	NOR	Direct distance from nasion (N) to the orbitale (Or).
4	Frontomalare-nasion length	FMTN	Direct distance from the frontomalare (Fmt) to nasion (N).

5	Frontomalare-nasospinale	FMTNS	Direct distance from frontomalare (Fmt) to nasospinale (Ns).
6	Malar height	MAH	Least distance from the most inferior point on the lower border of the orbit (Or) to the most superior point on the inferior border of the zygomatic.
7	Mastoid length	MPL	Direct distance from porion (Po) to mastoidale (Ms).
8	Mastoid breadth	MPB	Direct distance from the posterior border of the external auditory meatus (Pem) to the most anterior point along the posterior margin of the mastoid process (Pm).
9	Mastoidale-asterion	MSAST	Direct distance from mastoidale (Ms) to asterion (Ast).
10	Occipital condyle length	OCL	Maximum distance from the most anterior (Aoc) to the most posterior (Poc) point on the occipital condyles.
11	Opisthion-porion length	OPO	Direct distance from the opisthion (O) to porion (Po).
12	Basion-porion length	BAPO	Direct distance from basion (Ba) to porion (Po).

13	Nasion-mastoidale	NMS	Direct distance from nasion (N) to mastoidale (Ms).
14	Nasion-alare	NAL	Direct distance from nasion (N) to alare (Al)
15	Nasospinale-alare	NAAL	Direct distance from nasospinale (Ns) to alare (Al)

Finally, fluctuating asymmetry (FA) values (left-side measurement minus right-side measurement) were calculated for each individual. Since fluctuating indices can increase with trait size, a standardised scale needed to be used to assess asymmetry, allowing for an accurate comparison between traits with different magnitudes. Standard asymmetry formulae developed by Palmer and Strobeck (2003) were thus used. Average FA values were calculated for each trait for each individual and for a combination of traits (Palmer and Strobeck, 2003, Hagg et al., 2017) (refer to Table 3.4 for formula and definition of FA indices).

Table 3.4 *- Formulae of the indices used to evaluate asymmetry (Adapted from Hagg et al., 2017 and Palmer and Strobeck, 2003)*

Index	Formula	Description
FA8	$FA8 = \left\lvert \ln(R_d/L_d) \right\rvert$	The difference between the natural logs of the left and right measurements of a trait, in absolute values.
FA17	$FA\ 17 = \sum \left\lvert \ln(R_d/L_d) \right\rvert / T$	Average FA values computed from the FA8 values for multiple traits and combinations.

In addition to collecting measurements from the cranium, the crania, and long bones (humeri, ulnae, radii, femurs, tibias, and fibulas) were all examined for pathological lesions typically linked to non-specific signs of disease and nutritional diseases. This, however, was not performed on the micro-XCT scans, because these lesions were not easily observable and furthermore, not all the postcranial elements for the individuals have been scanned. Diagnostic aids such as palaeopathological textbooks were used to effectively analyse the pathological lesions (Ortner, 2019; Waldron, 2009). Specifically, the presence of cribra orbitalia (Figure 3.2), and porotic hyperostosis (Figure 3.3) was scored as present if pitting was seen on the orbital roofs, partial and occipital bones respectively. Enamel hypoplasia was scored as present if at least one hypoplastic defect was present on at least one tooth (Figure 3.4). Similarly, subperiosteal bone reactions (periostitis) were considered present if it was observed on at least one long bone (Figure 3.5). The pathological lesions were scored as present regardless of whether the lesion appeared active or healed/in the process of

healing. The pathological lesions, lesion location and the number of lesions seen on each individual were observed and noted.

Figure 3.2 *- Pictures illustrating cribra orbitalia : A- unaffected individual , B- active lesions of cribra orbitalia , and C- healing/healed lesions of cribra orbitalia.*

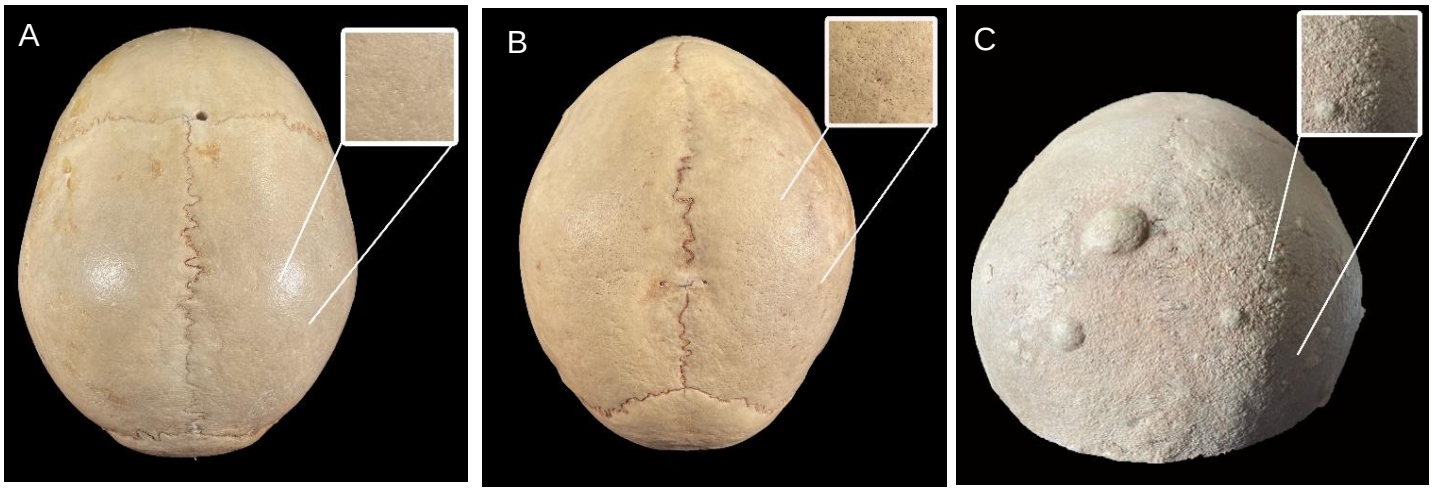

Figure 3.3 *- Pictures illustrating porotic hyperostosis. A- unaffected individual, B- pitting present and C- severe pitting*

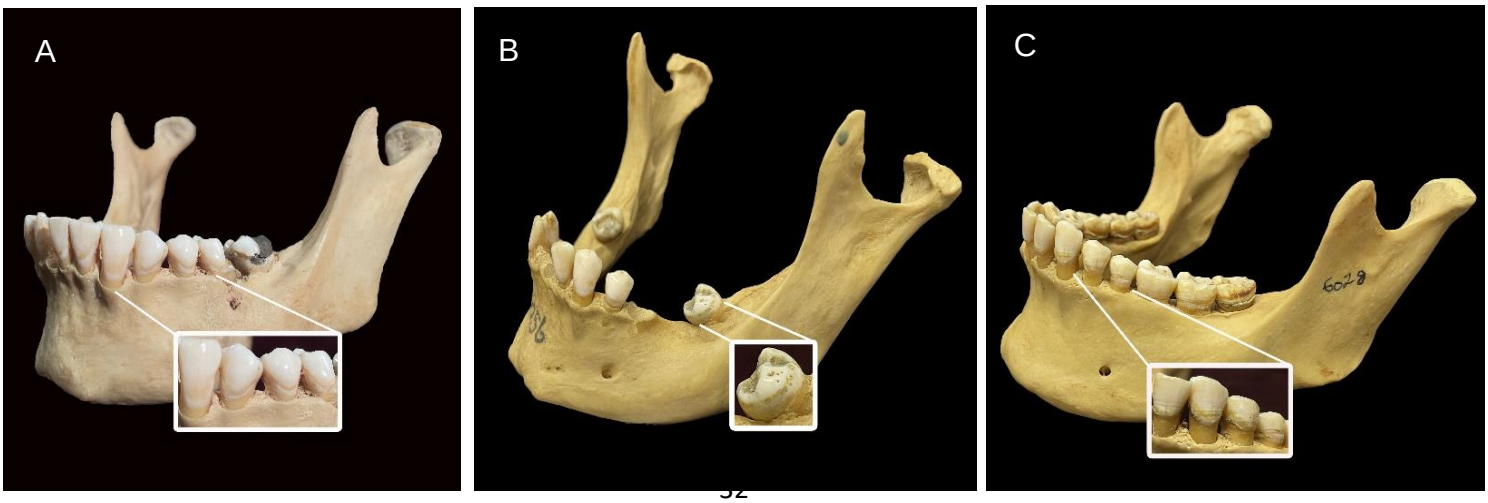

Figure 3.4 *- Pictures illustrating enamel hypoplasia A- unaffected individual, B- spotted defects and C- linear defects associated with enamel hypoplasia*

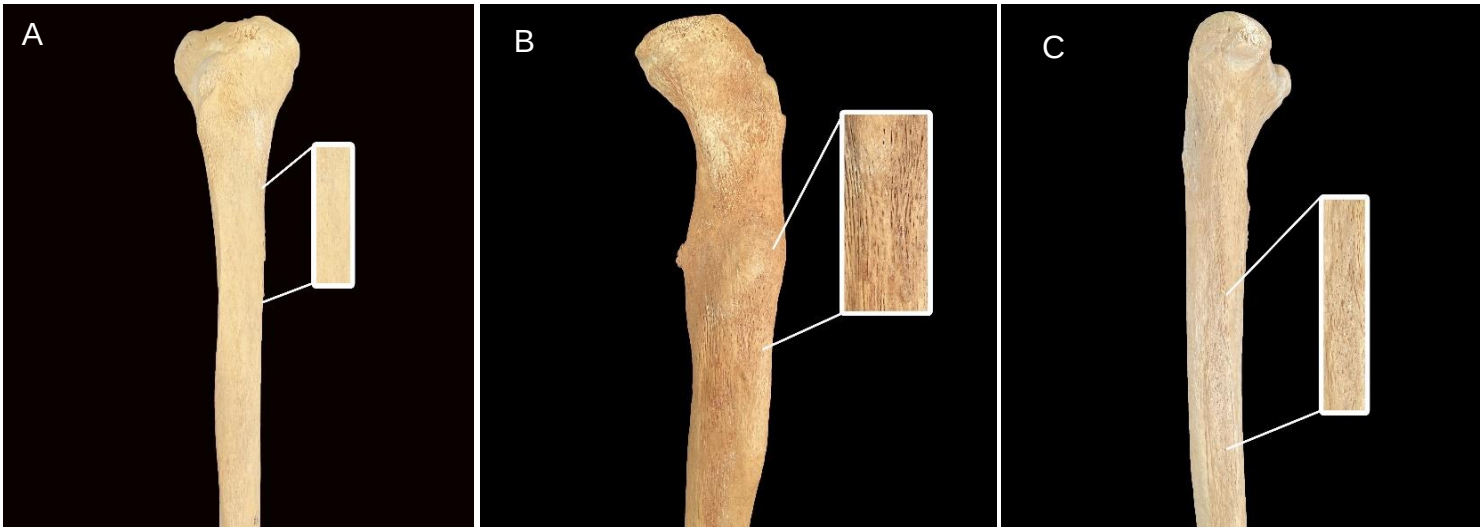

Figure 3.5 *- Pictures illustrating an individual without periostitis and individuals with varying degrees of periostitis: A- uninfected individual, B- active periosteal stripping and C- healed periostitis*

3.3. Statistical analysis

All statistical analyses were conducted in the R software and R studio environment (R Core Team, 2018; Trochim, 2020).

3.3.1 Intra and inter-observer repeatability

Repeatability testing was performed to assess the reproducibility of the landmark positioning by calculating intra- and inter-observer errors. For the intra-observer error, the landmark placement was performed twice on 15 randomly selected crania by the same observer with an interval of two weeks. For the inter-observer error, the landmark placement was performed by two different observers on the 15 random crania. The reproducibility of the landmark positioning was calculated using the dispersion Δ_{ij} for each landmark *i* and individual *j*. Dispersion is defined as the Mean Euclidean Distance (MED) of the sample landmark $\boldsymbol{p}_{ijk}$ to the mean $\overline{\boldsymbol{p}}_{ij}$of the (x, y, z)-coordinates of landmark *i* over all observation's *k* (inter, intra, resp.) for subject *j* *(Formula 3.1)*:

Formula 3.1

$$\Delta_{ij} = \sum_{k=1}^{K} \left\| \boldsymbol{p}_{ijk} - \overline{\boldsymbol{p}}_{ij} \right\| / K \text{ , with } \overline{\boldsymbol{p}}_{ij} = \sum_{k=1}^{K} \boldsymbol{p}_{ijk} / K$$

Boxplots of MED values were generated to show the variation of dispersion over different subjects. Global precision is reported as the global (averaged over all landmarks) mean (μ_{Δ}) and median (m_{Δ}) of the per landmark mean ($\mu_{\Delta i}$) and median ($m_{\Delta i}$) values (over all subjects).

3.3.2 Descriptive, exploratory, and correlative statistics

Descriptive statistics were calculated to summarise and describe the main features of the dataset for asymmetrical linear distances and FA values (Trochim, 2020). For normality testing, Shapiro-Wilk tests were conducted on the inter-landmark distances and on the FA indices. From these results, non-parametric Wilcoxon tests were chosen and performed between each corresponding left and right distances (e.g., left, and right OBH) to evaluate asymmetry. Asymmetrical differences between demographic profiles (population and sex) were further investigated for the inter-landmark distances, as well as for FA8 and FA17 indices, using Wilcoxon and Kruskal-Wallis tests.

Statistical analyses were then conducted to evaluate the frequency and presence of pathology in the South African population and between sexes. Frequency distributions (0 = absent , 1= present) were calculated for presence of the pathological lesions (for each disease), separated into sex and population groups and for population and sex, simultaneously. Kruskal-Wallis tests were conducted in conjunction with the frequency distributions to test for significant differences between the groups. Frequency distributions were also conducted to examine the number of pathologies an individual had (0 = none observed, 1 = one condition observed, etc.) over the entire sample for populations, sexes, and population and sex, simultaneously. Kruskal-Wallis testing was conducted to test for significant differences between the groups per the number of pathologies. Results were broken down to see which conditions were seen together more frequently.

Spearman's rank correlations were employed to assess the relationship between the pathological conditions and population/sex. Additionally, spearman's correlations were calculated to further explore the relationship between each of the conditions, as well as the relationship between the conditions and asymmetry in the measurements. A correlation value of -1 indicates a strongly negative correlation, while +1 indicates a

strongly positive correlation showing a decreased and increased likelihood of diseases have an association, respectively.

3.3.3 Geometric morphometric analysis

Lastly, geometric morphometric methods (GMM) analyses were conducted to assess asymmetrical shape variation in matrices and demographic profiles. Preliminary statistical testing was first needed. A Generalised Procrustes Analysis (GPA) was performed on the raw Cartesian coordinate data of the landmarks to obtain orientation-invariant shape coordinates (Dryden and Mardia, 2016). A Principal Component Analysis (PCA) was then conducted to alter the data to form a new coordinate system and identify the greatest variance between sex and population affinity of data lying on the first and second Principal Component (PC) and produce PC scores (Schlager, 2013; Ridel et al., 2018). Multivariate normality testing was performed for the PC score distribution by rendering Q-Q plots, showing a multivariate normal distribution (Schlager, 2013). Procrustes two-way, mixed model Analysis of Variances (ANOVAs) were then used to statistically evaluate fluctuating asymmetry (individuals (I) x sides (S) interaction) and its correlation to sex and sex/population. Individuals (I), consist of a random sample of individuals from the entire study sample, while sides (S) are a fixed effect that consist of two levels (left and right). An individual by side interaction (I x S) is a mixed effect and provides information on an individual's failure to be the same from side-to-side denoting fluctuating asymmetry (Ducos and Tabugo, 2014). Statistical methods for both matching/bilateral (traits with mirrored pairs) and object (single object is symmetric about a midline) symmetry were implemented (Mardia et al., 2000; Klingenberg et al., 2002). P-values were then obtained for each trait and for sex and sex/population affinity per trait to observe if fluctuating asymmetry was present in traits, and its influence on sex and sex/population affinity.

Chapter 4 - EXPLORATION OF CRANIOFACIAL ASYMMETRY

4.1. Chapter Overview

The purpose of this chapter was to explore the extent of craniofacial asymmetry in a South African sample (black and white South Africans) using both inter-landmark distances and geometric morphometric methods (GMM). This research demonstrates which regions in the cranium are affected by fluctuating asymmetry, as well as which population affinity and sex cohort exhibited the greatest magnitude of asymmetry.

Exploring craniofacial asymmetry in a South African sample.

M HARRIPERSHAD, CEG THEYE, AF RIDEL, L LIEBENBERG

Manuscript to be submitted for publication to the American Journal of Biological Anthropology

Abstract

Fluctuating asymmetry and its correlation to population history, health and its impact on the biological profile has been extensively studied by biological anthropologists. However, in South Africa, there have only been a few studies done on skeletal asymmetry. Thus, the following study aimed to assess the magnitude of craniofacial asymmetry in the South African population and the influence of sex and population affinity on fluctuating asymmetry. The sample analysed consisted of 115 adult individuals (59 black and 56 white South Africans, comprising 58 females and 57 males) and their associated micro-XCT scans. Craniometric landmarks were placed and used to calculate inter-landmark distances and perform shape analysis. Fluctuating asymmetry was first calculated from the left and right inter-landmark distances for various traits on the cranium, and subsequently assessed using geometric morphometrics for asymmetrical shape variation. Significantly high levels of fluctuating asymmetry were noted in the orbital, nasal and temporal regions. A significantly high degree of asymmetry was seen in females and black South Africans, which was consistent with the literature. While the potential influence of asymmetry on biological profile estimations can be minimal when taking measurements, forensic

anthropologists should have an understanding of the consequences asymmetry may have on the sides of skeletal elements or traits being employed on an individual basis.

Keywords: Fluctuating asymmetry, Micro-XCT, Geometric morphometrics, Biological anthropology, South African population

4.2. Introduction

Skeletal asymmetry refers to inequality in the size and shape of bilateral anatomical structures and is often studied by biological anthropologists (Graham and Özener, 2016). The literature classifies asymmetry into three types: fluctuating asymmetry, directional asymmetry, and antisymmetry (Graham and Özener, 2016). The main focus of this article is fluctuating asymmetry, which is defined as a random deviation from perfect symmetry with an inequality in the size or shape of bilateral (left and right sided) traits (Graham and Özener, 2016). Directional asymmetry is the constant growth of one side of a bilateral trait, with larger dimensions expressed on the dominant side, and is commonly referred to as handedness. As such, right bias is frequently observed in the postcranial skeleton of the general population (right-side traits are larger than left-side traits) (Hagg et al., 2017). Similarly, antisymmetry is defined in bilateral traits as one side being more developed. Antisymmetry, unlike directional asymmetry, is random and not caused by pattern limb dominance (Graham and Özener, 2016). Compared to postcranial elements, the cranium lacks a substantial pattern of one-sided dominance (Graham and Özener, 2016). Thus, the cranium is minimally affected by directional asymmetry, and can assist in providing a better gauge of fluctuating asymmetry in individuals (Graham and Özener, 2016).

Fluctuating asymmetry is often overlooked in literature (especially in modern human samples) because directional asymmetry is easier to quantify and is thus a popularly studied topic among anthropologists (Latimer and Lowrance, 1965; Hiramoto, 1993; Cuk et al., 2001; Auerbach and Ruff, 2006; Kanchan et al., 2008). Fluctuating asymmetry has been suggested to be the result of developmental instability and can potentially be used as an indicator of developmental stress (Graham and Özener, 2016). Developmental instabilities are described as an individual's inefficiency to produce a desired phenotype under a specific environmental condition (e.g., nutritional deficiencies, adverse living conditions or temperatures, and genetic mutations) (Palmer, 1994). While, the term developmental stressors are often used in biological

anthropology and refers to the event that results in physiological change caused by strain placed upon an individual brought about by environmental and genetic conditions during stages of growth. Often in childhood, developmental stress may arise from congenital defects, living in poverty, and poor health due to susceptibility to disease. Publications have shown that children from low socio-economic backgrounds tend to be frequently hospitalised, have an increased susceptibility to disease throughout their lifetime and demonstrate higher degrees of fluctuating asymmetry (Livshits et al.1988; Palmer, 1994). Due to the skeletal implications, biological anthropologists are interested in understanding developmental stressors that arise during ontogeny, their influence on adult health, and the overall impact on adult skeletal asymmetry (Livshits et al.1988).

Presently in South Africa, an estimated four million South Africans are experiencing multidimensional poverty (poor health, malnutrition, and lack of access to basic needs), which is in part due to the high levels of unemployment in the country (Daniel, 2020; Stoddard, 2022). Persistent inequalities and unemployment in the population largely stemmed from institutional racism associated with the apartheid regime (1948-1994), which prevented people of colour from having access to good education and jobs. Thus, the apartheid regime created a wealth and power imbalance between racial groups. In 2021, 61% of people of colour in South Africa are estimated to be living in poverty, while only 1% of the white South African population is experiencing poverty (*Government* Gazette, 2021).

By improving the understanding of skeletal asymmetry and the roles played by different stressors, anthropologists will be able to interpret and understand skeletal variation observed among individuals (De Coster et al., 2013). In addition, the diverse nature and history of the South African population yields an ideal sample to explore the effects of developmental stressors on fluctuating asymmetry. However, fluctuating asymmetry in the modern South African population has rarely been explored (Kieser,1998; Holland, 2015).

An understanding of asymmetry is required in forensic anthropology as it may potentially influence estimates of the biological profile resulting in misclassification (Cole et al., 2020). Multiple studies have shown that limb asymmetry may cause difficulty in the forensic and bioarchaeological assessment of the biological profile.

Asymmetry can influence the biological profile, particularly when assessing stature and age estimates, as well as when identifying the number of individuals in comingled remains (Zivanović, 1983; Kanchan et al., 2008; Krishan et al., 2010; Corron and Stull, 2017; Nandi et al., 2018). Both cranial and pelvic asymmetry have been shown to have implications on sex estimation and a better understanding of the magnitude of asymmetry expressed by an individual is imperative for accurate sex estimates (Cole et al., 2020). Knowledge of facial asymmetry is required in the medical field, as complications may arise when placing facial or dental implants (Srivastava et al., 2018). For instance, mental nerve injuries can occur due to misplacement of dental implants, as this nerve often arises from asymmetric foramina (Kim, 2011). A good grasp of facial asymmetry in the South African population and among individuals can therefore benefit medical professionals.

With regards to population affinity, research on asymmetrical population differences is greatly needed, not only to better comprehend the understanding of population history and instability, but also to assist the processes of facial approximation and identification in the medical and forensic fields. However, only a small amount of research has been conducted in relation to asymmetry. Since different populations experience different stressors or no stressors at all, asymmetry can be extremely helpful when studying the extent and correlation of fluctuating asymmetry. Furthermore, due to the socio-economic constraints experienced in the South African population by means of population stressors (e.g., apartheid and poverty), research by Kieser and Groeneveld (1988) found that black South Africans exhibited higher levels of dental asymmetry as opposed to the white South African population. This great degree of asymmetry in the South African population may potentially be attributed to the high prevalence of disease and malnutrition in this population group following the legacy of apartheid (Kieser and Groeneveld, 1988).

Sex estimation may be impacted by fluctuating asymmetry and should thus be considered when evaluating asymmetry (Cole et al., 2020). Females are thought to be more resistant to developmental instabilities due to their genotype; more specifically, XX-chromosomes can buffer deleterious recessive alleles, while the single X chromosome present in the male genotype (XY sex chromosomes) cannot (Graham and Özener, 2016). Hence, females are considered more “stable,” and males are predicted to express a greater degree of asymmetry (Graham and Özener, 2016).

Additionally, females are considered to have a ”maternal buffering system” which is a physiological response to physical stress. However, if the mother herself experienced stressful conditions while developing, her buffering system will not be as efficient. Thus, when the mother is pregnant and experiences stressful conditions, the infant will be susceptible to environmental stressors, consequently increasing developmental instability in the child (Reck et al., 2016; Howell et al., 2017). In this way, the generational effects of poverty and poor living conditions is observed (Howell et al., 2017). In a modern living Turkish sample, Özener and Fink (2010) noted asymmetrical sex differences, but only in males living in lower socio-economic conditions. Multiple other studies on various prehistoric and modern populations found no significant sex differences for fluctuating asymmetry when evaluating the crania, mandible, dentition, and postcranial skeleton (Perzigian, 1977; Townsend and Garcia-Godoy, 1984; Costa, 1986; Hallgrimsson, 1999). Owing to the myriad of contradictory results, literature has been highly inconsistent in describing the relationship between sex and fluctuating asymmetry; hence, more research is needed to understand the extent to which asymmetry may differ between the sexes, especially in a South African population.

Past research on facial asymmetry and odontology have focused on utilizing physical measurements (following traditional methods) and two-dimensional (2D) posteroanterior cephalometric images (Letzer and Kronman, 1967; Shah and Joshi, 1978; Cohen, 2005; de Moraes et al., 2011). However, there are multiple limitations to these methodologies. The traditional methods can often be time-consuming, based on small samples, requires the handling and contamination of skeletal material, and may not be practical in a clinical setting for medical professionals. Furthermore, literature has indicated low agreement between measurements taken on 2D digital images and physical measurements (Cohen, 2005; de Moraes et al., 2011). This poor agreement is due to the fact that cephalometric radiograph images are often distorted, magnified, and can have erroneous projections due to misalignment of the cephalostat (de Moraes et al., 2011).

On the other hand, multiple studies have employed three-dimensional (3D) imaging to study facial asymmetry and have found near-perfect agreement between measurements taken on 3D models and physical measurements (de Moraes et al., 2011; Akhil et al., 2015; Klingenberg, 2015). Virtual biological anthropology has become widely popular and used, as it provides an alternative method of conducting

research (Akhil et al., 2015 and Klingenberg, 2015). Micro-focus X-ray computed tomography (micro-XCT) is now considered the gold standard modality for bone and dental research compared to all other imaging technologies (Olejniczak et al., 2007; Grünheid et al., 2014; Andronowski et al., 2018). Micro-XCT imaging not only provides very high-resolution images but is also non-destructive and non-invasive in nature (Suwa and Kono, 2005; Marciano et al., 2012). Micro-XCT is highly effective in providing detailed images which can assist in assessing facial asymmetry and providing an accurate and a more precise way to take facial measurements (Akhil et al., 2015). In order to take facial measurements and assess biological shape on 3D models, anatomical landmarks have to be placed manually or automatically and were found to be highly accurate (Cavalcanti et al., 2004; Gribel et al., 2011; Schlager, 2013).

Geometric morphometric methods (GMM) have shown to be useful in the assessment of fluctuating asymmetry (Benítez et al., 2020). This method is highly beneficial as it can detect subtle asymmetrical shape differences. Furthermore, it is a more precise approach with low measurement error (ME) when using anatomical landmarks (Benítez et al., 2020). Unlike physical and 3D measurements that have been employed to study fluctuating asymmetry, shape analysis is highly sensitive to genetic and environmental stressors that influence asymmetry and provides a more complex and detailed way of examining fluctuating asymmetry (Benítez et al., 2020).

Consequently, this study aimed to assess craniofacial asymmetry in a South African population using craniometric landmarks collected on micro-XCT scans, in order to provide in-depth information on both size and shape asymmetrical. Standard anatomical landmarks were placed to obtain inter-landmark distances and perform shape analysis using the 3D coordinate data. The presence of craniofacial asymmetry from inter-landmark distances and shape analysis were assessed. Finally, the presence and magnitude of asymmetry between populations and sexes will be explored.

4.3. Materials and Methods

4.3.1. Sample size and collection

The sample consisted of micro-XCT scans of 115 crania from individuals sourced from the Pretoria Bone Collection (PBC), housed in the Department of Anatomy, University of Pretoria, South Africa (see Table 4.1). The PBC is a collection of modern South African individuals born between 1863 and 1996 and is a good indicator of modern variation seen amongst the South African populations (L'Abbé et al., 2005; L'Abbé et al., 2021). The collection is comprised of cadavers with known sex and population affinity that were unclaimed or donated to the University of Pretoria medical school (L'Abbé et al., 2005; Krüger et al., 2015; Liebenberg et al., 2019; L'Abbé et al.,2021).

Only adults were included in this study (mean age: 53 ± 16 years); however, the effects of age on asymmetry were not further investigated as it was beyond the scope of this study. Only well-preserved skulls were selected, with absence of trauma, bone alterations or metal restorations that affected scanning or the ability to collect measurements accurately. Ethical approval to conduct this research was obtained by the University of Pretoria Ethical committee (Ethical Number: 386/2021).

Table 4.1 - *Study sample distribution*

	black South Africans	white South Africans	Total
Females	30	27	57
Males	29	29	58
Total	59	56	115

4.3.2. Methods

Firstly, the micro-XCT scans had to be segmented (i.e., virtual extraction of the region of interest) using the semi-automatic watershed method available in Avizo 2019 (ThermoFisher Scientific Inc.), a 3D imaging software. The segmentation allows the generation of accurate 3D models that can be used in the subsequent analysing steps. All the 3D models were re-oriented and aligned according to a similar reference plane: the Frankfort plane. The orientation was performed by placing four anatomical standard landmarks: the right and left porion, and the right and left orbitale. Once all crania were in a standard position, 34 craniometric landmarks were manually placed (see Table 4.2 for definitions and Figure 4.1). Asymmetry was evaluated from the

landmarks by calculating inter-landmark distances,(refer to Table 4.3 for details on the inter-landmark distances) but also by analysing shapes using geometric morphometric methods.

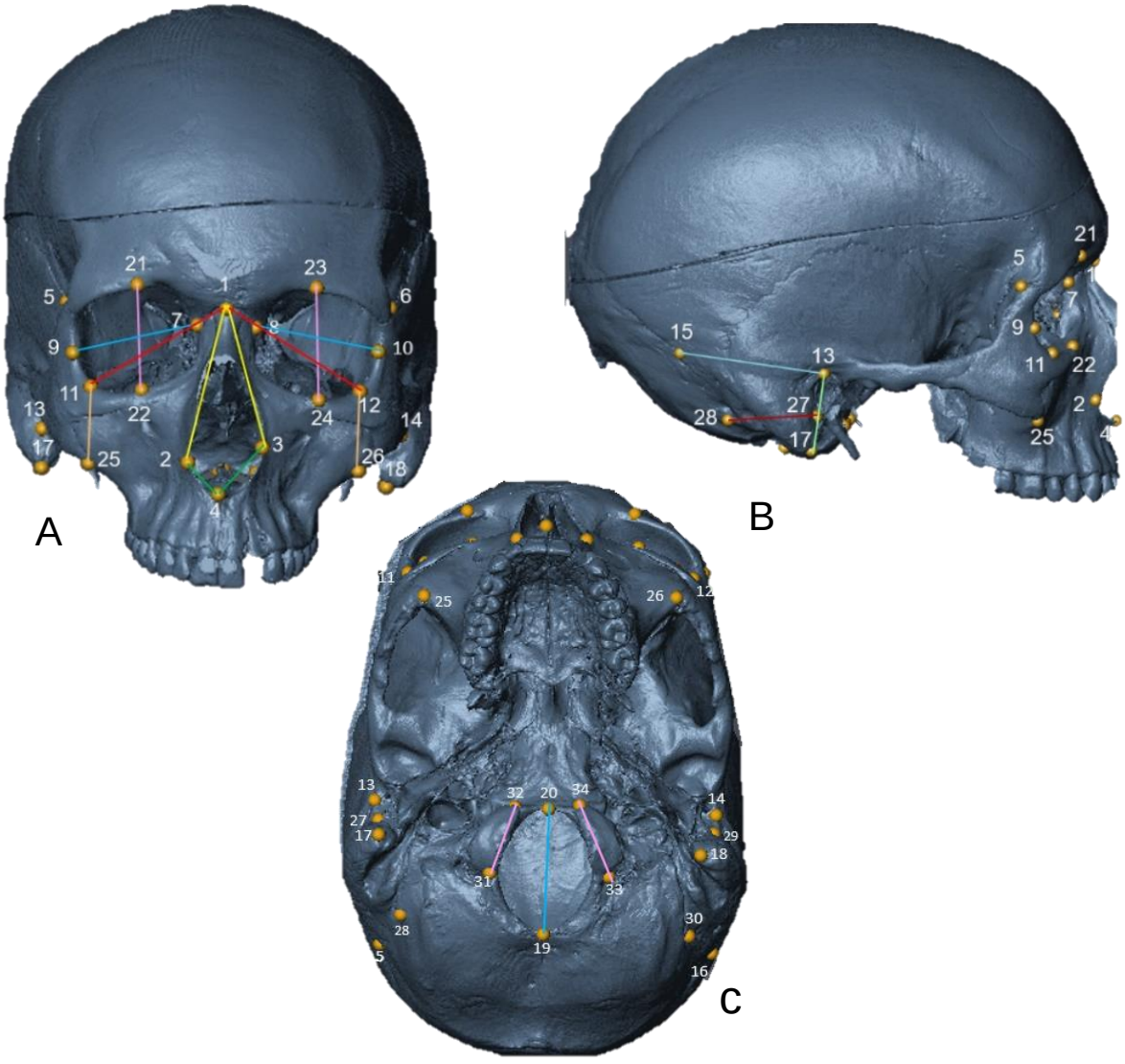

Figure 4.1 *- Landmarks (1 – 34) placed on the cranium (cf.Table 4.2). A: Frontal view; B: Lateral view; C: Inferior view*

Table 4.2 *- Craniometric landmarks placed on each cranium (adapted from Caple and Stephan, 2016; Langley et al., 2016; Ridel, 2019)*

Nr.	Name		Abr.	Definition
1	Nasion	Midline	N	Located on the frontal bone, at the intersection of the nasal bone and frontal bone.
2, 3	Alare	Bilateral	Al	Most lateral points on the nasal aperture.
4	Nasospinale	Midline	Ns	Located at the midpoint of a line connecting the lowest points of the inferior margin of the nasal aperture.
5,6	Frontomalaretemporale	Bilateral	Fmt	Most laterally positioned point on the frontomalare suture.
7,8	Dacryon	Bilateral	D	Intersection of the lacrimomaxillary suture and the frontal bone. If the suture cannot be seen, it is aligned with lacrimal fossa.
9,10	Ectoconchion	Bilateral	Ec	Located on the lateral margin of the orbits such that when a straight line is drawn from dacryon to the lateral margin, the line runs parallel to the supraorbital margin and bisects the orbit into two.
11,12	Orbitale	Bilateral	Or	Most inferior point on the lower orbital rim.
13,14	Porion	Bilateral	Po	Located at the most superior point along the upper margin of the external acoustic meatus.
15,16	Asterion	Bilateral	Ast	Located on the occipital bone where sutures intersect, between temporal, occipital, and parietal bones.
17,18	Mastoidale	Bilateral	Ms	Most inferior point on the tip of the mastoid process.
19	Opisthion	Midline	O	Most inferior point at the posterior margin of the foramen magnum, on the midsagittal plane.
20	Basion	Midline	Ba	Located at the midpoint of the ridge forming the anterior border of foramen magnum.
21,23	Superior Orbital	Bilateral	So	Located on the superior orbital margin perpendicular to orbital breadth
22,24	Inferior Orbital	Bilateral	Io	Located on the inferior orbital margin perpendicular to orbital breadth
25,26	Zygomatic	Bilateral	Z	Located superiorly on the Inferior border of the zygoma
27,29	Posterior External Meatus	Bilateral	Pem	Located on the posterior border of the of the external meatus
28,30	Posterior Mastoid	Bilateral	Pm	Located on the most anterior point on the Posterior margin of the mastoid
31,33	Posterior Occipital Condyle	Bilateral	Poc	Located on the most posterior point on the occipital condyle
32,34	Anterior Occipital Condyle	Bilateral	Aoc	Located on the most anterior point on the occipital condyle

Table 4.3 *- Inter-landmark distances calculated from the craniometric landmarks (adapted from Hagg et al., 2017). Refer to Table 2 for landmark definitions*

Nr.	Name:	Abr.	Definition:
1	Orbital breadth	OBB	Lateral distance from the dacryon (D) to ectoconchion (Ec).
	Orbital height	OBH	Direct distance between the superior (So) and inferior (I0) orbital margins perpendicular to the orbital breadth.
3	Diagonal orbital breadth	NOR	Direct distance from nasion (N) to the orbitale (Or).
4	Frontomalare-nasion length	FMTN	Direct distance from the frontomalare (Fmt) to nasion (N).
5	Frontomalare-nasospinale	FMTNS	Direct distance from frontomalare (Fmt) to nasospinale (Ns).
6	Malar height	MAH	Least distance from the most inferior point on the lower border of the orbit (Or) to the most superior point on the inferior border of the zygomatic.
7	Mastoid length	MPL	Direct distance from porion (Po) to mastoidale (Ms).
8	Mastoid breadth	MPB	Direct distance from the posterior border of the external auditory meatus (Pem) to the most anterior point along the posterior margin of the mastoid process (Pm).
9	Mastoidale-asterion	MSAST	Direct distance from mastoidale (Ms) to asterion (Ast).
10	Occipital condyle length	OCL	Maximum distance from the most anterior (Aoc) to the most posterior (Poc) point on the occipital condyles.
11	Opisthion-porion length	OPO	Direct distance from the opisthion (O) to porion (Po).
12	Basion-porion length	BAPO	Direct distance from basion (Ba) to porion (Po).
13	Nasion-mastoidale	NMS	Direct distance from nasion (N) to mastoidale (Ms).
14	Nasion-alare	NAL	Direct distance from nasion (N) to alare (Al)
15	Nasospinale-alare	NAAL	Direct distance from nasospinale (Ns) to alare (Al)

Finally, fluctuating asymmetry (FA) values (left-side measurement minus right-side measurement) were calculated for each individual. Since fluctuating indices can increase with trait size, a standardised scale needed to be used to assess asymmetry, allowing for an accurate comparison between traits with different magnitudes. Standard asymmetry formulae developed by Palmer and Strobeck (2003) were thus used. Average FA values were calculated for each trait for each individual and for a combination of traits (Hagg et al., 2017; Palmer and Strobeck, 2002) (refer to Table 4.4 for formula and definition of FA indices).

Table 4.4 *- Formulae of the indices used to evaluate asymmetry (Adapted from Hagg et al., 2017 and Palmer and Strobeck , 2003)*

Index	Formula	Description
FA8	$FA8 = \left\lvert \ln(R_d/L_d) \right\rvert$	The difference between the natural logs of the left and right measurements of a trait, in absolute values.
FA17	$FA\ 17 = \sum \left\lvert \ln(R_d/L_d) \right\rvert / T$	Average FA values computed from the FA8 values for multiple traits and combinations.

The FA8 Index is univariate and assesses asymmetry per inter-landmark distance, while the FA17 index is a multivariate combination of all FA8 indices. Essentially, FA8 provides information on specific regions of the cranium, while FA17 provides an overall picture of asymmetry within and among individuals. Subgroups were created from the FA8 indices for each cranial inter-landmark distance, and for FA17 to represent specific cranial regions (e.g., orbital, nasal etc.; see Table 4.5 for more information on which measurements were employed to calculate all FA17 indices).

Table 4.5 *- Definitions of all FA17 matrices*

Matrices	Abr.	Definition
FA17		Average of all FA8 values
FA17_Orbital	FA17_Orbs	Average of FA8_OBB, FA8_OBH and FA8_NOR
FA17_Face	FA17_Fac	Average of FA8_FMTN, FA8_FMTNS, FA8_MAH ,FA8_NAL, and FA8_NAAL
FA17_Temporal	FA17_Temp	Average of FA8_MPL, FA8_MPB,FA8_MSAST and FA8_NMS
FA17_Base	FA17_Bas	Average of FA8_OCL, FA8_OPO and FA8_BAPO

4.3.3. Statistical analysis

All statistical analyses were conducted in the R software and R studio environment (R Core Team, 2018; Trochim, 2020) . Repeatability testing was performed to assess the reproducibility of the landmark positioning. This was done by placing the landmarks on 15 randomly selected scans and calculating intra- and inter-observer agreement. For the intra-observer repeatability, the landmark placement was performed twice by the same observer with an interval of two weeks. For the inter-observer agreement, an additional observer performed the landmark placement. The reproducibility of the landmark positioning was calculated using the dispersion Δ_{ij} for each landmark *i* and individual *j*. Dispersion is defined as the Mean Euclidean Distance (MED) of the sample landmark $\boldsymbol{p}_{ijk}$ to the mean $\overline{\boldsymbol{p}}_{ij}$of the (x, y, z)-coordinates of landmark *i* over all observation's *k* (inter, intra, resp.) for subject *j (Formula 4.1)*:

Formula 4.1

$$\Delta_{ij} = \sum_{k=1}^{K} \left\| \boldsymbol{p}_{ijk} - \overline{\boldsymbol{p}}_{ij} \right\| / K \text{ , with } \overline{\boldsymbol{p}}_{ij} = \sum_{k=1}^{K} \boldsymbol{p}_{ijk} / K$$

Plots of MED values were generated to show the variation of dispersion over different subjects. Global precision is reported as the global (averaged over all landmarks) mean (μ_{Δ}) and median (m_{Δ}) of the per landmark mean ($\mu_{\Delta i}$) and median ($m_{\Delta i}$) values (over all subjects).

Descriptive statistics were calculated to summarise and describe the main features of the dataset for asymmetrical linear distances and FA values (Trochim, 2020). Normality testing was conducted using Shapiro-Wilks tests on the inter-landmark distances and on the FA indices. From these results, non-parametric Wilcoxon tests were chosen and performed between each corresponding left and right distances (e.g., left, and right OBH) to evaluate asymmetry. Asymmetrical differences between demographic profiles were further investigated for the inter-landmark distances, as well as for FA8 and FA17, using Wilcoxon and Kruskal-Wallis tests.

Lastly, GMM analyses were conducted to assess asymmetrical shape variation in matrices and demographic profiles. GMM matrices, were divided into two groups:

landmarks grouped together into the orbital, temporal, midface, and base region without midline landmarks and landmarks grouped together into nasion, midface, face, opisthion and base including midline landmarks. Preliminary statistical testing was first needed. A Generalised Procrustes Analysis (GPA) was performed on the raw Cartesian coordinate data of the landmarks to obtain orientation-invariant shape coordinates (Dryden and Mardia, 2016). A Principal Component Analysis (PCA) was then conducted to alter the data to form a new coordinate system and identify the greatest variance between sex and population groups of data lying on the first and second Principal Component (PC) and produce PC scores (Ridel et al., 2018; Schlager, 2013). Multivariate normality testing was then performed for the PC score distribution by rendering Q-Q plots, showing a multivariate normal distribution (Schlager, 2013; Ridel et al., 2020b). Procrustes two-way, mixed model Analysis of Variances (ANOVAs) were then used to statistically evaluate fluctuating asymmetry (individuals (I) x sides (S) interaction) and its correlation to sex and sex/population using the R Geomorph package. Individuals (I), consist of a random sample of individuals from the entire study sample while, sides (S) are a fixed effect that consist of two levels (left and right). An individual by side interaction (I x S), is a mixed effect and provides information on an individual's failure to be the same from side-to-side denoting fluctuating asymmetry (Ducos and Tabugo, 2015). Statistical methods for both object and matching symmetry were implemented (Klingenberg et al., 2002; Mardia et al., 2000) as defined by the Geomorph package for the assessment of fluctuating asymmetry. Object symmetry refers to corresponding landmarks with a common landmark located on the midline. While matching symmetry refers to corresponding landmarks that are mirrored on the left and right sides but does not include a common landmark on the midline. P-values were then obtained for each trait and for sex and sex/population affinity per trait to observe if fluctuating asymmetry was present in traits and its influence on sex and sex/population affinity.

4.4. Results

4.4.1. Repeatability testing

Observer repeatability for craniometric landmark positioning was tested to ensure accurate results. For intra-observer error, the mean dispersion values ranged between 0.28mm (SD ± 0.13) to 1.43mm (SD ± 1.87); while for inter-observer error, the mean value ranged between 0.36mm (SD ± 0.18) to 5.04mm (SD ± 2.86). Mean results of intra- and inter-observer measurement error of craniometric landmark positioning are summarised in Table 4.6. Overall, lower mean values were obtained for intra-observer compared to inter-observer mean values.

Table 4.6 *- Mean dispersion errors (mm) of craniometric landmark placement from 15 crania*

Observations	Intra-observer error		Inter-observer error	
	Mean	**SD**	**Mean**	**SD**
	0.700	0.530	1.300	0.840

Figure 4.2 graphically presents the comparison between mean values for intra- and inter-observer error for craniometric landmark placement on the 15 crania. With regards to intra-observer repeatability, all craniometric landmarks presented with a measurement error of less than 2mm, showing high intra-observer reproducibility. For inter-observer repeatability, majority of the craniometric landmarks presented with a measurement error of less than 2mm, while three landmarks, the right inferior orbital margin (22), and the right and left landmarks on the posterior margin of the mastoid (28, 30) fell above 2mm. However, due to limited discrepancies with the intra-observer dispersion, the was considered acceptable and retained. Therefore, any asymmetrical differences noted I this region is assumed to be due to true asymmetry rather than measurement error. The right inferior orbital margin landmark yielded an inter-observer error of 2.2mm, while the right and left landmark on the posterior margin of the mastoid yielded an inter-observer error of 5.04mm and 4.63mm, respectively. Overall, the repeatability testing showed high agreement for most of the craniometric landmarks.

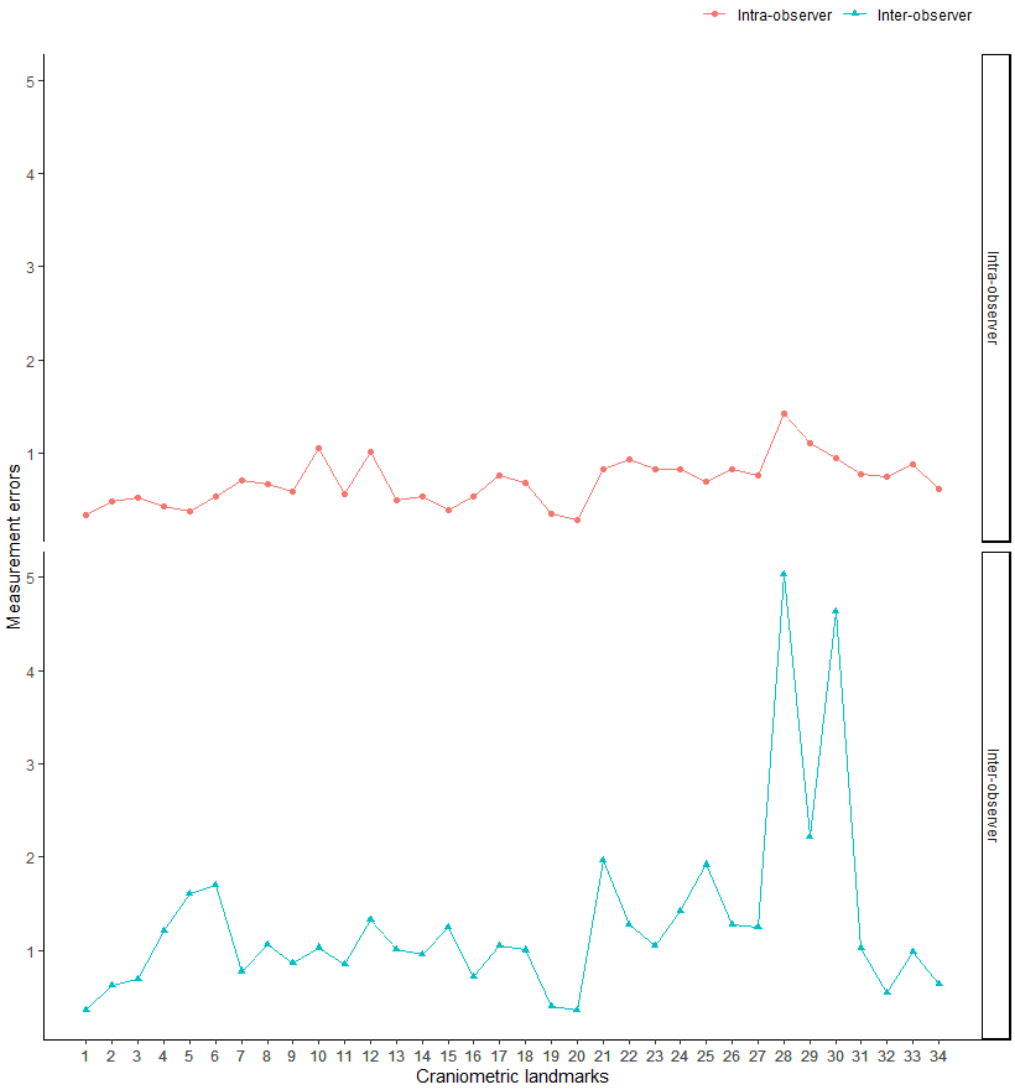

Figure 4.2 *- Graphical representation of the intra- and inter-observer mean dispersion values for landmark positioning*

4.4.2. Size Variation: Inter-landmark distances

Inter-landmark distances were used to quantify size variation of the craniofacial skeleton and the left and right sides were compared to explore differences attributable to sex and population variation. Mean values were calculated for the left and right inter-landmark distances (see Table 4.7 for descriptive statistics). For both sex and population, the means for the left and right sides were similar for most traits, with some

exceptions. More specifically, when comparing mean left vs. right traits, the OBB, NOR, FMTN, FMTNS, MPL, MSAST, OCL, OPO, BAPO, NMS, NAL and NAAL showed differences between males and females. Similarly, when comparing mean values for black and white South Africans (with the sexes pooled), left vs. right differences were noted for OBH, FMTN, MSAST, OCL, OPO, BAPO and NAL. These results provide information on the mean values for each left and right inter-landmark distances that described where the greatest variation lied, so asymmetry could be better quantified within the sample.

Table 4.7 *- Descriptive statistics for left and right inter-landmark distances per sex (F: females, M: males) and population (B: black, W: white). Refer to Table 4.3 for measurement definitions*

	Sex		Population		
	F (N=57)	**M (N=58)**	**B (N=59)**	**W (N=56)**	**Total (N=115)**
OBB_r					
Mean (SD)	42.909 (1.761)	44.320 (2.761)	43.737 (2.438)	43.497 (2.408)	43.621 (2.416)
Range (min-max)	39.899 - 46.109	39.715 - 50.393	39.715 - 49.552	40.008 - 50.393	39.715 - 50.393
OBB_l					
Mean (SD)	42.611 (1.897)	43.744 (2.627)	43.350 (2.509)	43.006 (2.187)	43.183 (2.354)
Range (min-max)	38.682 - 47.091	38.141 - 49.191	38.141 - 49.191	39.334 - 48.598	38.141 - 49.191
OBH_r					
Mean (SD)	36.498 (2.183)	36.265 (2.409)	36.047 (2.287)	36.733 (2.265)	36.381 (2.292)
Range (min-max)	31.204 - 41.452	29.504 - 41.751	29.504 - 40.308	33.113 - 41.751	29.504 - 41.751
OBH_l					
Mean (SD)	36.085 (2.078)	36.439 (2.292)	35.697 (2.292)	36.861 (1.912)	36.264 (2.186)
Range (min-max)	31.480 - 39.992	29.965 - 43.406	29.965 - 43.406	32.523 - 42.536	29.965 - 43.406
NOR_r					
Mean (SD)	52.816 (2.500)	55.281 (2.766)	54.250 (2.415)	53.858 (3.353)	54.059 (2.903)
Range (min-max)	48.018 - 57.989	50.347 - 62.657	48.018 - 58.842	48.726 - 62.657	48.018 - 62.657
NOR_l					
Mean (SD)	53.466 (2.483)	55.556 (2.731)	54.639 (2.646)	54.395 (2.979)	54.520 (2.803)
Range (min-max)	46.790 - 59.137	49.834 - 61.143	46.790 - 60.511	48.415 - 61.143	46.790 - 61.143
FMTN_r					
Mean (SD)	55.960 (2.205)	58.279 (3.040)	57.977 (2.831)	56.236 (2.703)	57.129 (2.892)

Range (min-max)	51.312 - 61.088	52.312 - 64.457	52.112 - 64.457	51.312 - 62.703	51.312 - 64.457
FMTN_l					
Mean (SD)	56.331 (2.263)	58.426 (3.131)	58.291 (2.988)	56.437 (2.542)	57.388 (2.920)
Range (min-max)	49.797 - 60.733	51.241 - 65.393	49.797 - 65.393	51.241 - 61.529	49.797 - 65.393
FMTNS_r					
Mean (SD)	74.424 (2.943)	77.704 (4.092)	75.837 (4.142)	76.333 (3.684)	76.078 (3.916)
Range (min-max)	69.053 - 81.719	64.626 - 85.105	64.626 - 85.105	69.428 - 84.654	64.626 - 85.105
FMTNS_l					
Mean (SD)	74.650 (3.067)	77.994 (3.819)	76.357 (3.889)	76.315 (3.819)	76.337 (3.838)
Range (min-max)	67.734 - 81.623	68.955 - 86.083	68.955 - 86.083	67.734 - 83.312	67.734 - 86.083
MAH_r					
Mean (SD)	21.234 (9.252)	22.139 (3.325)	22.014 (3.226)	21.349 (9.373)	21.690 (6.913)
Range (min-max)	15.933 - 87.339	14.812 - 30.593	15.967 - 30.593	14.812 - 87.339	14.812 - 87.339
MAH_l					
Mean (SD)	20.910 (9.167)	22.192 (3.087)	21.664 (3.168)	21.443 (9.257)	21.556 (6.816)
Range (min-max)	14.295 - 86.804	15.920 - 31.061	14.295 - 31.061	15.920 - 86.804	14.295 - 86.804
MPL_r					
Mean (SD)	30.252 (2.848)	33.079 (3.453)	31.229 (3.656)	32.151 (3.202)	31.678 (3.459)
Range (min-max)	20.917 - 35.992	25.550 - 40.526	20.917 - 38.857	26.322 - 40.526	20.917 - 40.526
MPL_l					
Mean (SD)	30.213 (3.048)	33.441 (3.468)	31.429 (3.902)	32.276 (3.307)	31.841 (3.634)
Range (min-max)	22.441 - 38.978	24.745 - 41.957	22.441 - 40.724	27.075 - 41.957	22.441 - 41.957
MPB_r					
Mean (SD)	31.489 (3.418)	33.610 (5.594)	32.931 (5.314)	32.166 (4.073)	32.559 (4.745)
Range (min-max)	20.953 - 38.538	23.300 - 50.112	24.883 - 50.112	20.953 - 39.591	20.953 - 50.112

MPB_l					
Mean (SD)	31.522 (3.451)	33.119 (5.034)	32.630 (3.968)	32.008 (4.788)	32.327 (4.378)
Range (min-max)	23.761 - 38.183	24.160 - 45.073	25.136 - 42.984	23.761 - 45.073	23.761 - 45.073
MSAST_r					
Mean (SD)	50.655 (5.314)	55.342 (6.099)	52.054 (5.467)	54.036 (6.725)	53.019 (6.166)
Range (min-max)	41.557 - 63.689	42.022 - 77.131	41.744 - 71.861	41.557 - 77.131	41.557 - 77.131
MSAST_l					
Mean (SD)	50.024 (4.977)	55.617 (5.903)	50.939 (5.212)	54.852 (6.406)	52.845 (6.122)
Range (min-max)	42.951 - 66.155	43.408 - 74.469	42.951 - 64.866	44.186 - 74.469	42.951 - 74.469
OCL_r					
Mean (SD)	21.087 (2.404)	22.478 (2.647)	20.667 (2.175)	22.971 (2.529)	21.789 (2.613)
Range (min-max)	16.086 - 29.934	17.621 - 29.328	16.086 - 29.328	17.621 - 29.934	16.086 - 29.934
OCL_l					
Mean (SD)	21.598 (2.821)	22.577 (2.848)	20.985 (2.337)	23.257 (2.924)	22.092 (2.864)
Range (min-max)	16.336 - 30.195	17.032 - 30.388	16.336 - 27.571	17.032 - 30.388	16.336 - 30.388
OPO_r					
Mean (SD)	72.971 (3.374)	76.827 (3.312)	73.623 (3.647)	76.277 (3.609)	74.916 (3.850)
Range (min-max)	64.768 - 80.660	69.880 - 85.319	64.768 - 80.067	70.091 - 85.319	64.768 - 85.319
OPO_l					
Mean (SD)	72.971 (2.964)	76.534 (3.470)	73.595 (3.371)	76.003 (3.612)	74.768 (3.679)
Range (min-max)	64.999 - 80.597	70.469 - 84.497	64.999 - 80.639	70.012 - 84.497	64.999 - 84.497
BAPO_r					
Mean (SD)	60.113 (3.008)	63.858 (3.252)	60.755 (3.145)	63.315 (3.695)	62.002 (3.643)
Range (min-max)	53.604 - 66.646	57.775 - 71.508	53.604 - 67.903	54.627 - 71.508	53.604 - 71.508
BAPO_l					

Mean (SD)	60.803 (2.909)	63.853 (3.179)	61.363 (3.382)	63.371 (3.127)	62.341 (3.399)
Range (min-max)	53.644 - 68.858	57.113 - 70.647	53.644 - 69.758	57.845 - 70.647	53.644 - 70.647
NMS_r					
Mean (SD)	121.325 (4.897)	127.727 (6.114)	124.196 (6.404)	124.931 (6.406)	124.554 (6.388)
Range (min-max)	110.810 - 131.237	115.691 - 144.131	113.902 - 139.498	110.810 - 144.131	110.810 - 144.131
NMS_l					
Mean (SD)	120.892 (4.923)	128.238 (5.652)	123.930 (6.359)	125.299 (6.509)	124.597 (6.441)
Range (min-max)	111.208 - 133.124	111.517 - 143.133	111.208 - 136.077	112.642 - 143.133	111.208 - 143.133
NAL_r					
Mean (SD)	43.446 (3.481)	46.257 (3.949)	43.441 (3.735)	46.362 (3.670)	44.863 (3.968)
Range (min-max)	37.312 - 51.210	36.069 - 54.401	36.069 - 52.246	38.132 - 54.401	36.069 - 54.401
NAL_l					
Mean (SD)	43.182 (3.321)	45.341 (4.049)	42.790 (3.592)	45.831 (3.496)	44.271 (3.846)
Range (min-max)	36.708 - 52.061	33.872 - 52.141	33.872 - 52.141	37.482 - 52.061	33.872 - 52.141
NAAL_r					
Mean (SD)	16.837 (1.892)	17.727 (1.881)	17.349 (1.956)	17.219 (1.919)	17.286 (1.931)
Range (min-max)	13.537 - 21.260	12.827 - 22.299	12.827 - 22.299	13.537 - 21.260	12.827 - 22.299
NAAL_l					
Mean (SD)	16.616 (1.920)	18.000 (1.850)	17.470 (1.899)	17.149 (2.109)	17.314 (2.001)
Range (min-max)	11.770 - 20.130	12.931 - 21.478	12.931 - 21.478	11.770 - 21.070	11.770 - 21.478

After normality testing (refer to Figure A1-A3), Wilcoxon tests were performed on all cranial inter-landmark distances to test for asymmetry (between the left and right sides) in the entire sample with all the groups pooled, and in subgroups according to sex and population, respectively. Table 4.8 outlines the results for the asymmetrical differences observed in cranial inter-landmark distances. Significant statistical left vs. right differences were observed for OBB (p=0.002), NOR (p=0.001) and NAL (p<0.001), which are variables pertaining to the orbital and nasal regions. When comparing the left and right distances of males and females, slightly different patterns were observed (refer to Table 4.9 and Figure 4.3). Similar to the pooled sample, males displayed significant statistical asymmetrical differences only for OBB (p=0.011) and NAL (p<0.001). Conversely, for females, statistically significant asymmetrical differences were detected for four distances: OBH (p=0.025), NOR (p=0.001), FMTN (p=0.043) and BAPO (p=0.029). While these variables pertain largely to the nasal and orbital regions, they include other inter-landmark distances than those reported for the pooled sample.

Table 4.8 *- Wilcoxon tests comparing left and right bilateral distances for the pooled sample. Bold indicates statistically significant differences (p<0.05)*

IL distance	p-value
OBB	**0.002**
OBH	0.442
NOR	**0.001**
FMTN	0.071
FMTNS	0.144
MAH	0.343
MPL	0.367
MPB	0.981
MSAST	0.444
OCL	0.146
OPO	0.630
BAPO	0.090
NMS	0.724
NAL	**<0.001**
NAAL	0.917

Table 4.9 *- Wilcoxon tests comparing left and right bilateral distances for sex (F: females, M: males), population (B: black, W: white), and sex and population simultaneously (BF: black females, BM: black males, WF: white females; WM: white males). Bold indicates statistically significant differences (p<0.05)*

	Sex		**Population**		**Sex/population**			
	F	M	B	W	BF	BM	WF	WM
IL distance	**p-value**	**p-value**	**p-value**	**p-value**	**p-value**	**p-value**	**p-value**	**p-value**
OBB	0.0812	**0.011**	**0.048**	**0.027**	0.262	0.096	0.201	0.062
OBH	**0.025**	0.204	**0.032**	0.2908	**0.001**	0.782	0.859	0.132
NOR	**0.001**	0.180	**0.016**	**0.019**	0.080	0.137	**0.004**	0.639
FMTN	**0.043**	0.506	0.119	0.306	0.070	0.733	0.361	0.594
FMTNS	0.427	0.196	**0.007**	0.716	**0.029**	0.101	0.413	0.815
MAH	0.047	0.593	0.128	0.835	**0.033**	0.949	0.500	0.417
MPL	0.994	0.196	0.600	0.446	1.000	0.417	0.972	0.256
MPB	0.849	0.926	0.616	0.633	0.245	0.624	0.148	0.522
MSAST	0.157	0.804	**0.011**	0.185	**0.043**	0.101	0.934	0.063
OCL	0.095	0.687	0.217	0.390	0.280	0.442	0.155	0.815
OPO	0.849	0.322	0.824	0.554	0.777	0.468	0.915	0.417
BAPO	**0.029**	0.822	**0.022**	0.867	0.177	**0.041**	0.069	0.284
NMS	0.263	0.099	0.584	0.318	0.440	0.915	0.427	**0.027**
NAL	0.129	**<0.001**	**0.003**	**0.010**	0.229	**0.003**	0.279	**0.012**
NAAL	0.305	0.289	0.4572	0.549	0.903	0.304	0.194	0.733

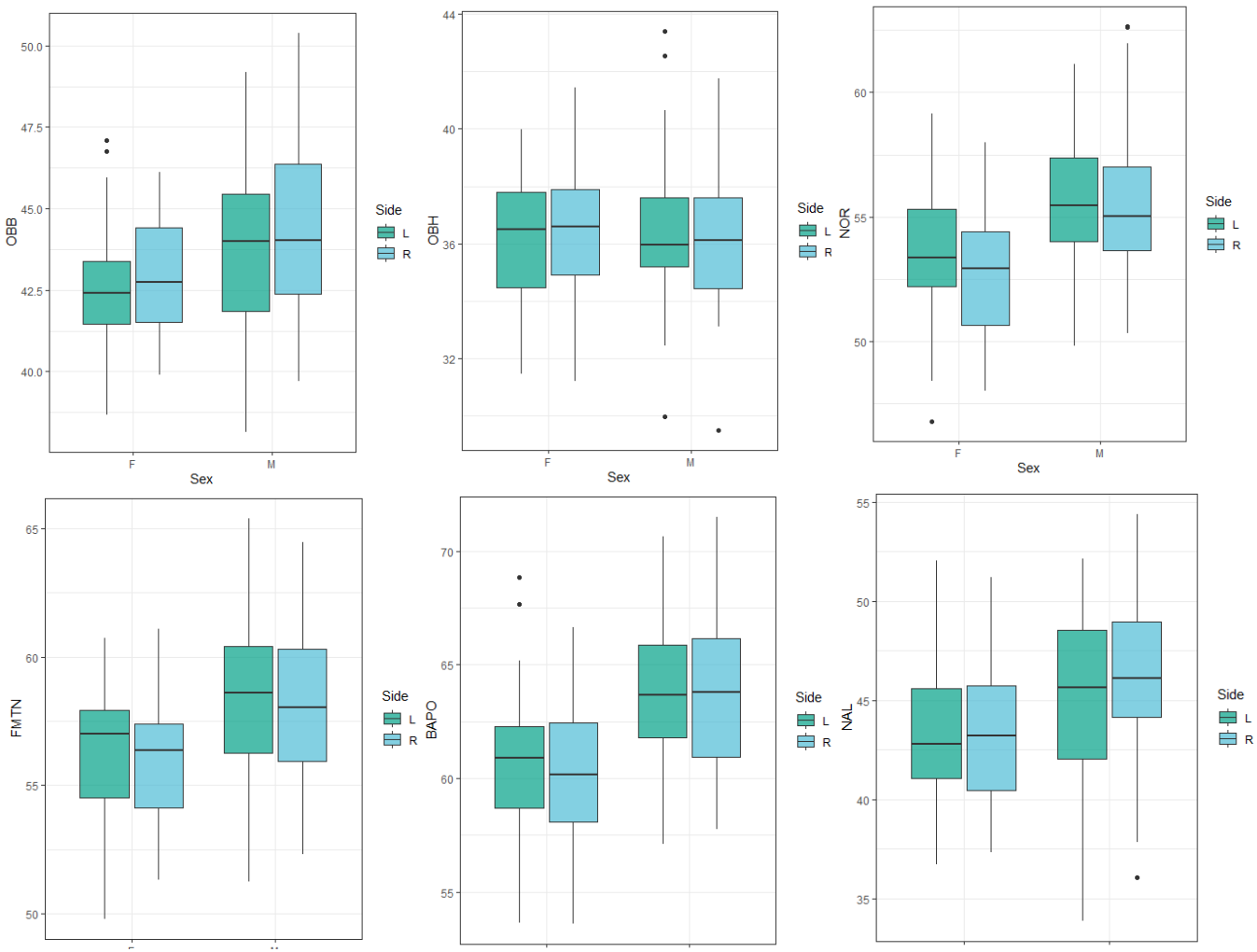

Figure 4.3 *- Boxplots illustrating the asymmetry in females (F) and males (M), for the statistically significant inter-landmark distances (p<0.05)*

Regarding population affinity, both black and white South Africans demonstrated similar results, where statistically significant asymmetry was detected for OBB, OBH, NOR, FMTNS, MSAST, BAPO and NAL ($p<0.05$) (Refer to Table 4.9 and Figure 4.4). White South Africans demonstrated significant differences for OBB ($p=0.027$), NOR ($p=0.019$) and NAL ($p=0.010$) (like the pooled sample); while black South Africans displayed significant differences for OBB ($p=0.048$), OBH ($p=0.032$), NOR ($p=0.016$), FMTNS ($p=0.007$), MSAST ($p=0.011$), BAPO ($p=0.022$) and NAL ($p=0.003$), which pertains to other cranial areas in addition to the orbital and nasal regions. However, for OBB, white South Africans only showed a greater asymmetrical variation ($p=0.027$) when directly compared to black South Africans ($p=0.048$). Lastly, black South Africans expressed overall greater asymmetrical variation in the six inter-landmark distances compared to white South Africans.

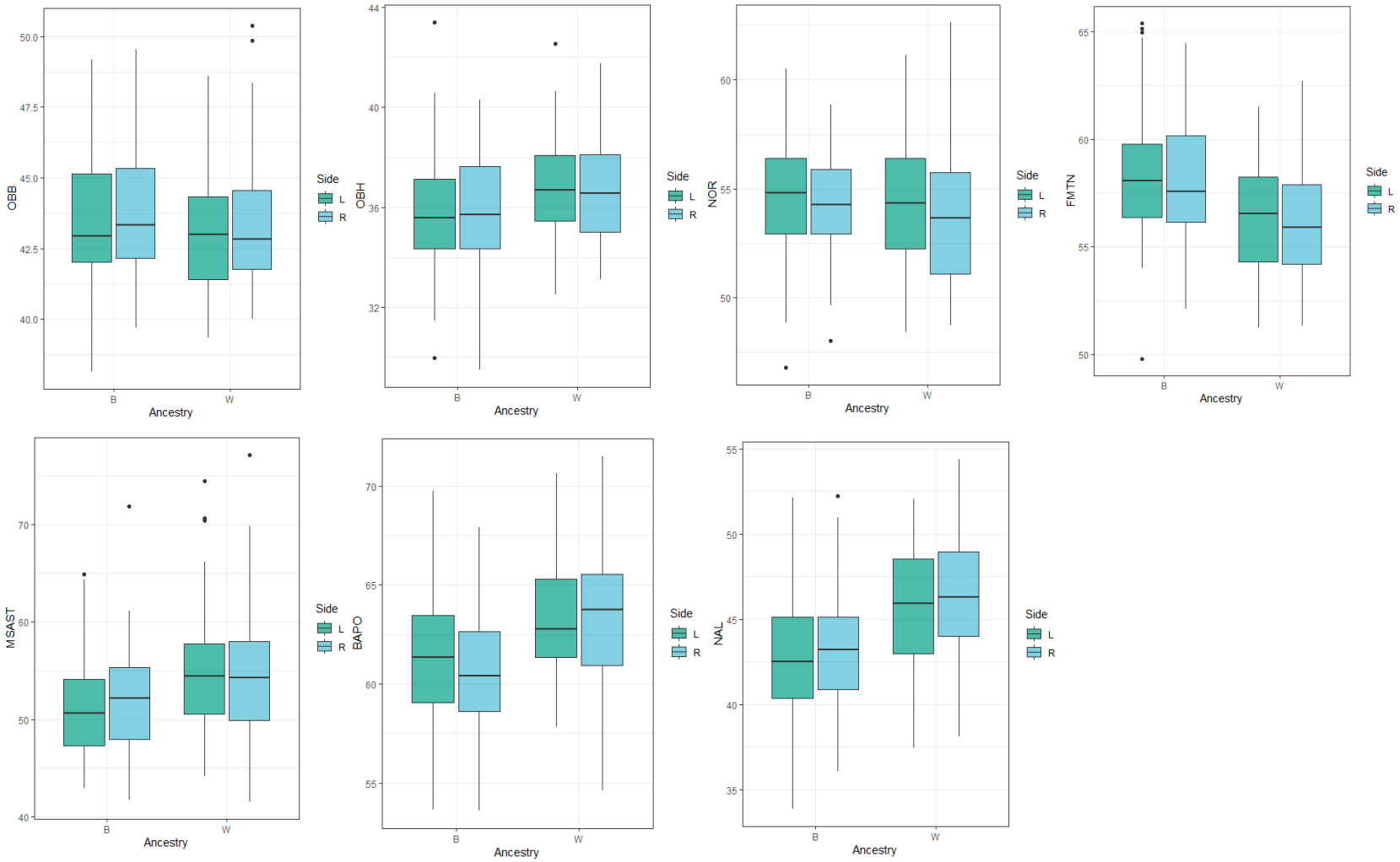

Figure 4.4 *- Boxplots illustrating the asymmetry in black (B) and white (W) South Africans for the statistically significant inter-landmark distances (p<0.05)*

When assessing each sex and population subgroup simultaneously, significant asymmetrical differences were noted for OBH, NOR, FMTNS, MAH, MSAST, BAPO, NMS and NAL ($p<0.05$) (refer to Table 4.9 and Figure 4.5 for more information). Most notably, black South African females demonstrated statistically significant differences for the following four inter-landmark distances: OBH ($p=0.01$), FMTNS ($p=0.029$), MAH ($p=0.033$), and MSAST ($p=0.043$). Overall, black South African females showed greater asymmetrical variation among all subgroups.

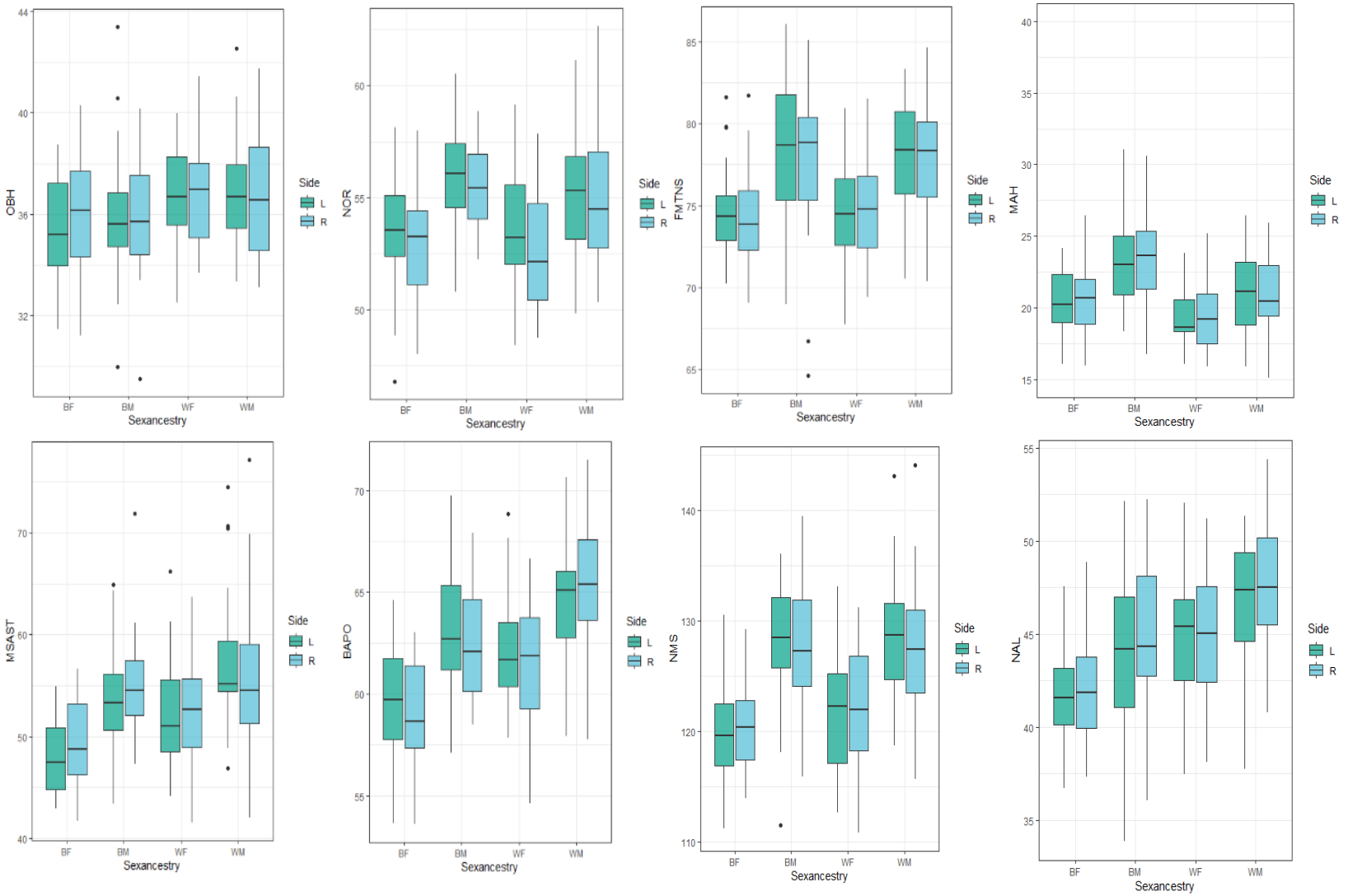

Figure 4.5 *- Boxplots illustrating the asymmetry in sex/population subgroups (BF: black females, BM: black males, WF: white females, and WM: white males) for the statistically significant inter-landmark distances (p<0.05)*

4.4.3. Indices of fluctuating asymmetry

From the inter-landmark distances, two types of indices were calculated: FA8 and FA17. Mean values of FA8 and FA17 indices were calculated (descriptive statistics available in Tables 4.10 and 4.11). The mean asymmetry per individual for South African males and females were alike in magnitude for all FA8 indices. In other words, no inter-landmark distances, or indices showed differences between the sexes. However, when assessing FA17 and FA17_Temp (which is the sum of all FA8 temporal traits), asymmetrical differences were noted between males and female

Table 4.10 *- Descriptive statistics for FA8 values per sex and in the entire sample*

Index_IL distance	F (N=57)	M (N=58)	Total (N=115)
FA8_OBB			
Mean (SD)	0.026 (0.019)	0.029 (0.026)	0.027 (0.023)
Range (min-max)	0.001 - 0.074	0.001 - 0.112	0.001 - 0.112
FA8_OBH			
Mean (SD)	0.030 (0.023)	0.027 (0.021)	0.028 (0.022)
Range (min-max)	0.001 - 0.087	0.000 - 0.079	0.000 - 0.087
FA8_NOR			
Mean (SD)	0.024 (0.018)	0.021 (0.016)	0.023 (0.017)
Range (min-max)	0.001 - 0.077	0.000 - 0.073	0.000 - 0.077
FA8_FMTN			
Mean (SD)	0.018 (0.014)	0.022 (0.015)	0.020 (0.015)
Range (min-max)	0.000 - 0.059	0.001 - 0.066	0.000 - 0.066
FA8_FMTNS			
Mean (SD)	0.015 (0.012)	0.017 (0.014)	0.016 (0.013)
Range (min-max)	0.000 - 0.044	0.000 - 0.065	0.000 - 0.065

FA8_MAH			
Mean (SD)	0.056 (0.045)	0.064 (0.054)	0.060 (0.050)
Range (min-max)	0.000 - 0.174	0.004 - 0.234	0.000 - 0.234
FA8_MPL			
Mean (SD)	0.048 (0.035)	0.051 (0.038)	0.049 (0.037)
Range (min-max)	0.001 - 0.142	0.002 - 0.148	0.001 - 0.148
FA8_MPB			
Mean (SD)	0.080 (0.072)	0.112 (0.101)	0.096 (0.089)
Range (min-max)	0.000 - 0.420	0.004 - 0.511	0.000 - 0.511
FA8_MSAST			
Mean (SD)	0.056 (0.054)	0.074 (0.081)	0.065 (0.069)
Range (min-max)	0.001 - 0.319	0.000 - 0.366	0.000 - 0.366
FA8_OCL			
Mean (SD)	0.069 (0.066)	0.075 (0.058)	0.072 (0.062)
Range (min-max)	0.005 - 0.279	0.003 - 0.244	0.003 - 0.279
FA8_OPO			
Mean (SD)	0.023 (0.018)	0.021 (0.016)	0.022 (0.017)
Range (min-max)	0.000 - 0.085	0.000 - 0.067	0.000 - 0.085
FA8_BAPO			

Mean (SD)	0.034 (0.031)	0.028 (0.021)	0.031 (0.026)
Range (min-max)	0.000 - 0.121	0.001 - 0.093	0.000 - 0.121
FA8_NMS			
Mean (SD)	0.017 (0.011)	0.017 (0.013)	0.017 (0.012)
Range (min-max)	0.000 - 0.046	0.001 - 0.054	0.000 - 0.054
FA8_NAL			
Mean (SD)	0.029 (0.019)	0.034 (0.027)	0.032 (0.023)
Range (min-max)	0.000 - 0.082	0.001 - 0.097	0.000 - 0.097
FA8_NAAL			
Mean (SD)	0.061 (0.056)	0.071 (0.060)	0.066 (0.058)
Range (min-max)	0.007 - 0.359	0.001 - 0.345	0.001 - 0.359

Table 4.11 *- Descriptive statistics for FA17 values per sex and in the entire sample*

Index	F (N=57)	M (N=58)	Total (N=115)
FA17			
Mean (SD)	0.039 (0.010)	0.044 (0.013)	0.042 (0.012)
Range (min-max)	0.017 - 0.074	0.023 - 0.073	0.017 - 0.074
FA17_Orbital			
Mean (SD)	0.026 (0.013)	0.026 (0.013)	0.026 (0.013)
Range (min-max)	0.002 - 0.061	0.006 - 0.067	0.002 - 0.067
FA17_Face			
Mean (SD)	0.030 (0.015)	0.034 (0.020)	0.032 (0.018)
Range (min-max)	0.005 - 0.075	0.007 - 0.090	0.005 - 0.090
FA17_Temporal			
Mean (SD)	0.061 (0.035)	0.079 (0.046)	0.070 (0.042)
Range (min-max)	0.007 - 0.229	0.017 - 0.272	0.007 - 0.272
FA17_Base			
Mean (SD)	0.036 (0.019)	0.035 (0.018)	0.035 (0.018)
Range (min-max)	0.007 - 0.094	0.007 - 0.082	0.007 - 0.094

Wilcoxon tests were conducted to assess asymmetrical differences between the sexes and populations groups for fluctuating asymmetry (FA) indices (see Table 4.12 for detailed results). Between the sexes, significant differences were noted for FA17 and FA17_Temp indices ($p < 0.05$). Females demonstrated the highest values for FA17 ($p=0.035$) and FA17_Temp ($p=0.029$) indices compared to males. A visualisation of the asymmetrical differences is provided in Figure 4.6. However, there was no statistically significant differences in and between population groups for FA8 and FA17, as all p-values were higher than 0.05.

Table 4.12 *- Wilcoxon tests on fluctuating asymmetry values based on FA8 and FA17 indices, between sexes and population groups. Bold indicates significance (p<0.05)*

	Sex		Population	
Index_IL distance	**W**	**p-value**	**W**	**p-value**
FA8_OBB	1637	0.931	1382	0.132
FA8_OBH	1750	0.590	1613	0.829
FA8_NOR	1755	0.570	1406	0.170
FA8_FMTN	1353	0.094	1769	0.515
FA8_FMTNS	1493	0.372	1385	0.136
FA8_MAH	1543	0.540	1710	0.748
FA8_MPL	1577	0.673	1522	0.469
FA8_MPB	1339	0.080	1599	0.769
FA8_MSAST	1551	0.570	1478	0.332
FA8_OCL	1494	0.375	1462	0.289
FA8_OPO	1748	0.597	1430	0.215
FA8_BAPO	1682	0.873	1634	0.922
FA8_NMS	1788	0.451	1538	0.525
FA8_NAL	1523	0.468	1790	0.442
FA8_NAAL	1463	0.298	1659	0.971
FA17	1275	**0.035**	1470	0.310
FA17_Orbs	1734	0.653	1399	0.158
FA17_Fac	1466	0.297	1656	0.984
FA17_Temp	1261	**0.029**	1521	0.465
FA17_Bas	1677	0.895	1529	0.493

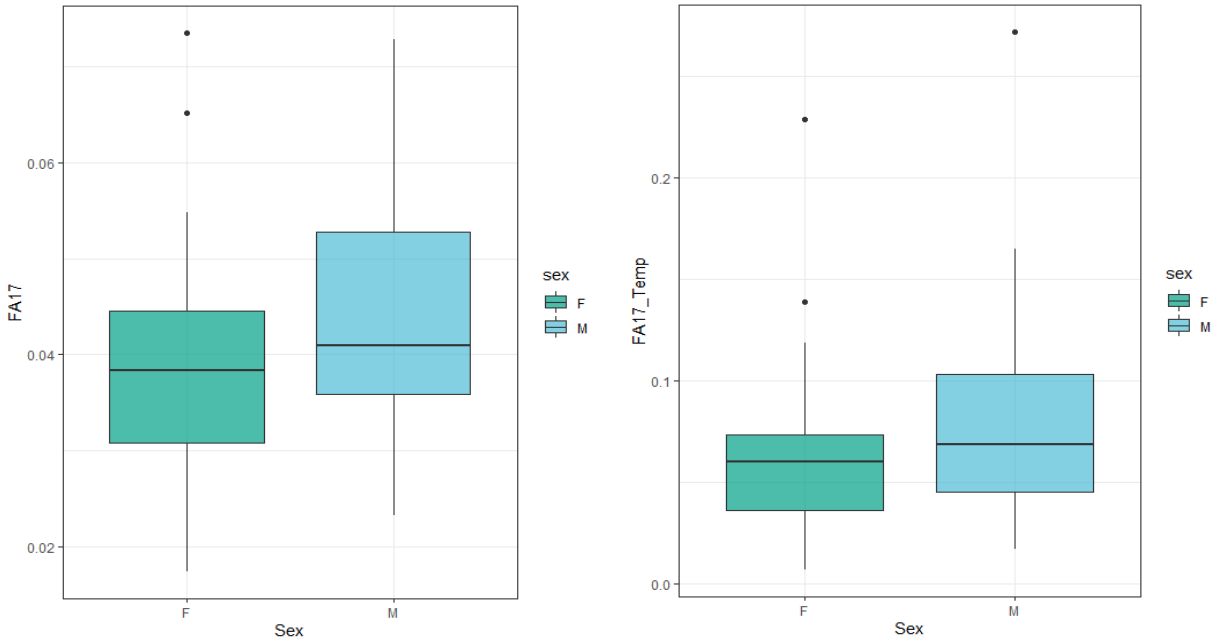

Figure 4.6 *- Boxplots illustrating FA17 and FA17_Temp in females (F) and males (M) (p<0.05)*

When taking into account sex and population simultaneously, Kruskal-Wallis tests were conducted to assess asymmetrical differences among these groups for the FA indices (refer to Table 4.13 for sex/population differences). When comparing sex and population simultaneously, statistically significant differences were noted for the FA17_Temp indices (p <0.05). More specifically, black South African females (p=0.031) differed significantly from the other groups, as confirmed by a *post-hoc* test (Table 4.14) and displayed a lower level of asymmetry than the others (see Figure 4.7).

Table 4.13 *- Kruskal-Wallis tests on fluctuating asymmetry values based on FA8 and FA17 indices between sex/population subgroups. Bold indicates significance (p<0.05)*

Index_IL distance	Chi-squared	Df	p-value
FA8_OBB	2.505	3	0.475
FA8_OBH	1.102	3	0.777
FA8_NOR	2.648	3	0.449
FA8_FMTN	6.721	3	0.081
FA8_FMTNS	3.163	3	0.367
FA8_MAH	2.005	3	0.571
FA8_MPL	5.740	3	0.125
FA8_MPB	4.737	3	0.192
FA8_MSAST	1.303	3	0.728
FA8_OCL	7.685	3	0.053
FA8_OPO	5.404	3	0.145
FA8_BAPO	3.369	3	0.338
FA8_NMS	1.270	3	0.736
FA8_NAL	2.321	3	0.509
FA8_NAAL	2.126	3	0.547
FA17	6.219	3	0.101
FA17_Orbs	3.514	3	0.319
FA17_Fac	3.993	3	0.262
FA17_Temp	8.842	3	**0.031**
FA17_Bas	1.249	3	0.741

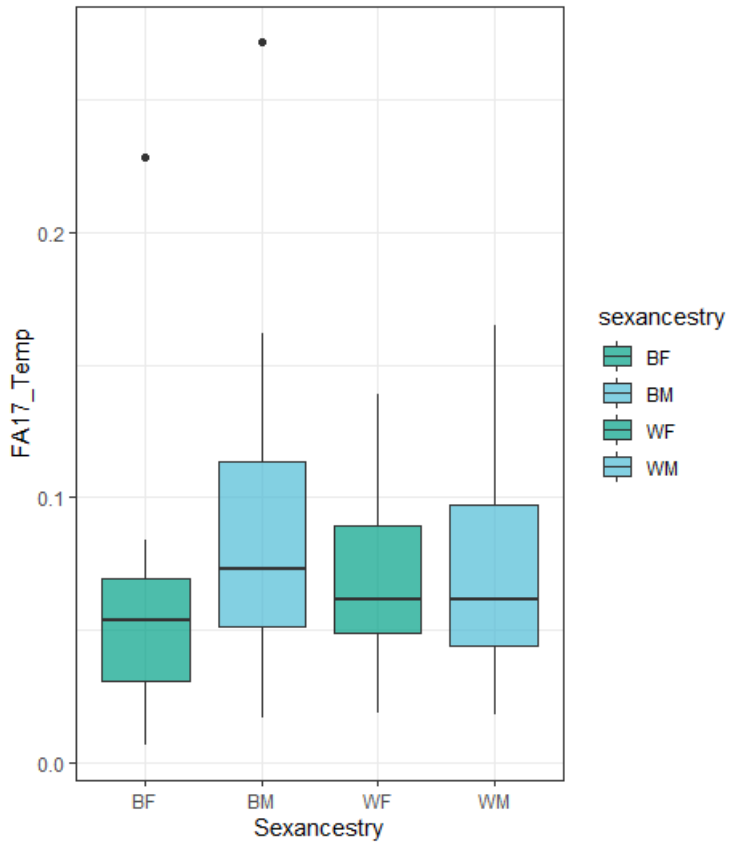

Figure 4.7 *- Boxplots illustrating FA17_Temp in black South African females (BF), black South African males (BM), white South African females (WF), and white South African males (WM) (p<0.05)*

Table 4.14 *- Post-hoc pairwise comparison test on FA17_Temp between sex/population subgroups. Bold indicates significance (p<0.05).*

Sex-ancestry	BF	BM	WF
BM	**0.017**	-	-
WF	0.288	0.936	-
WM	0.264	0.936	0.936

4.4.4. Shape variation: GMM

All preliminary tests such as GPA, PCA, and multivariate normality testing on the 3D coordinate data were conducted and statistical tests were employed to assess asymmetrical shape differences. On the QQ plots, 3D coordinates points indicated normal distribution (Refer to Figure A4-A7). All data lies on or near the 45-degree reference line, thus indicating univariate normality.

ANOVA was conducted to assess shape differences for matching and object asymmetry. Matching asymmetry refers to mirrored, paired landmarks that do not include a midline point, while object asymmetry refers to landmarks that join to a common point on the midline. The shape variables demonstrated the same pattern as the inter-landmark distances. More specifically, the results yielded statistically significant shape differences for the orbits, temporal, and midface for matching asymmetry ($p < 0.05$) (see Table 3.15). The greatest variation was noted in the orbital region, followed by the midface and then the temporal region, as demonstrated by the F-value (greater F-value demonstrates greater variation in a trait) (Table 4.15). No statistically significant difference was noted for the base matching landmarks ($p > 0.05$) (Table 4.15).

When looking at object symmetry, statistically significant shape differences were noted for the nasion, midface, facial and base regions ($p < 0.05$) (Table 4.16). The greatest variation was found in the facial region, followed by the base, the midface and the nasion (Table 4.16). No statistically significant differences were noted for the opisthion ($p > 0.05$) (Table 4.16).

ANOVA was also conducted on matching and object asymmetry for sex, and sex and population simultaneously. The results demonstrated statistically significant shape differences in sex for the orbits, temporal, and midface in matching asymmetry ($p < 0.05$). The greatest variation in traits was seen in males compared to females for matching asymmetry. Indeed, males showed the greatest variation for the orbits, temporals, and midface (greater F-value than females) (Table 4.15). It was also noted that white South African males showed the greatest variation in the orbits and midface region compared to all the other groups, while black South African males exhibited the greatest variation for the temporals ($p < 0.05$) (see the F-values in Table 4.15). This is

different from what was seen with the inter-landmark distances in which black females were noted to be more variable in the temporal region.

The results for object asymmetry demonstrated statistically significant shape differences in sex for the nasion, midface, facial and base regions ($p < 0.05$) (Table 4.16). The greatest variation was observed in females compared to males (greater F-value in females compared to males), even if it is worth noting that males showed greater variation in the midface (greatest F-value) ($p < 0.05$) (see Table 4.15). However, upon closer examination among subgroups, black South African females showed the overall greatest variation for object asymmetry (greatest F-value) ($p < 0.05$) (Table 4.16).

Table 4.15 *- Shape ANOVA test output for matching asymmetry traits, sexes, and sex/population groups. Bold indicates significance (p<0.05)*

Shape ANOVA_ Orbits			**Shape ANOVA_Temporals**		
Trait / Individual	**F- Value**	**Pr (>F)**	**Trait / Individual**	**F-Value**	**Pr (>F)**
Orbits	788.523	**0.007****	**Temporal**	37.729	**0.007****
F	297.471	**0.007****	**F**	15.898	**0.007****
M	563.028	**0.007****	**M**	22.646	**0.007****
BF	306.454	**0.007****	**BF**	14.109	**0.007****
BM	231.426	**0.007****	**BM**	16.690	**0.007****
WF	107.156	**0.007****	**WF**	5.261	**0.007****
WM	377.825	**0.007****	**WM**	9.094	**0.007****
Signif.codes: 0.001***	**0.01****	**0.05***	**Signif.codes: 0.001*****	**0.01****	**0.05***
Shape ANOVA_Midface			**Shape ANOVA_Base**		
Trait / Individual	**F-Value**	**Pr (>F)**	**Trait / Individual**	**F-Value**	**Pr (>F)**
Midface	396.060	**0.007****	**Base**	0.292	0.787
F	144.170	**0.007****	**F**	0.856	0.460
M	300.296	**0.007****	**M**	0.437	0.640
BF	148.573	**0.007****	**BF**	0.667	0.567
BM	124.645	**0.007****	**BM**	0.306	0.740
WF	47.194	**0.007****	**WF**	0.719	0.467
WM	197.934	**0.007****	**WM**	1.440	0.227
Signif.codes: 0.001***	**0.01****	**0.05***	**Signif.codes: 0.001*****	**0.01****	**0.05***

Table 4.16 *- Shape ANOVA test output for object asymmetry traits, sexes, and sex/population groups. Bold indicates significance (p<0.05)*

Shape ANOVA_Base			**Shape ANOVA_Face**		
Trait / Individual	**F- Value**	**Pr (>F)**	**Trait / Individual**	**F- Value**	**Pr (>F)**
Base	13028.027	**0.002 ****	**Face**	42046.051	**0.002 ****
F	6552.139	**0.002 ****	**F**	22258.811	**0.002 ****
M	6498.360	**0.002 ****	**M**	20282.293	**0.002 ****
BF	3919.769	**0.002 ****	**BF**	12340.834	**0.002 ****
BM	3214.937	**0.002 ****	**BM**	10126.525	**0.002 ****
WF	2871.267	**0.002 ****	**WF**	10144.435	**0.002 ****
WM	3295.603	**0.002 ****	**WM**	10530.174	**0.002 ****
Signif.codes: 0.001***	**0.01****	**0.05***	**Signif.codes: 0.001*****	**0.01****	**0.05***
Shape ANOVA_Midface			**Shape ANOVA_Nasion**		
Trait / Individual	**F- Value**	**Pr (>F)**	**Trait / Individual**	**F- Value**	**Pr (>F)**
Midface	7761.777	**0.002 ****	**Nasion**	455.635	**0.002 ****
F	2732.542	**0.002 ****	**F**	280.415	**0.002 ****
M	6212.601	**0.002 ****	**M**	194.813	**0.002 ****
BF	3882.510	**0.002 ****	**BF**	176.158	**0.002 ****
BM	3082.034	**0.002 ****	**BM**	118.122	**0.002 ****
WF	826.368	**0.002 ****	**WF**	107.276	**0.002 ****
WM	3659.341	**0.002 ****	**WM**	79.975	**0.002 ****
Signif.codes: 0.001***	**0.01****	**0.05***	**Signif.codes: 0.001*****	**0.01****	**0.05***
Shape ANOVA_Opistion					
Trait / Individual	**F- Value**	**Pr (>F)**			
Opistion	2.214	0.088			
F	3.042	0.074			
M	0.232	0.848			
BF	2.166	0.088			
BM	0.601	0.593			
WF	1.375	0.244			
WM	0.483	0.627			
Signif.codes: 0.001***	**0.01****	**0.05***			

4.5. Discussion and Conclusion

Skeletal asymmetry is often discussed in the literature and used to better understand the overall health, lifestyle, and diseases in a sample (DeLeon, 2007; Kujanová et al., 2008; Graham and Özener, 2016; Hagg et al.,2017). Asymmetry can affect different populations in various ways depending on the stressors placed upon them. As such, studying asymmetry in different populations can give invaluable insights on how stressors may have implications on the overall skeletal health of a sample. This research is the first study to assess craniofacial asymmetry in a modern South African sample, using 3D imaging and a combination of inter-landmark distances and GMM shape analyses. The following section will discuss the prevalence of craniofacial FA between sexes and populations, the general trends and patterns observed within the cranium for linear distances and GMM, as well as the overall implications of asymmetry in the South African population.

Black South Africans expressed the greatest degree of asymmetry compared to white South Africans. This is assumed to be in part due to the lasting effect of apartheid on the South African population. Similar findings were reported by Kieser and Groeneveld (1988) when assessing dental asymmetry in the South African population. They attributed the high degree of asymmetry seen in the black South African population to the legacy of apartheid. Indeed, apartheid resulted in prolonged unequal living conditions between the groups. Black South Africans were subjected to harsh living conditions and poverty, while white South Africans were typically of higher socio-economic status and lived wealthy lifestyles due to the implementation of apartheid racial laws (Liebenberg et al., 2015). Thus, black South Africans experienced numerous stressors such as poor nutrition, limited resources leading to poorer sanitation and susceptibility to illness, which had dire implications on skeletal growth and formation (Kieser and Groeneveld, 1988; Liebenberg et al., 2015). Even though the apartheid regime ended in 1994, black South African individuals continued to be affected despite the onset of democracy. As a consequence of population history and low-socioeconomic status, many black South Africans have experienced developmental stressors (environmental, genetic, and nutritional stress) that may contribute to asymmetry present on the skeleton. Within the South African population, females expressed the most asymmetry overall compared to males. This is similar to

other populations studied in the literature, such as Hagg et al., (2017) or Kujanova et al. (2008). Indeed, the study found females to be more asymmetrical than males in archaeological populations, even if it was not significant in the studies. While Özener and Fink (2010) did not find any differences between males and females living in good conditions, they observed that males living in poor conditions were the most asymmetric, and that males from a mixed-ethnic samples showed significant asymmetry. Therefore, asymmetry expression is variable and is dependent on the population studied, as well as the environmental stressors placed on the populations. While females are often thought to be the least asymmetrical, it should be noted that if females experienced stressful conditions during their development, their buffering system becomes inefficient (Graham and Özener, 2016). With generational poverty, which is likely assumed to be the case for the present sample, black females may have been unable to buffer negative stressors. As such, it comes to no surprise that black South African females would exhibit the most asymmetry overall due their population history, and stressors placed upon them.

Furthermore, general trends in the cranium for both inter-landmark distances and GMM indicated that the orbits, nasion and temporals were the traits that exhibited the most asymmetry in the South African population. Asymmetry in the temporal bones and orbits is consistent with findings in the literature (Storm and Knusel, 2005; Gawlikowaka et al., 2007; DeLeon, 2007; Hagg et al., 2017). It would be expected to see these asymmetrical changes in the temporal region, as their phenotypic plasticity is often influenced by the environment and has no genetic constraints (von Cramon-Taubadel, 2014). However, functional areas on the face such as the orbits and nose, show high heritability and are under stricter genetic control exhibiting genetic variance (Martínez-Abadías et al., 2009). Although the nose is under strict genetic control, it should be noted that nasal breadth does not show an additive genetic variance. The face is extremely sensitive to non-genetic factors (Siebert & Swindler, 2002). Craniofacial traits can exhibit genetic variation but factors such as sex, year of birth, population, environment, growth, and development can affect the expression of facial traits (Martínez-Abadías et al., 2009). Consequently, population, sex and the environment should be considered when examining the expression of asymmetry in facial traits (Martínez-Abadías et al., 2009). The expression of FA in traits and matrices is highly dependent on canalisation strength and ability, i.e., certain traits may buffer

stressors differently. Therefore, the results of the present study correspond to the literature, with a fluctuation of the expression of FA across traits and matrices (Blackburn, 2011; Hagg et al., 2017; Møller and Swaddle, 1997; Storm, 2009). Due to the population history and environmental conditions in the South African population, important asymmetrical influences in different regions of the crania are expected. It is worth noting that GMM detected more subtle asymmetrical changes in shape compared to inter-landmark distances for size variation, allowing us to conclude that there is more asymmetry in shape variation than in size variation, as reported in other studies (Schlager, 2013; Klingenberg, 2015; Benítez et al., 2020).

While the potential influence of asymmetry on estimating the biological profile may be minimal when taking measurements, anthropologists should always consider its presence and be cognisant of the sides and elements being used in methods on an individual basis. In terms of morphological scoring (specifically methods developed by Walker (2008) and Hefner (2009) for sex and ancestry estimation), both left and right sides should be included during the process, especially when scoring the orbits and mastoids, as this may potentially influence estimates in the populations. Indeed, high magnitudes of asymmetry were observed in the orbital region of the South African sample. Medical doctors should consider the vast variation and asymmetry seen in the South African sample, especially when designing their craniofacial treatment plan.

While the cranium is a good indicator for the study of fluctuating asymmetry, the literature also indicates the potential of dentition in assessing fluctuating asymmetry and its correlation to stressors. Future research should further explore fluctuating asymmetry through odontometrics to assess patterns of asymmetry and its correlation to craniofacial asymmetry in the South African population. As teeth preserves well and do not remodel after adolescence, they retain information on childhood stress and its association to asymmetry, whereas craniofacial asymmetry can change at any period in an individual's life and may be prone to remodelling which potentially limits information gained about an individual. Holistic studies combining the crania and post crania may also provide more information on the influence of stressors on individuals in the South African population and the overall health of each individual.

4.6. References

Akhil, G., Senthil Kumar, K.P., Raja, S., Janardhanan, K., 2015. Three-Dimensional Assessment of Facial Asymmetry: A Systematic Review. Journal of Pharmacy Bioallied Science 77, S433–S437. https://doi.org/10.4103/0975-7406.163491

Andronowski, J.M., Crowder, C. and Soto Martinez, M. 2018. Recent Advancements in the Analysis of Bone Microstructure: New Dimensions in Forensic Anthropology. Forensic Sciences Research 3(4),294–309. https://doi.org/10.1080/20961790.2018.1483294

Auerbach, B.M., Ruff, C.B., 2006. Limb Bone Bilateral Asymmetry: Variability and Commonality Among Modern Humans. Journal of Human Evolution 50, 203–218. https://doi.org/10.1016/j.jhevol.2005.09.004

Benítez, H.A., Lemic, D., Villalobos-Leiva, A., Bažok, R., Órdenes-Claveria, R., Pajač Živković, I., Mikac, K.M., 2020. Breaking Symmetry: Fluctuating Asymmetry and Geometric Morphometrics as Tools for Evaluating Developmental Instability under Diverse Agroecosystems. Symmetry 12, 1789. https://doi.org/10.3390/sym12111789

Blackburn, A., 2011. Bilateral Asymmetry of the Humerus During Growth and Development. American Journal of Physical Anthropology 145, 639–646. https://doi.org/10.1002/ajpa.21555

Caple, J., Stephan, C.N., 2016. A Standardized Nomenclature for Craniofacial and Facial Anthropometry. International Journal of Legal Medicine 130, 863–879. https://doi.org/10.1007/s00414-015-1292-1

Cavalcanti, M.G.P., Rocha, S.S., Vannier, M.W., 2004. Craniofacial measurements based on 3D-CT volume rendering: implications for clinical applications. Dentomaxillofacial Radiology 33, 170–176. https://doi.org/10.1259/dmfr/13603271

Cohen, J.M., 2005. Comparing Digital and Conventional Cephalometric Radiographs. American Journal of Orthodontics and Dentofacial Orthopedics 128, 157–160. https://doi.org/10.1016/j.ajodo.2005.03.017

Cole, S.J., Hulse, C.N., Stull, K.E., 2020. The Effects of Skeletal Asymmetry on Accurate Sex Classification, in A.R. Klales (Ed.): Sex Estimation of the Human Skeleton: History, Methods, and Emerging Techniques. Elsevier, pp. 307–325. https://doi.org/10.1016/B978-0-12-815767-1.00019-5

Corron, L., Stull, K., 2017. The Effects of Epiphyseal Fusion Asymmetry on Juvenile Age Estimation. 86th Annual meeting of the American Association of Physical Anthropologists, Nouvelle-Orléans, United States. Available from: https://hal.archives-ouvertes.fr/hal-01819886 (accessed 3.7.2021)

Costa, R.L., 1986. Asymmetry of the Mandibular Condyle in Haida Indians. American Journal of Physical Anthropology 70, 119–123. https://doi.org/10.1002/ajpa.1330700116

Coster, G.D., Dongen, S.V., Malaki, P., Muchane, M., Alcántara-Exposito, A., Matheve, H., Lens, L., 2013. Fluctuating Asymmetry and Environmental Stress: Understanding the Role of Trait History. PLOS ONE 8, e57966. https://doi.org/10.1371/journal.pone.0057966

Daniel, L., 2020. One in Five South Africans Now Lives on Less Than R28 a Day, The UN Finds. Business insider. Available from: https://www.businessinsider.co.za/heres-how-many-south-africans-live-on-less-than-r28-a-day-and-why-its-getting-worse-2020-12 (accessed 7.24.22).

DeLeon, V., 2007. Fluctuating Asymmetry and Stress in a Medieval Nubian Population. American Journal of Physical Anthropology, 132, 520–534. https://doi.org/10.1002/ajpa.20549

de Moraes, M.E.L., Hollender, L.G., Chen, C.S.K., Moraes, L.C., Balducci, I., 2011. Evaluating Craniofacial Asymmetry with Digital Cephalometric Images and Cone-Beam Computed Tomography. American Journal of Orthodontics and Dentofacial Orthopedics 139, e523–e531. https://doi.org/10.1016/j.ajodo.2010.10.020

Dryden. Ian. L, Mardia, K.V., 2016. Procrustes analysis, in: Statistical Shape Analysis, with Applications in R. John Wiley & Sons, Ltd, pp. 125–173. https://doi.org/10.1002/9781119072492.ch7

Ducos, M.B., Tabugo, S.R., 2015. Fluctuating Asymmetry as Bioindicator of Stress and Developmental Instability in Gafrarium Tumidum (Ribbed Venus Clam) From Coastal Areas of Iligan Bay, Mindanao, Philippines. AACL Bioflux 8, 292–300

Gawlikowska, A., Szczurowski, J., Czerwiński, F., Miklaszewska, D., Adamiec, E., Dzieciołowska, E., 2007. The Fluctuating Asymmetry of Medieval and Modern Human Skulls. Journal of Comparative Human Biology 58, 159–172. https://doi.org/10.1016/j.jchb.2006.10.001

Government Gazette, 2021. Final Report. South Africa. Available from: https://www.gov.za/sites/default/files/gcis_document/201409/report0.pdf

Graham, J., Özener, B., 2016. Fluctuating Asymmetry of Human Populations: A Review. Symmetry 8, 154. https://doi.org/10.3390/sym8120154

Gribel, B.F., Gribel, M.N., Frazão, D.C., McNamara, J.A., Manzi, F.R., 2011. Accuracy and Reliability of Craniometric Measurements on Lateral Cephalometry and 3D Measurements on CBCT Scans. The Angle Orthodontist. 81, 26–35. https://doi.org/10.2319/032210-166.1

Grünheid, T., Patel, N., De Felippe, N.L., Wey, A., Gaillard, P.R., Larson, B.E., 2014. Accuracy, Reproducibility, and Time Efficiency of Dental Measurements Using Different Technologies. American Journal of Orthodontics and Dentofacial Orthopedics 145,157–164. https://doi.org/10.1016/j.ajodo.2013.10.012

Hagg, A.C., Van der Merwe, A.E., Steyn, M., 2017. Developmental instability and its relationship to mental health in two historic Dutch populations. International Journal of Paleopathology. 17, 42–51. https://doi.org/10.1016/j.ijpp.2017.04.001

Hallgrimsson, B., 1999. Ontogenetic Patterning of Skeletal Fluctuating Asymmetry in Rhesus Macaques and Humans: Evolutionary and Developmental Implications. International Journal of Primatology 20, 121–151. https://doi.org/10.1023/A:1020540418554

Hefner, J.T., 2009. Cranial Nonmetric Variation and Estimating Ancestry. Journal of Forensic Sciences 54, 985–995. https://doi.org/10.1111/j.1556-4029.2009.01118.x

Hiramoto, Y., 1993. Right-Left Differences in the Lengths of Human Arm and Leg Bones. Kaibogaku Zasshi 68, 536–543. PMID: 8279264

Holland, A.J., 2016. Assessment of fluctuating asymmetry as an indicator of water quality stress in South Africa. PhD thesis, Rhodes University, South Africa. Available from: http://vital.seals.ac.za:8080/vital/access/services/Download/vital:19958/SOURCE1

Howell, B.R., McMurray, M.S., Guzman, D.B., Nair, G., Shi, Y., McCormack, K.M., Hu, X., Styner, M.A., Sanchez, M.M., 2017. Maternal Buffering Beyond Glucocorticoids: Impact of Early Life Stress on Corticolimbic Circuits That

Control Infant Responses to Novelty. Social Neuroscience 12, 50–64. https://doi.org/10.1080/17470919.2016.1200481

Kanchan, T., Mohan Kumar, T.S., Pradeep Kumar, G., Yoganarasimha, K., 2008. Skeletal asymmetry. Journal of Forensic Legal Medicine 15, 177–179. https://doi.org/10.1016/j.jflm.2007.05.009

Kieser, J.A., Groeneveld, H.T., 1988. Fluctuating Odontometric Asymmetry in an Urban South African Black Population. Journal of Dental Research 67, 1200–1205. https://doi.org/10.1177/00220345880670091001

Kim, S.G., 2011. Clinical Complications of Dental Implants. Implant Dentistry - A Rapidly Evolving Practice. https://doi.org/10.5772/17262

Klingenberg, C., 2015. Analysing Fluctuating Asymmetry with Geometric Morphometrics: Concepts, Methods, and Applications. Symmetry 7, 843–934. https://doi.org/10.3390/sym7020843

Klingenberg, C.P., Barluenga, M., Meyer, A., 2002. Shape Analysis of Symmetric Structures: Quantifying Variation among Individuals and Asymmetry. Evolution 56, 1909–1920

Krishan, K., Kanchan, T., DiMaggio, J.A., 2010. A Study of Limb Asymmetry and Its Effect on Estimation of Stature in Forensic Case Work. Forensic Science International 200, 181.e1–5. https://doi.org/10.1016/j.forsciint.2010.04.015

Krüger, G.C., L'Abbé, E.N., Stull, K.E., Kenyhercz, M.W., 2015. Sexual Dimorphism in Cranial Morphology Among Modern South Africans. International Journal of Legal Medicine 129, 869–875. https://doi.org/10.1007/s00414-014-1111-0

Kujanová, M., Bigoni, L., Velemínská, J., Veleminsky, P., 2008. Limb Bones Asymmetry and Stress in Medieval and Recent Populations of Central Europe. International Journal of Osteoarchaeology 18, 476–491. https://doi.org/10.1002/oa.958

L'Abbé, E.N., Krüger, G.C., Theye, C.E.G., Hagg, A.C., Sapo, O., 2021. The Pretoria Bone Collection: A 21st Century Skeletal Collection in South Africa. Forensic Science 1, 220–227. https://doi.org/10.3390/forensicsci1030020

L'Abbé, E.N., Loots, M., Meiring, J.H., 2005. The Pretoria Bone Collection: A modern South African skeletal sample. HOMO 56, 197–205 https://doi.org/10.1016/j.jchb.2004.10.004

Langley, N.R., Jantz, L.M., Ousley, S.D., Jantz, R.L., Milner, G., 2016. Data Collection Procedures for Forensic Skeletal Material 2.0. University of Tennessee and Lincoln Memorial University

Latimer, H.B., Lowrance, E.W., 1965. Bilateral Asymmetry in Weight and in Length of Human Bones. The Anatomical Record 152, 217–224. https://doi.org/10.1002/ar.1091520213

Letzer, G.M., Kronman, J.H., 1967. A Posteroanterior Cephalometric Evaluation of Craniofacial Asymmetry. Angle Orthodontist 37, 205–211. https://doi.org/10.1043/0003-3219(1967)037<0205:APCEOC>2.0.CO;2

Liebenberg, L., Krüger, G.C., L'Abbé, E.N., Stull, K.E., 2019. Postcraniometric Sex and Ancestry Estimation in South Africa: A Validation Study. International Journal of Legal Medicine 133, 289–296. https://doi.org/10.1007/s00414-018-1865-x

Liebenberg, L., L'Abbé, E.N., Stull, K.E., 2015. Population Differences in The Postcrania of Modern South Africans and the Implications for Ancestry Estimation. Forensic Science International 257, 522–529. https://doi.org/10.1016/j.forsciint.2015.10.015

Livshits, G., Davidi, L., Kobyliansky, E., Ben-Amitai, D., Levi, Y., Merlob, P., Optiz, J.M., Reynolds, J.F., 1988. Decreased Developmental Stability as Assessed by Fluctuating Asymmetry of Morphometric Traits in Preterm Infants. American Journal of Medicine and Genetics 29, 793–805. https://doi.org/10.1002/ajmg.1320290409

Marciano, M.A., Duarte, M.A.H., Ordinola-Zapata, R., Del Carpio Perochena, A., Cavenago, B.C., Villas-Bôas, M.H., Minotti, P.G., Bramante, C.M. and Moraes, I.G. 2012. Applications of Micro-Computed Tomography in Endodontic Research. In: Méndez-Vilas (ed.). Current Microscopy Contributions to Advances in Science and Technology. pp. 782–788. ISBN: 8493984361, 9788493984366

Mardia, K.V., Bookstein, F.L., Moreton, I.J., 2000. Statistical Assessment of Bilateral Symmetry of Shapes. Biometrika 87, 285–300

Martínez-Abadías, N., Esparza, M., Sjøvold, T., Gonzalez-Jose, R., Santos, M., Hernández, M., 2009. Heritability of Human Cranial Dimensions: Comparing the Evolvability of Different Cranial Regions. Journal of Anatomy 214, 19–35. https://doi.org/10.1111/j.1469-7580.2008.01015.x

Møller, A.P., Swaddle, J.P., 1997. Asymmetry, Developmental Stability, and Evolution. Oxford University Press

Nandi, M.E., Olabiyi, O., Okubike, E., Cyprain, I., 2018. A Study of Bilateral Asymmetry of Upper Extremity and its Effects on Stature Reconstruction amongst Nigerians. Australian. Journal of Forensic Science 1, 978–988. https://doi.org/10.26735/16586794.2018.023

Olejniczak, A., Tafforeau, P., Smith, T., Temming, H., Hublin, J.-J., 2007. Technical Note: Compatibility of Microtomographic Imaging Systems for Dental Measurements. American Journal of Physical Anthropology 134, 130–4. https://doi.org/10.1002/ajpa.20615

Özener, B., Fink, B., 2010. Facial Symmetry in Young Girls and Boys from a Slum and a Control Area of Ankara, Turkey. Evolution and Human Behaviour 31, 436–441. https://doi.org/10.1016/j.evolhumbehav.2010.06.003

Palmer, A., Strobeck, C., 2002. Fluctuating Asymmetry and Developmental Stability: Heritability of Observable Variation vs. Heritability of Inferred Cause. Journal of Evolutionary Biology 10, 39–49. https://doi.org/10.1046/j.1420-9101.1997.10010039.x

Palmer, A.R., 1994. Fluctuating Asymmetry Analyses: A Primer, in: Markow, T.A. (Ed.), Developmental Instability: Its Origins and Evolutionary Implications, Contemporary Issues in Genetics and Evolution. Springer Netherlands, Dordrecht, pp. 335–364. https://doi.org/10.1007/978-94-011-0830-0_26

Perzigian, A.J., 1977. Fluctuating Dental Asymmetry: Variation Among Skeletal Populations. American Journal of Physical Anthropology 47, 81–88. https://doi.org/10.1002/ajpa.1330470114

Reck, C., Zietlow, A.-L., Müller, M., Dubber, S., 2016. Perceived Parenting Stress in the Course of Postpartum Depression: The Buffering Effect of Maternal Bonding. Archives of Women's Mental Health 19, 473–482. https://doi.org/10.1007/s00737-015-0590-4

Ridel, A.F., Demeter, F., Liebenberg, J., L'Abbé, E.N., Vandermeulen, D., Oettlé, A.C., 2018. Skeletal Dimensions as Predictors for the Shape of the Nose in a South African Sample: A Cone-Beam Computed Tomography (CBCT) Study. Forensic Science International 289, 18–26. https://doi.org/10.1016/j.forsciint.2018.05.011

Schlager S. 2013. Soft-Tissue Reconstruction of the Human Nose: Population Differences and Sexual Dimorphism. PhD thesis, Universitatsbibliothek Freiburg. http://dx.doi.org/10.13140/RG.2.1.2564.5528

Shah, S.M., Joshi, M.R., 1978. An Assessment of Asymmetry in the Normal Craniofacial Complex. Angle Orthodontist 48, 141–148. https://doi.org/10.1043/0003-3219(1978)048<0141:AAOAIT>2.0.CO;2

Siebert, J.R., Swindler, D.R., 2002. Evolutionary Changes in the Midface and Mandible: Establishing the Primate Form, in: Understanding Craniofacial Anomalies. John Wiley & Sons, Ltd, pp. 343–378. https://doi.org/10.1002/0471221953.ch15

Srivastava, D., Singh, H., Mishra, S., Sharma, P., Kapoor, P., Chandra, L., 2018. Facial asymmetry revisited: Part I- diagnosis and treatment planning. J. Oral Biol. Craniofacial Res. 8, 7–14. https://doi.org/10.1016/j.jobcr.2017.04.010

Stoddard, E., 2022. DISMAL ASCENT: South African Unemployment Rate Hits Record 35.3% In Q4 2021. Daily Maverick. Available from: https://www.dailymaverick.co.za/article/2022-03-29-south-african-unemployment-rate-hits-record-35-3-in-q4-2021/ (accessed 7.24.22)

Storm, R.A., 2009. Human Skeletal Asymmetry. A Study of Directional and Fluctuating Asymmetry in Assessing Health, Environmental Conditions, and Social Status in English Populations from the 7th to the 19th Centuries. Doctor of Philosophy. University of Bradford. Available from: http://hdl.handle.net/10454/4325 (accessed 2.9.21)

Storm, R., & Knüsel, C., 2005. Fluctuating Asymmetry: A Potential Osteological Application. Paper Presented at Proceedings of the Fifth Annual Conference of the British Association for Biological Anthropology and Osteoarchaeology, Southampton, England.

Suwa, G., Kono, R.T., 2005. A Micro-CT Based Study of Linear Enamel Thickness in the Mesial Cusp Section of Human Molars: Revaluation of Methodology and Assessment of Within-Tooth, Serial, And Individual Variation. Anthropological Science 113, 273–289. https://doi.org/10.1537/ase.050118

Townsend, G.C., Garcia-Godoy, F., 1984. Fluctuating Asymmetry in the Deciduous Dentition of Dominican Mulatto Children. Archives of Oral Biology 29, 483–486. https://doi.org/10.1016/0003-9969(84)90067-0

Trochim, W.M.K., 2020. The Research Methods Knowledge Base. Available from : https://conjointly.com/kb/cite-kb/(accessed 11.03.21)

von Cramon-Taubadel, N., 2014. Evolutionary Insights into Global Patterns of Human Cranial Diversity: Population History, Climatic and Dietary Effects. Journal of Anthropological Science 92, 43–77. https://doi.org/10.4436/jass.91010

Walker, P.L., 2008. Sexing Skulls Using Discriminant Function Analysis of Visually Assessed Traits. American Journal of Forensic Anthropology 136. https://doi.org/10.1002/ajpa.20776

Živanović, S., 1983. A note on the effect of asymmetry in suture closure in mature human skulls. American Journal Physical Anthropology 60, 431–435. https://doi.org/10.1002/ajpa.1330600404

The previous chapter evaluated the extent and effect of fluctuating asymmetry on the cranium by assessing craniofacial asymmetry. The cranium was chosen as the ideal skeletal element as it is minimally affected by side-bias and thus provided a better gauge of fluctuating asymmetry in this sample. The results from the previous chapter revealed that females and black South Africans expressed the greatest degree of asymmetry. A possible reason for these results may be due to the lasting effects of apartheid and the overall strain it had on the black South Africa sample. Throughout history black South Africans have been experiencing numerous stressors such as poor nutrition, unsanitary living conditions and susceptibility to infection which can affect the normal process of skeletal growth and formation (Kieser and Groeneveld, 1988; Liebenberg et al., 2015). This disruption on normal skeletal formation can lead to the development of pathological lesions resulting in skeletal markers of disease being present on different regions of the skeleton. As such, to go further, the next Chapter explore the link between asymmetry and the health and lifestyle of the South African population. This was done by assessing non-specific signs of disease on the entire skeleton of each individual.

Chapter 5 - AN ASSESSMENT OF THE CORRELATION OF ASYMMETRY TO SKELETAL SIGNS OF STRESS

5.1. Chapter Overview

The following chapter will explore the correlation between asymmetry and non-specific signs of disease. This research explored and discussed the frequency of non-specific signs of disease, the relationship between the disease and its overall correlation to sexes and population affinities.

The frequency of non-specific signs of disease in a modern South African sample and its relationship with fluctuating asymmetry
M HARRIPERSHAD, CEG THEYE, AF RIDEL, L LIEBENBERG
Manuscript to be submitted for publication to the Anthropologischer Anzeiger

Abstract

The study of skeletal asymmetry and its correlation to health and disease has become of particular interest to biological anthropologists. By gaining a better understanding of the relationship between these two factors, anthropologists are able to interpret the overall implication of disease on skeletal growth and formation and gain a better understanding of the variation seen within and between population affinities. This study aimed to evaluate the frequency of non-specific signs of disease in a South African sample and its overall correlation to fluctuating asymmetry. The sample comprised of 115 individuals (59 black and 56 white south Africans, comprising 58 females and 57 males). Fluctuating asymmetry values were obtained from 3D left and right inter-landmark distances calculated from landmarks placed on the micro-XCT scans of crania of these 115 individuals. Four types of non-specific signs of disease were documented and scored. Statistical analysis was then conducted for frequency distributions of each disease and to explore the relationship between asymmetry and disease. Twenty-six individuals were found to be significantly asymmetrical and periostitis was commonly present among those individuals. While white South Africans did show a weak significant correlation between asymmetry and periostitis, no other correlations were detected between asymmetry and pathological lesions. Overall,

black South Africans exhibited the highest frequency of porotic hyperostosis and enamel hypoplasia which may be indicative of stress due to socio-economic circumstances.

Keywords: Fluctuating asymmetry, Developmental stress, Craniometric, Cribra orbitalia, Enamel hypoplasia, Porotic hyperostosis, landmarks, Micro-XCT

5.2. Introduction

Pathological conditions often interrupt bone formation and remodelling, which may lead to the formation of lesions in response to the type of disease or stressor experienced by the bone (Ortner, 2019; Waldron, 2009). Biological anthropologists examine skeletal lesions on bone to provide a possible identification of diseases, to understand the pathogenesis of the disease, and to learn more about the living conditions and lifestyle of individuals or populations. Therefore, an understanding of how lesions were formed, and the main process of the disease is required to give a possible diagnosis of the type of pathology from examination of bone (Ortner, 2019; Waldron, 2009). The pathogenesis and expression of non-specific skeletal markers of disease related to malnutrition or harsh living conditions and its development throughout childhood into adulthood has been extensively studied. More specifically, many authors discuss the potential links of non-specific signs of disease and stunted growth and development, as commonly being associated with low socio-economic status (SES) (Kim et al., 2015; Miszkiewicz and Cooke, 2019; Casna and Schrader, 2022;). Individuals that are considered lower SES are typically defined to be part of households with little income or wealth and are thus unable to buffer negative impacts that have been applied upon them from adverse conditions (Leonard et al., 2017). Hence, children living in low socio-economic families are in frequent need of hospitalization due to the susceptibility to disease. As such, childhood stress tends to have lasting effects into adulthood and usually results in a higher susceptibility to more health problems throughout an individual's lifetime (Coolidge, 2015).

In South Africa, apartheid has contributed largely to disparities in economic status between individuals within the country. Between 1948 and 1994, apartheid was a system of institutionalised racial segregation which created a wealth and power imbalance among the racial groups (particularly in favour of white South Africans

compared to black and coloured South Africans) (Linford, 2011). As a result of apartheid, access to high-level jobs, education, and urban areas were limited for people of colour, leaving many black and coloured South Africans poorly educated and possibly without jobs to improve their living conditions (Linford, 2017; Fogel, 2019). Presently, the economic effects of apartheid are still prevalent in South Africa even after the end of apartheid in the early 1990's. Many people of colour in South Africa are thus experiencing multidimensional (poor health, lack of education and inadequate living standard) generational poverty due to the lasting effects of the apartheid regime. As a result, this population has inadequate access to health care and is highly susceptible to disease and the development of pathological lesions (Daniel, 2020; Stoddard, 2022).

The literature documents a higher degree of skeletal asymmetry among populations of lower SES, especially in cases where foetal development occurred while the mother lived in a polluted environment, underwent physiological stress, or contracted an infectious disease and suffered severe nutritional deficits (Harris and Nweeia, 1980; Livshits et al., 1988; Gawlikowska et al., 2007; Storm, 2009). Fluctuating asymmetry, the term commonly used to describe asymmetry associated with developmental stressors, refers to the random deviation from perfect symmetry with an inequality in size or shape of bilateral (left and right sided) traits (Graham and Özener, 2016). Because fluctuating asymmetry has been shown to have a positive correlation with developmental instabilities, it can be employed as a useful indicator of developmental stress and congenital defects that arise during ontogeny and continue to affect adult health (Livshits et al., 1988). The term developmental stressors are often used in biological anthropology and refers to the event that results in physiological change caused by strain placed upon an individual brought about by environmental and genetic conditions during stages of growth. Hence, improved knowledge and the understanding of the role played by developmental stressors and its correlation to skeletal asymmetry enable anthropologists to better interpret human variation and its implications for medical and forensic applications. The present study will explore the correlation between skeletal asymmetry and pathological lesions of stress. The study will also focus on the frequency of pathological stress indicators found on the skeleton that are often associated with childhood stress and its longevity into adulthood, inclusive of cribra orbitalia, porotic hyperostosis, enamel hypoplasia and periostitis.

Cribra orbitalia presents as porosities or pitting, paired with a thickening of the roof of the orbits (Zariła et al., 2016). As the lesions tend to be more severe and active in children, the condition has typically been associated with nutritional stress during childhood. In adults, the condition is noted less frequently, and when present, the lesions tend to be healed with less severe expressions of pitting (Ortner, 2019). More recent literature discusses a proposed aetiology of anaemia-induced marrow hypertrophy resulting from haemolytic and/or megaloblastic anaemia as a cause for cribra orbitalia to develop. Haemolytic anaemias, such as thalassemia or sickle cell anaemia, has shown to be caused when red blood cells are destroyed prematurely, producing the expression of osseous haemopoietic marrow expansion (Walker et al., 2009). On the other hand, megaloblastic anaemia has shown to be acquired in infants through nursing, due to the combination of the mother being deficient in vitamin B12 and experiencing poor living conditions (low SES), resulting in the infant developing the deficiency from birth producing active, expansive pitting on the roof of the orbits (Walker et al., 2009). Lastly, Walker et al. (2009) noted that another probable cause for cribra orbitalia may be due to subperiosteal bleeding that occurs with a deficiency for both vitamin B12 as well as vitamin C. Hence, individuals that have suffered or are suffering from scurvy often have a vitamin C deficiency, which can cause a decrease in collagen synthesis and susceptibility to infectious disease and haemorrhage, and often exhibit pitting on the lateral sides of the orbit roofs.

Porotic hyperostosis manifests in a manner similar to cribra orbitalia and therefore, a direct correlation between the two conditions may exist (Walker et al., 2009). However, this pathological lesion differs from cribra orbitalia as it usually occurs because of marrow hypertrophy between the inner and outer tables of the cranium; and thus, producing lesions across the cranial vault rather than the orbits (Rinaldo, 2018; Ortner, 2019). When in an anaemic state, the body becomes hypoxic (starved of oxygen), which stimulates haemopoietic marrow red blood cell production (Salvadei et al., 2001). This results in an enlargement of the diploë through the outer table of the cranial vault with porosities or pitting on it (Ortner, 2019). In severe cases, expansion of the diploë may even cause exposure of the underlying trabecular bone. The porotic lesions are seen with massive marrow hypertrophy that can only be produced by high levels of erythropoiesis, such as haemolytic and/or megaloblastic anaemia (Walker et al., 1997). If the number of dead red blood cells exceeds the number of red blood cells

produced, this will stimulate the bone marrow expansion (Walker et al., 1997). Walker et al. (2009) noted many active lesions in the skeletons of subadults in an archaeological sample, while healed lesions were typically noted in older adults. It was therefore concluded that the appearance of porotic hyperostosis is most likely a reflection of childhood anaemia. This is supported by bioarchaeological data as well as modern clinical data that have shown that children have much lower capacity to support elevated levels of red blood cell production, which increases the likelihood of porotic hyperostosis being frequently observed in children (Hagg et al., 2017).

Periostitis occurs due to inflammation or lifting at an infected area under the periosteum (Ortner, 2019). The periosteum is the membranous soft tissue layer that encapsulates the bone and stimulates circumferential growth of bones during the physiological growth of subadults, as well as remodelling in response to stress or strain in adults (Waldron, 2009). Bone reacts to pathological responses related to the periosteum by continuously depositing bone at sites of infection and inflammation. These subperiosteal bone reactions are highly variable as it can be unilateral, bilateral, or diffuse, and are mostly exhibited on long bones (Waldron, 2009). Active lesions are attached loosely to the cortical bone with signs of newly formed bone having a loose and irregularly striated appearance. To identify periostitis, the area of the active lesions displays striations, pits, and porous bone with well-defined margins (Ortner, 2019). When the lesions start to heal the bone will begin to remodel from primary woven bone to secondary cortical bone, which appears smoother with some residual pitting or striations (Ortner, 2019). While commonly attributed to infection, periostitis is considered a non-specific sign of disease as it may also be the result of trauma, bacterial infections, neoplasms, scurvy, chronic distribution of drugs into the periosteum using a needle and venous insufficiency (which can occur frequently in individuals of low SES) (Waldron, 2003; Hagg et al., 2017).

Lastly, enamel tends to carry vital information on the history of childhood stress, with lasting signs in adulthood seen as enamel hypoplasia. This usually occurs during enamel formation. Ameloblasts are single cells that develop the enamel of the outer tooth crown by differentiating, maturing, and orientating themselves into bundles forming prisms with cross-striations known as striae of Retzius (Ortner, 2019). Any occurrence that disrupts this process, such as infections, poor nutrition, trauma during

birth, low weight at birth, or genetic predisposition may result in defects in the enamel (Ortner, 2019). These hypoplastic defects can be observed as pits, furrows, grooves, and lines with uneven distribution of thickness on the enamel layer (Ortner, 2019). Enamel hypoplasia can start to form in the second trimester of pregnancy up to the age of ten years and will be retained into adulthood, as the enamel cannot repair or remodel itself once its formation has been disrupted (Goodman and Rose, 1990; Brook, 2009; Upex, 2012; Schuurs, 2013; Ortner, 2019). Enamel hypoplasia can therefore be seen on both permanent and deciduous teeth. Furthermore, anterior teeth generally exhibit higher levels of enamel hypoplasia than posterior teeth, with mandibular canines being mainly affected in adult populations (Wright, 1997). As such, enamel hypoplasia can be an indicator for developmental stress due to its link to infection or nutritional deficiencies, and its persistence into adulthood.

Since the pathogenesis of cribra orbitalia, porotic hyperostosis, enamel hypoplasia, and periostitis is linked to developmental instabilities, these lesions are ideal to assess disease and fluctuating asymmetry in a South African sample. Therefore, this study aimed to assess the frequency of non-specific signs of disease and its correlation to facial asymmetry in a South African population. The cranium was selected for the assessment of fluctuating asymmetry as it is minimally affected by confounding factors such as side-bias (directional asymmetry) and muscular development.

5.3. Materials and Methods

5.3.1. Sample

The sample consisted of crania (dry bone and micro-XCT scans) and post-crania (dry bone) of 115 individuals (Table 5.1), sourced from the Pretoria Bone Collection (PBC), housed in the Department of Anatomy, University of Pretoria, South Africa (L'Abbé et al., 2005; L'Abbé et al., 2021). To explore any difference in the prevalence of the conditions, the sample included male and female black and white South Africans, with all individuals older than 18 years of age. Only well-preserved skulls and long bones with the absence of bone alterations and with the absence of metal restorations were selected. The PBC is a moderately contemporary sample that consists of South African individuals born between 1863 to 1996 and is a good gauge of modern variation seen amongst the South African populations (L'Abbé et al., 2005; L'Abbé et al., 2021). The skeletons were obtained from cadavers that are composed of unclaimed and donated

bodies that were acquired by the University of Pretoria medical school (L'Abbé et al., 2005; Krüger et al., 2015; Liebenberg et al., 2019; L'Abbé et al., 2021). Micro-XCT imaging has shown to be extremely effective in providing detailed visualisation of facial structures that assists in identifying facial asymmetry without causing damages or destruction to skeletal material. However, the examination of pathology could not be done on micro-XCT imaging as the pathological lesions were not easily visible on scans and full-body micro-XCT scans were not available. Ethical approval for this study was obtained by the Faculty of Health Sciences Research Ethics committee (University of Pretoria) (Ethical Number: 386/2021).

Table 5.1 *- Study sample distribution*

	black South Africans	**white South Africans**	**Total**
Females	30	27	57
Males	29	29	58
Total	59	56	115

5.3.2. Methods

All cranial micro-XCT scans had to be segmented using the semi-automatic watershed method and re-oriented and aligned standardly according to the Frankfort plane to place landmarks. A total of 15 inter-landmark distances were obtained from 34 landmarks placed on micro-XCT scans of crania using Avizo 2019 (ThermoFisher Scientific Inc.) Table 5.2 details the definitions of the landmarks and distances included in the study. Several calculations were done to quantify asymmetry. First, fluctuating asymmetry (FA) values were calculated for each individual by subtracting the right-side measurements from the left-side measurements. Standard asymmetry formulae developed by Palmer and Strobeck (2003) were employed, in order to take size into consideration (Table 5.3). Average FA values were calculated for multiple traits for each individual and for a combination of traits (Palmer and Strobeck, 2003, Hagg et al., 2017) (Table 5.3).

In addition to collecting measurements from the cranium, the crania, and long bones (humeri, ulnae, radii, femurs, tibias, and fibulas) of the same individuals were all examined for pathological lesions typically linked to non-specific signs of disease and nutritional diseases. Diagnostic aids, such as palaeopathological textbooks were used

to effectively analyse the pathological lesions (Waldron, 2009; Ortner, 2019). Specifically, the presence of cribra orbitalia, porotic hyperostosis, enamel hypoplasia and subperiosteal bone reaction (periostitis) were recorded. Cribra orbitalia was scored as present if pitting was observed on the orbital roofs (Figure 5.1). Porotic hyperostosis was scored as present if pitting was observed on the partial and occipital bones (Figure 5.2). Enamel hypoplasia was scored as present if at least one hypoplastic defect was present on at least one tooth (Figure 5.3). Similarly, subperiosteal bone reactions (periostitis) were considered present if it was observed on at least one long bone (Figure 5.4). The pathological lesions were scored as present regardless of whether the lesion appeared active or healed/in the process of healing. The pathological lesions, lesion location and the number of lesions seen on each individual was also observed and recorded.

Figure 5.1 *- Pictures illustrating cribra orbitalia : A- unaffected individual , B- active lesions of cribra orbitalia , and C- healing/healed lesions of cribra orbitalia.*

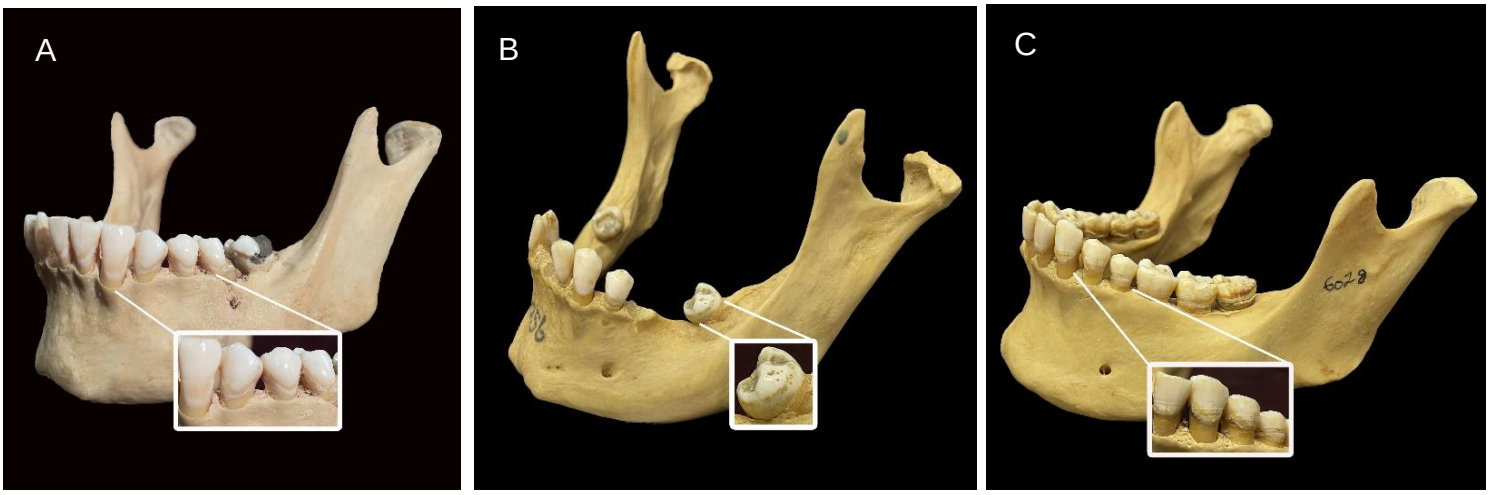

Figure 5.3 *- Pictures illustrating enamel hypoplasia A- unaffected individual, B- spotted defects and C- linear defects associated with enamel hypoplasia*

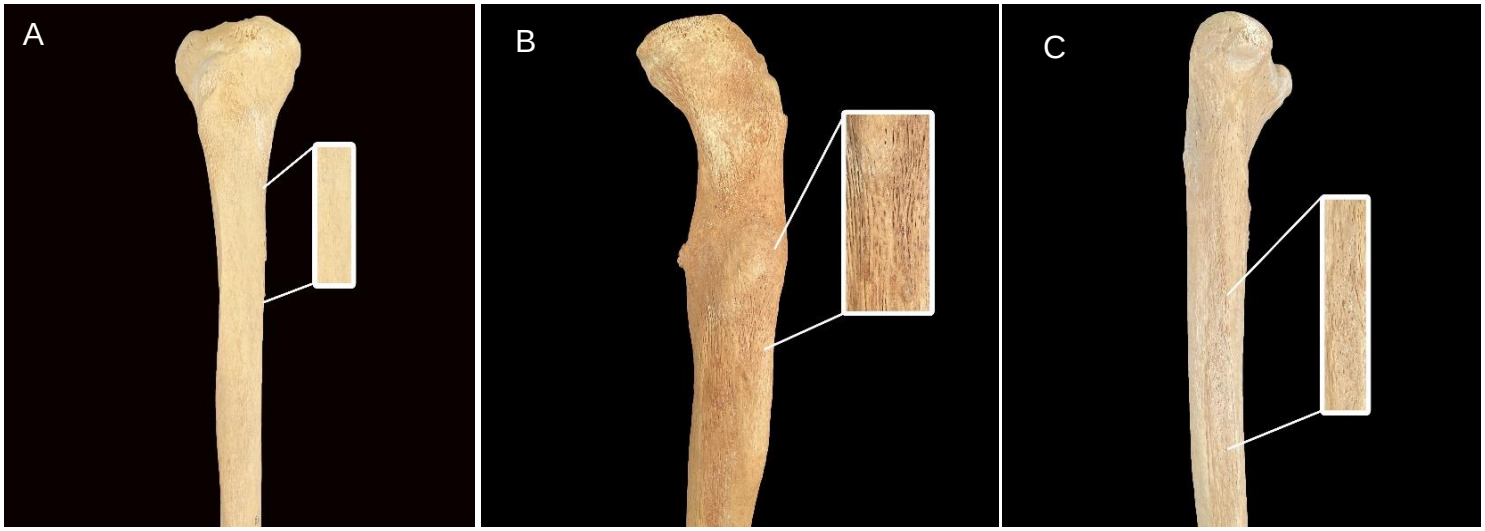

Figure 5.4 *- Pictures illustrating an individual without periostitis and individuals with varying degrees of periostitis: A- uninfected individual, B- active periosteal stripping and C- healed periostitis*

Table 5.2 *- Craniometric measurements (adapted from Hagg et al., 2017)*

Nr.	Name	Abr.	Definition
1	Orbital breadth	OBB	Lateral distance from the dacryon (D) to ectoconchion (Ec).
2	Orbital height	OBH	Direct distance between the superior (So) and inferior (I0) orbital margins perpendicular to the orbital breadth.
3	Diagonal orbital breadth	NOR	Direct distance from nasion (N) to the orbitale (Or).
4	Frontomalare-nasion length	FMTN	Direct distance from the frontomalare (Fmt) to nasion (N).
5	Frontomalare-nasospinale	FMTNS	Direct distance from frontomalare (Fmt) to nasospinale (Ns).
6	Malar height	MAH	Least distance from the most inferior point on the lower border of the orbit (Or) to the most superior point on the inferior border of the zygomatic.
7	Mastoid length	MPL	Direct distance from porion (Po) to mastoidale (Ms).
8	Mastoid breadth	MPB	Direct distance from the posterior border of the external auditory meatus (Pem) to the most anterior point along the posterior margin of the mastoid process (Pm).
9	Mastoidale-asterion	MSAST	Direct distance from mastoidale (Ms) to asterion (Ast).
10	Occipital condyle length	OCL	Maximum distance from the most anterior (Aoc) to the most posterior (Poc) point on the occipital condyles.
11	Opisthion-porion length	OPO	Direct distance from the opisthion (O) to porion (Po).
12	Basion-porion length	BAPO	Direct distance from basion (Ba) to porion (Po).
13	Nasion-mastoidale	NMS	Direct distance from nasion (N) to mastoidale (Ms).
14	Nasion-alare	NAL	Direct distance from nasion (N) to alare (Al)
15	Nasospinale-alare	NAAL	Direct distance from nasospinale (Ns) to alare (Al)

Table 5.3 *- Description and formula of the indices used to evaluate asymmetry (Adapted from Hagg et al., 2017 and Palmer and Strobeck , 2003)*

Index	Formula	Description
FA8	FA8 = $\left\lvert \ln(R_d/L_d) \right\rvert$	The difference between the natural logs of the left and right measurements of a trait, in absolute values.
FA17	FA 17 = $\sum \left\lvert \ln(R_d/L_d) \right\rvert$ / T	Average FA values computed from the FA8 values for multiple traits and combinations.

5.3.3. Statistical analysis

All statistical analyses were conducted in the R software and R studio environment (R Core Team, 2018) (Trochim, 2020). Repeatability testing was performed to assess the reproducibility of the landmark positioning. This was done by placing the landmarks on 15 randomly selected scans and calculating intra- and inter-observer agreement. For the intra-observer agreement, the landmark placement was performed twice by the same observer with an interval of two weeks. For the inter-observer agreement, an additional observer performed the landmark placement. The reproducibility of the landmark positioning was calculated using the dispersion Δ_{ij} for each landmark *i* and individual *j*. Dispersion is defined as the Mean Euclidean Distance (MED) of the sample landmark $\boldsymbol{p}_{ijk}$ to the mean $\bar{\boldsymbol{p}}_{ij}$ of the (x, y, z)-coordinates of landmark *i* over all observation's *k* (inter, intra, resp.) for subject *j (Formula 5.1)*:

Formula 5.1

$$\Delta_{ij} = \sum_{k=1}^{K} \left\| \boldsymbol{p}_{ijk} - \bar{\boldsymbol{p}}_{ij} \right\| / K \text{ , with } \bar{\boldsymbol{p}}_{ij} = \sum_{k=1}^{K} \boldsymbol{p}_{ijk} / K$$

Plots of MED values were also generated to show the variation of dispersion over different subjects. Global precision is reported as the global (averaged over all

landmarks) mean (μ_{Δ}) and median (m_{Δ}) of the per landmark mean ($\mu_{\Delta i}$) and median ($m_{\Delta i}$) values (over all subjects).

Craniometric measurements were used to obtain FA8 and FA17 values (Table 5.2). Once all the values for FA8 per trait were obtained, FA17 could then be obtained for each individual to assess the total asymmetry expressed by each individual (all traits combined). An individual was considered asymmetrical if they had an FA17 value higher than 0.05. Lastly, descriptive statistics was used to summarise and describe the main features of the dataset for FA values (Trochim, 2020). The mean, standard deviation, and range for each FA8 trait and for FA17 were calculated in RStudio for populations, sexes, and population and sex simultaneously.

Statistical analysis was then conducted to evaluate the frequency and presence of pathology in the South African population and between sexes. Frequency distributions (0 = absent, 1= present) were calculated for presence of the pathological lesions (for each disease) separated into sex and population groups, and for population and sex, simultaneously. Kruskal-Wallis tests were conducted in conjunction with the frequency distributions to test for significant differences between the groups. Frequency distributions were also conducted to examine the number of pathologies (0 = none observed, 1 = one condition observed, etc.) an individual had over the entire sample for populations, sexes, and population and sex, simultaneously. Kruskal-Wallis testing was conducted to test for significant differences between the groups per the number of pathologies. Results were broken down to see which conditions were seen together more frequently.

Finally, Spearman's rank correlations were employed to assess the relationship between the pathological conditions and population/sex subgroups. Additionally, spearman's correlations were calculated to further explore the relationship between each of the conditions, as well as the relationship between the conditions and asymmetry in the measurements. A value of -1 indicates a strongly negative correlation, while +1 indicates a strongly positive correlation showing a decreased and increased likelihood of diseases have an association, respectively.

5.4. Results

5.4.1. Repeatability testing

Observer repeatability for craniometric landmark positioning was tested to ensure accurate results. For intra-observer error, the mean dispersion values ranged between 0.28mm (SD ± 0.13) to 1.43mm (SD ± 1.87). While for inter-observer error, the value ranged between 0.36mm (SD ± 0.18) to 5.04mm (SD ± 2.86). Mean results of intra- and inter-observer measurement error of craniometric landmark positioning are summarised in Table 5.4. Overall, lower mean values were obtained for intra-observer compared to inter-observer mean values.

Table 5.4 *- Mean dispersion errors (mm) of craniometric landmark placement from 15 crania.*

Observations	**Intra-observer error**		**Inter-observer error**	
	Mean	**SD**	**Mean**	**SD**
	0.700	0.530	1.300	0.840

Figure 5.5 presents a graphical output depicting the comparison between mean values for intra- and inter-observer error for craniometric landmark placement on 15 crania. With regards to intra-observer repeatability, all craniometric landmarks presented with a measurement error of less than 2 mm, showing high intra-observer reproducibility. For inter-observer repeatability, majority of the craniometric landmarks presented with a measurement error of less than 2mm, while three landmarks, the right inferior orbital margin (22), and the right and left landmarks on the posterior margin of the mastoid (28, 30) fell above 2mm. The right inferior orbital margin landmark yielded an inter-observer error of 2.21mm, while the right and left landmark on the posterior margin of the mastoid yielded an inter-observer error of 5.04mm and 4.63mm, respectively. However, due to limited discrepancies with the intra-observer dispersion, the was considered acceptable and retained. Therefore, any asymmetrical differences noted I this region is assumed to be due to true asymmetry rather than measurement error. Overall, the repeatability testing showed high agreement for most of the craniometric landmarks.

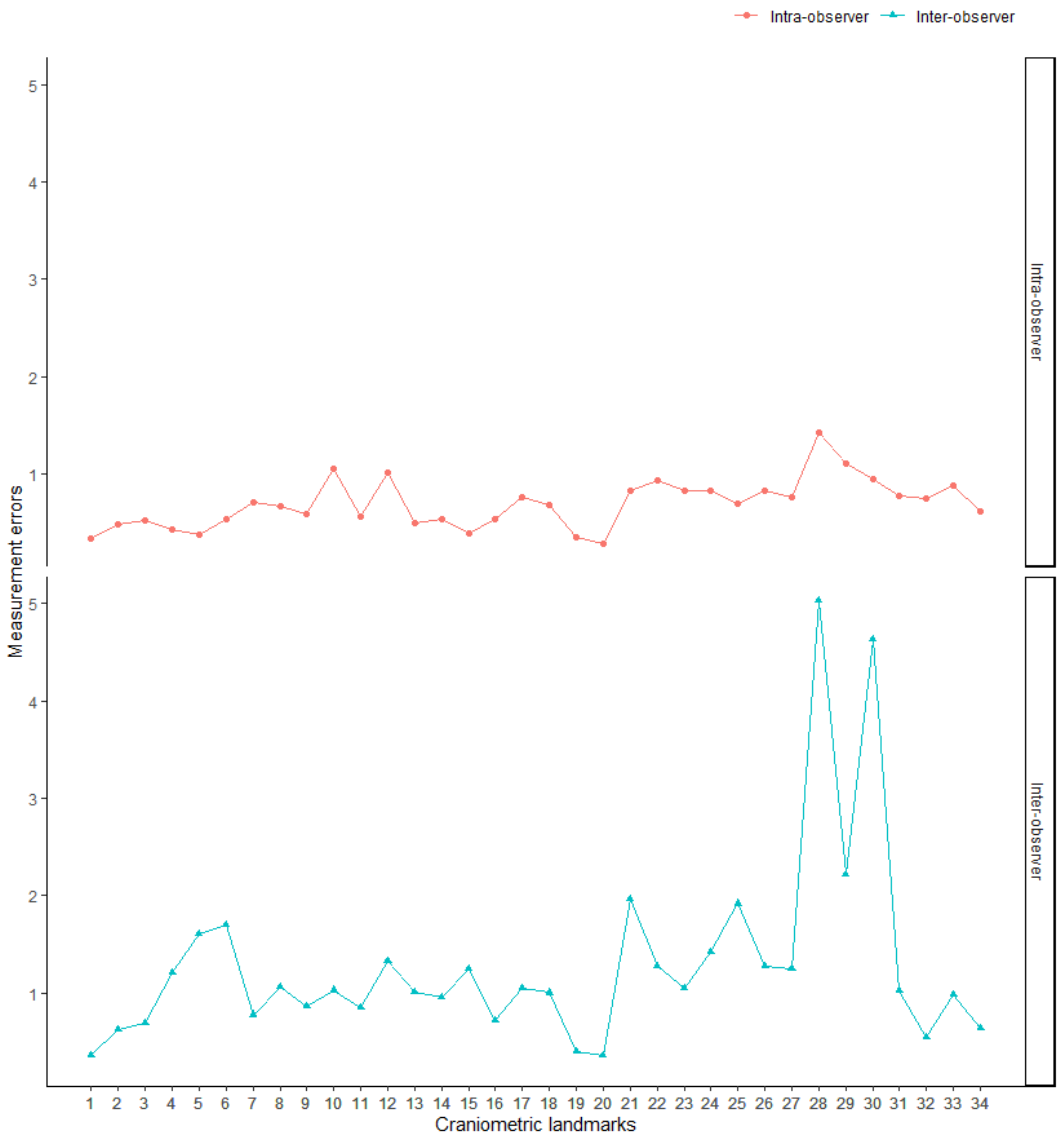

Figure 5.5 *- Graphical representation illustrating intra- and inter-observer mean dispersion values for landmark positioning.*

5.4.2. Descriptive statistics

Asymmetry values were calculated for each trait and each individual using the formulae adapted from Palmer and Strobeck (2003) to assess the presence of skeletal asymmetry (Table 5.3). First, FA8 (the difference between the natural logs of the left and right measurements of a trait) was calculated for each individual for each measurement. Majority of the mean asymmetry per trait was equal between males and females (see Table 5.5); however, differences in means were seen between males and females for MAH, MPB, MSAST AND NAAL. Next, FA17 (the total mean for all FA8

traits) was calculated to further explore asymmetry in a multivariate manner (see detailed results in Table 5.5). Only a slight difference was seen between males and females for the mean distribution of asymmetry. Descriptive statistics were also calculated for the population groups. Mean FA8 values were then analysed in population subgroups (Table 5.5). Differences between means for black and white South Africans were noted for MPB, MSAST and NAL; the rest of traits had similar mean distributions between black and white South Africans. For the FA17 results (detailed in Table 5.5), an equal mean distribution between the population groups was noted. Overall, of the 115 individuals in the sample, 26 individuals were found to express the most asymmetry (an individual was noted as asymmetrical with an FA17 value > than 0.05). Statistically significant asymmetrical differences were only seen between sexes for FA17 (which is the sum of all FA8 traits per an individual) and FA17_Temp (Mean total of FA8_MPL, FA8_MPB, FA8_MSAST and FA8_NMS). No asymmetrical differences were noted between population groups.

Table 5.5 *- Descriptive statistics for the mean values of FA8 and FA17 in females (F), males (M) and in the entire sample*

Trait Index	F (N=57)	M (N=58)	B (N=59)	W (N=56)	Total (N=115)
FA8_OBB					
Mean (SD)	0.026 (0.019)	0.029 (0.026)	0.024 (0.021)	0.031 (0.024)	0.027 (0.023)
Range	0.001 - 0.074	0.001 - 0.112	0.001 - 0.095	0.001 - 0.112	0.001 - 0.112
FA8_OBH					
Mean (SD)	0.030 (0.023)	0.027 (0.021)	0.028 (0.023)	0.029 (0.022)	0.028 (0.022)
Range	0.001 - 0.087	0.000 - 0.079	0.000 - 0.085	0.001 - 0.087	0.000 - 0.087
FA8_NOR					
Mean (SD)	0.024 (0.018)	0.021 (0.016)	0.020 (0.016)	0.025 (0.018)	0.023 (0.017)
Range	0.001 - 0.077	0.000 - 0.073	0.000 - 0.077	0.000 - 0.073	0.000 - 0.077
FA8_FMTN					
Mean (SD)	0.018 (0.014)	0.022 (0.015)	0.020 (0.013)	0.019 (0.016)	0.020 (0.015)
Range	0.000 - 0.059	0.001 - 0.066	0.000 - 0.049	0.000 - 0.066	0.000 - 0.066
FA8_FMTNS					
Mean (SD)	0.015 (0.012)	0.017 (0.014)	0.015 (0.014)	0.017 (0.012)	0.016 (0.013)
Range	0.000 - 0.044	0.000 - 0.065	0.000 - 0.065	0.001 - 0.058	0.000 - 0.065
FA8_MAH					

Mean (SD)	0.056 (0.045)	0.064 (0.054)	0.061 (0.048)	0.060 (0.052)	0.060 (0.050)
Range	0.000 - 0.174	0.004 - 0.234	0.000 - 0.204	0.006 - 0.234	0.000 - 0.234
FA8_MPL					
Mean (SD)	0.048 (0.035)	0.051 (0.038)	0.049 (0.040)	0.050 (0.034)	0.049 (0.037)
Range	0.001 - 0.142	0.002 - 0.148	0.001 - 0.148	0.009 - 0.142	0.001 - 0.148
FA8_MPB					
Mean (SD)	0.080 (0.072)	0.112 (0.101)	0.103 (0.107)	0.088 (0.064)	0.096 (0.089)
Range	0.000 - 0.420	0.004 - 0.511	0.000 - 0.511	0.004 - 0.262	0.000 - 0.511
FA8_MSAST					
Mean (SD)	0.056 (0.054)	0.074 (0.081)	0.057 (0.062)	0.073 (0.076)	0.065 (0.069)
Range	0.001 - 0.319	0.000 - 0.366	0.000 - 0.366	0.003 - 0.319	0.000 - 0.366
FA8_OCL					
Mean (SD)	0.069 (0.066)	0.075 (0.058)	0.069 (0.064)	0.075 (0.061)	0.072 (0.062)
Range	0.005 - 0.279	0.003 - 0.244	0.005 - 0.263	0.003 - 0.279	0.003 - 0.279
FA8_OPO					
Mean (SD)	0.023 (0.018)	0.021 (0.016)	0.020 (0.017)	0.023 (0.017)	0.022 (0.017)
Range	0.000 - 0.085	0.000 - 0.067	0.000 - 0.063	0.000 - 0.085	0.000 - 0.085
FA8_BAPO					
Mean (SD)	0.034 (0.031)	0.028 (0.021)	0.031 (0.027)	0.030 (0.026)	0.031 (0.026)

Range	0.000 - 0.121	0.001 - 0.093	0.001 - 0.105	0.000 - 0.121	0.000 - 0.121
FA8_NMS					
Mean (SD)	0.017 (0.011)	0.017 (0.013)	0.016 (0.012)	0.018 (0.012)	0.017 (0.012)
Range	0.000 - 0.046	0.001 - 0.054	0.001 - 0.048	0.000 - 0.054	0.000 - 0.054
FA8_NAL					
Mean (SD)	0.029 (0.019)	0.034 (0.027)	0.033 (0.023)	0.031 (0.024)	0.032 (0.023)
Range	0.000 - 0.082	0.001 - 0.097	0.000 - 0.097	0.000 - 0.096	0.000 - 0.097
FA8_NAAL					
Mean (SD)	0.061 (0.056)	0.071 (0.060)	0.061 (0.042)	0.071 (0.071)	0.066 (0.058)
Range	0.007 - 0.359	0.001 - 0.345	0.001 - 0.174	0.007 - 0.359	0.001 - 0.359
FA8_FA17					
Mean (SD)	0.039 (0.010)	0.044 (0.013)	0.041 (0.012)	0.043 (0.011)	0.042 (0.012)
Range	0.017 - 0.074	0.023 - 0.073	0.017 - 0.074	0.025 - 0.071	0.017 - 0.074

5.4.3. Frequency distribution and Kruskal-Wallis test

The frequency distributions were calculated for the presence of conditions and the results showed that 28/115 individuals presented with cribra orbitalia, 34/113 individuals presented with porotic hyperostosis, 40/92 individuals presented with enamel hypoplasia and 59/115 individuals presented with periostitis throughout the entire sample. The results were broken down to examine if significant differences were present between population, sex, and population and sex groups simultaneously.

Frequency distributions and Kruskal-Wallis tests provided results on the number of pathologies an individual had over the entire sample (0 = none, 1 = had one pathology, 2 = had two, 3 = had three and 4 = had four). Results were broken down to see the correlations between pathological lesion and populations, sex, and sex/population groups. Overall, 24 individuals had no pathological lesions, 45 individuals had one pathological lesion (24 had periostitis and 25 had enamel hypoplasia), 30 individuals had two pathological lesions (eight had enamel hypoplasia and periostitis, while seven had cribra orbitalia and periostitis), 13 individuals had three pathological lesions (six individuals had cribra orbitalia, porotic hyperostosis and periostitis, and four individuals had four pathological lesions).

The frequency of pathological lesions was then tested for correlations between the individuals that were noted asymmetrical based on the indices (n=26). Among these 26 asymmetrical individuals, four presented without any pathologies, nine individuals had one pathology, 11 individuals presented with two pathologies and two individuals had three pathologies. From these 26 asymmetrical individuals,13 had periostitis, nine had enamel hypoplasia and porotic hyperostosis and six had cribra orbitalia.

Significant differences for the presence of porotic hyperostosis were seen between black and white South Africans, with a high prevalence in black South Africans compared to white individuals ($p=0.003$). Significant differences were noted for enamel hypoplasia between black and white South Africans, with the occurrence being higher in black South Africans ($p=0.019$). Significant differences for disease frequency were seen between population groups with black South African individuals exhibiting at least more than three pathological lesions ($p=0.04$). While no other significant differences

were detected between populations for cribra orbitalia and periostitis. These results are detailed in Tables 5.6 and 5.7 and illustrated in Figures 5.6 and 5.7.

Table 5.6 *- Frequency distribution and Kruskal-Wallis results for the presence of pathological lesions between black and white South Africans (* Indicates significant differences between groups, p <0.05)*

	Cribra Orbitalia (n = 115)		**Porotic Hyperostosis (n = 113)**		**Enamel Hypoplasia (n = 92)**		**Periostitis (n = 115)**	
	0	**1**	**0**	**1**	**0**	**1**	**0**	**1**
Black	43	16	34	25	25	29	29	29
White	44	12	45	9	27	11	27	30
	KW: p = 0.479		KW: p = **0.003***		KW: p = **0.019***		KW: p = 0.779	

(0 = absent; 1 = present)

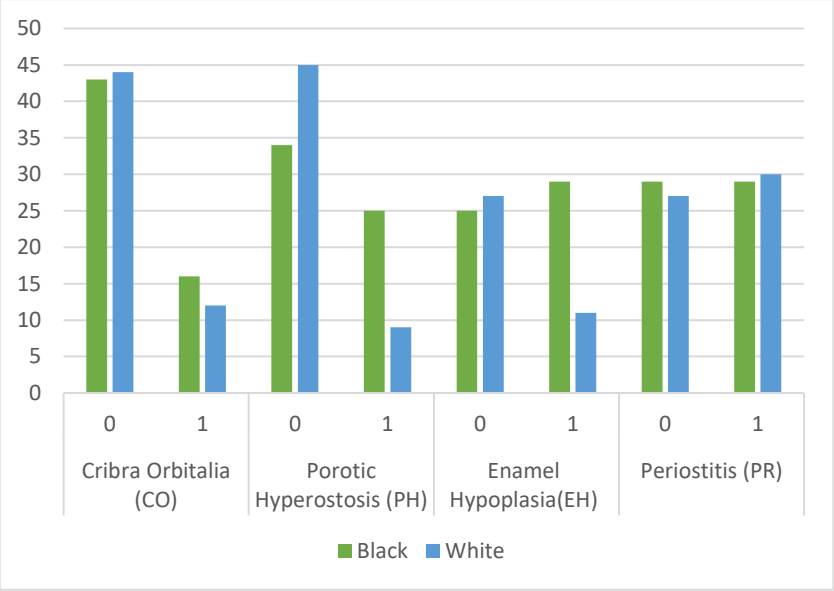

Figure 5.6 *- Frequency of pathological lesions absence (0) or presence (1) between black and white South Africans*

Table 5.7 *- Frequency of pathological lesions in black and white South Africans.* Indicates significant differences between populations (p<0.05)*

	Number of pathological lesions				
	0	1	2	3	4
black	9	20	15	11	4
white	15	25	15	2	0
N = 116					
					KW: p = **0.004***

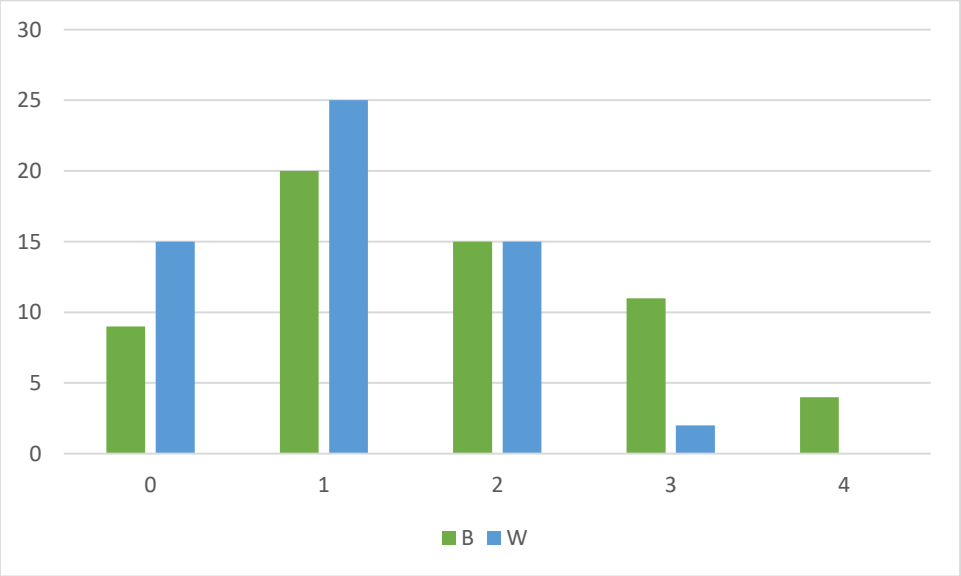

Figure 5.7 *- Bar plot illustrating the number of pathological lesions in black and white South Africans*

Statistically significant differences for porotic hyperostosis were noted between males and females, with males having a high prevalence for porotic hyperostosis (p=0.001). No significant sex differences were detected for enamel hypoplasia, where both males and females were equally affected. No other significant differences were observed between populations for cribra orbitalia and periostitis. Similarly, no significant differences were seen between females and males for disease frequency. These results are all detailed in Tables 5.8 and 5.9 and illustrated in Figures 5.8 and 5.9.

Table 5.8 *- Frequency distribution and Kruskal-Wallis results for the presence of pathological lesions between South African females and males. (* Indicates significant differences between groups, p <0.05)*

	Cribra Orbitalia (n = 115)		**Porotic Hyperostosis (n = 113)**		**Enamel Hypoplasia (n = 92)**		**Periostitis (n = 115)**	
	0	**1**	**0**	**1**	**0**	**1**	**0**	**1**
Female	45	13	48	9	27	20	29	29
Male	42	15	31	25	25	20	27	30
	KW: p = 0.627		KW: p = **0.001***		KW: p = 0.856		KW: p = 0.779	

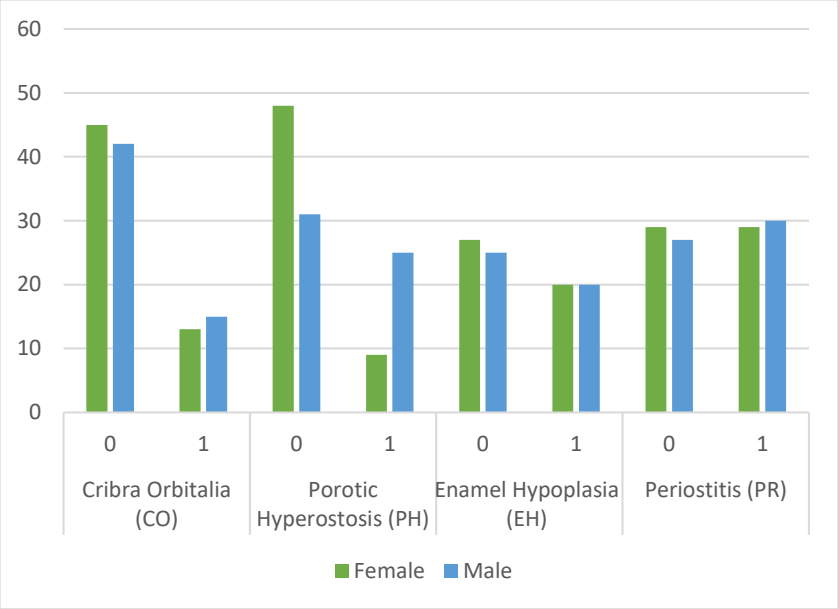

Figure 5.8 *- Frequency of pathological lesion absence (0) or presence (1) in South African females and males*

Table 5.9 *- Frequency of pathological lesions in South African males and females. * Indicates significant differences between populations (p<0.05)*

	Number of pathological lesions				
	0	**1**	**2**	**3**	**4**
Female	17	23	9	6	3
Male	7	22	21	7	1
N = 116					
					KW: p = 0.379

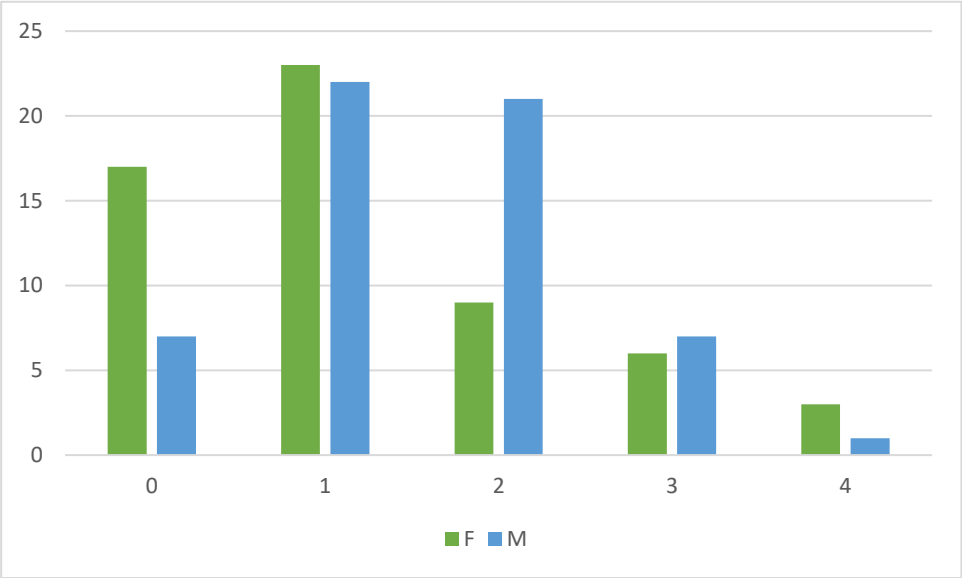

Figure 5.9 *- Bar plot illustrating the number of pathological lesions in South African females (F) and males (M)*

Lastly, black South African males showed the highest occurrence for porotic hyperostosis (p=0.00001); while no other statistically significant differences were observed between population and sex groups simultaneously, for any of the other conditions. Significant differences for disease frequency were noted in black South African males and females, exhibiting at least more than three pathological lesions (p=0.003). It should also be highlighted those black South African males exhibited the most pathological lesions among all subgroups. These results are detailed in Tables 5.10 and 5.11 and illustrated in Figures 5.10 and 5.11.

Table 5.10 *- Frequency distribution and Kruskal-Wallis results for the presence of pathological lesions between black and white South Africans females and males. (* Indicates significant differences between sex/population groups, p <0.05)*

	Cribra Orbitalia (n = 115)		Porotic Hyperostosis (n = 113)		Enamel Hypoplasia (n = 92)		Periostitis (n = 115)	
	0	**1**	**0**	**1**	**0**	**1**	**0**	**1**
BF	23	7	23	7	14	15	16	14
BM	20	9	11	18	11	14	13	15
WF	22	6	25	2	13	5	13	15
WM	22	6	20	7	14	6	14	15
	KW: p = 0.808		KW: p = **0.00001***		KW: p = 0.132		KW: p = 0.946	

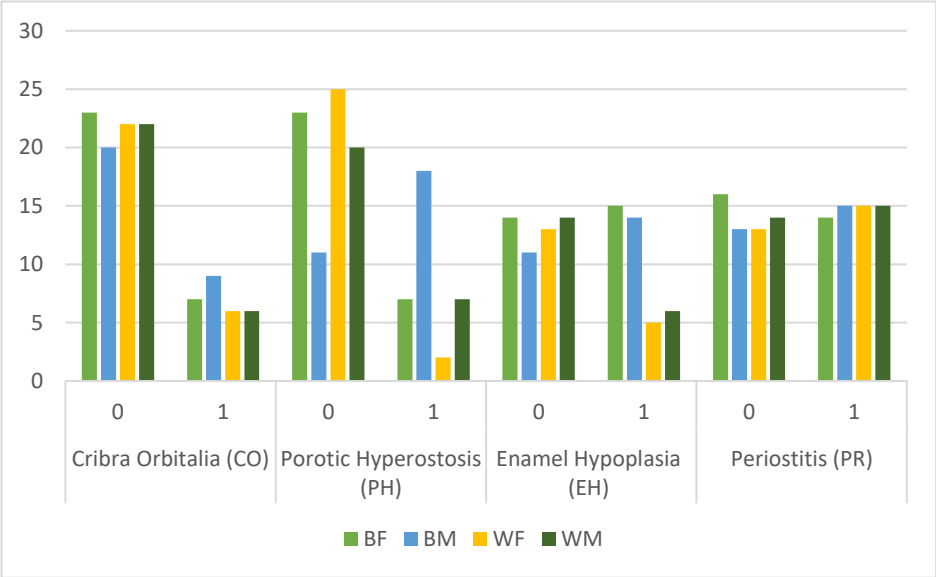

Figure 5.10 *- Bar plot illustrating the absence (0) or presence (1) of pathological lesions in black and white South African females and males*

Table 5.11 *- Frequency of pathological lesions in black and white South African males and females. * Indicates significant differences between populations (p<0.05)*

	Number of pathological lesions				
	0	**1**	**2**	**3**	**4**
BF	9	9	5	4	3
BM	0	11	10	7	1
WF	8	14	4	2	0
WM	7	11	11	0	0
N = 116					
					KW: p = 0,003*

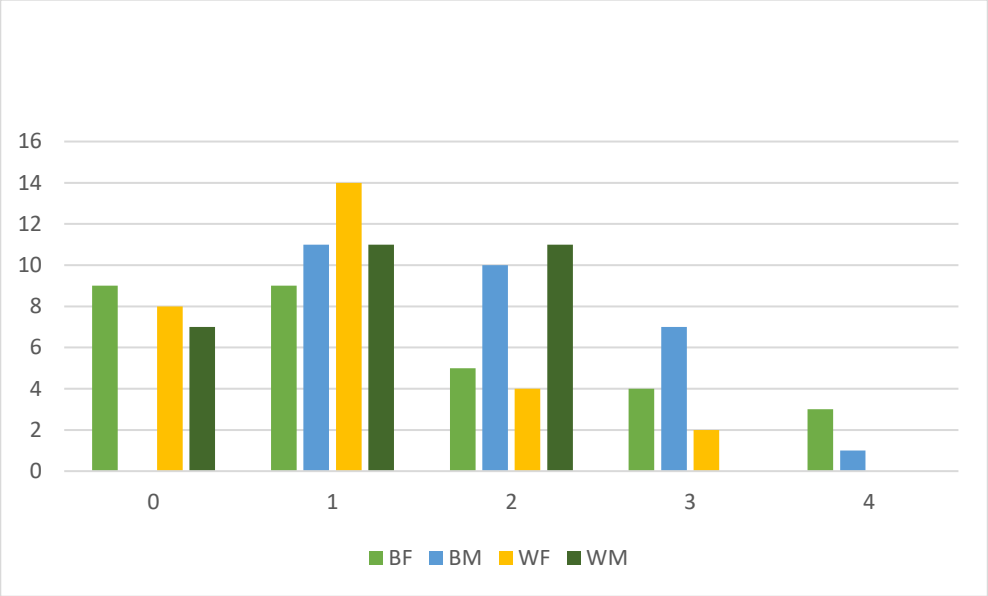

Figure 5.11 *- Bar plot illustrating the number of pathological lesions in black and white South African females and males*

5.4.4. Spearman's correlation tests

Spearman's correlations evaluate the association between diseases. In a pooled sample, a fair positive correlation (increased likelihood of having one with the other) was observed between cribra orbitalia and porotic hyperostosis, and between cribra orbitalia and periostitis (Table 5.12). Spearman's correlations were then run per sex and population groups and different patterns were noted. The correlation tests showed that white South Africans had a significantly fair negative correlation (decreased likelihood of having one with the other) between porotic hyperostosis and enamel

hypoplasia (p=0.036). However, black South Africans showed a significantly moderate positive association between cribra orbitalia and porotic hyperostosis (p=0.002), as well as between cribra orbitalia and periostitis (p=0.002) (Table 5.12). Interesting results were also noted when comparing the sexes. Indeed, males showed a moderate negative correlation between enamel hypoplasia and periostitis (p=0.003), while females showed a significantly moderate positive correlation between cribra orbitalia and porotic hyperostosis (p=0.000006). All other correlations were weak and not significant (Table 5.12).

Table 5.12 *- Spearman's correlation tests showing the relationships between diseases for a pooled sample, per population and per sex group. *Indicates significant correlations (p<0.05)*

	Spearman's correlations	Pooled	W	B	M	F
Cribra Orbitalia - Porotic Hyperostosis	**Correlation coefficient**	0.338	0.161	0.415	0.074	0.643
	P-value	**(0.0002)***	-0.340	**(0.002)***	-0.632	**(0.000006)***
Cribra Orbitalia - Enamel Hypoplasia	**Correlation coefficient**	-0.007	-0.024	-0.002	-0.122	0.128
	P-value	-0.947	-0.888	-0.991	-0.431	-0.391
Cribra Orbitalia - Periostitis	**Correlation coefficient**	0.208	-0.101	0.411	0.122	0.281
	P-value	**(0.027)***	-0.551	**(0.002)***	-0.431	-0.056
Porotic Hyperostosis - Enamel Hypoplasia	**Correlation coefficient**	0.036	-0.345	0.165	-0.086	0.183
	P-value	-0.753	**(0.036)***	-0.233	-0.581	-0.219
Porotic Hyperostosis- Periostitis	**Correlation coefficient**	0.063	-0.045	0.182	-0.01	0.236
	P-value	-0.507	-0.791	-0.189	-0.526	-0.110
Enamel Hypoplasia - Periostitis	**Correlation coefficient**	-0.170	-0.117	-0.146	-0.444	0.104
	P-value	-0.106	-0.790	-0.293	**(0.003)***	-0.489

Spearman’s correlations were also used to examine the relationship between pathological lesions and the presence of asymmetry (Table 5.13). Correlation tests were performed on pooled samples, per population and for each sex subgroup. When examining the pooled sample, there was no significant correlations between asymmetry and pathological lesions. Further examination was done according to sex and population. Only one fair and positive correlation was significant between the

presence of asymmetry and periostitis in white South Africans (p=0.027). No other significant correlations were observed.

Table 5.13 *- Spearman's correlation test showing the relationship between the presence of asymmetry and pathological lesions. * Indicates significant correlation*

	Spearman's correlations	Pooled	W	B	M	F
Asymmetry/Cribra Orbitalia	**Correlation coefficient**	-0.047	-0.053	-0.045	0.033	-0.186
	P-value	-0.655	-0.756	-0.744	-0.831	-0.210
Asymmetry/Porotic Hyperostosis	**Correlation coefficient**	0.033	0.092	-0.007	0.084	-0.173
	P-value	-0.753	-0.587	-0.959	-0.588	-0.244
Asymmetry/Enamel Hypoplasia	**Correlation coefficient**	0.008	-0.103	0.060	-0.035	0.058
	P-value	-0.938	-0.546	-0.665	-0.822	-0.701
Asymmetry/Periostitis	**Correlation coefficient**	0.090	0.363	-0.078	0.035	0.136
	P-value	-0.395	**(0.027)***	-0.576	-0.822	-0.363

5.5. Discussion and Conclusion

The health and wellness of an individual may have implications on the growth, development and remodelling of the human skeleton, which in turn may affect any skeletal analyses or medical procedures involving bone. Although the health and living conditions have improved in some areas of South Africa, little progress has been made with regards to the eradication of a myriad of socio-economic issues, inclusive of extreme poverty, a lack of access to healthcare and education, and unemployment (Bernitz et al., 2015; Steyn et al., 2016). These social issues are reflected in the unidentified human remains received by mortuaries and anthropologists annually (Steyn et al., 2016), as the deceased often represent the country's poor and destitute. An abundance of literature is available on the skeletal implications resulting from unfavourable or stressful living conditions (Wippert et al., 2017; McFadden and Oxenham, 2020). This study is the first to use a combination of skeletal material and micro-XCT scans to explore skeletal asymmetry and its association with the development of osteopathological lesions in a modern South African sample. While we may not know the population history and conditions of specific individuals in the sample, we are able to comment on the trends discussed in literature, the present South African context and what is observed on the skeletal remains in this sample.

The results from the present study indicated that certain regions of the cranium more frequently demonstrated significant differences between the left and right sides; this includes the orbital, nasal and temporal regions. It was important to note the cranial regions that are highly affected by asymmetry, as measurements or scoring done in these regions can be used in biological profile estimations, and thus high levels of asymmetry in these areas can affect classification accuracies. When assessing the FA17 indices, various multivariate combinations of all FA8 variables to better explore overall levels of asymmetry, only 26 individuals from the sample were significantly asymmetrical (individuals were considered asymmetric when FA17 >0.05). Among these 26 individuals, the most commonly observed lesions were sub-periosteal reactions (i.e., periostitis), which is not particularly surprising, given the multitude of causes that may lead to the formation of this type of lesion. Periostitis often occurs due to inflammation of the periosteum which can develop due to stress and poor living conditions but may also be due to chronic disease, such as cancer or as a result of

trauma or fractures (Waldron, 2003; Hagg et al., 2017). Interestingly, a significant correlation was seen between periostitis and asymmetry in the white South African population; however, the correlation was weak (r=0.363), and the possible relationship is not entirely understood. It is highly likely the case that many of the individuals that presented with periostitis suffered from other concurrent conditions as mentioned above. Ultimately, the presence of periostitis did not provide much information pertaining to developmental stress for this sample.

The next most prevalent conditions were porotic hyperostosis and enamel hypoplasia. In this study, it was found that porotic hyperostosis was frequently observed especially among black South Africans. Porotic hyperostosis is commonly caused by megaloblastic anaemia which is due to a vitamin B9 and B12 deficiency, typically related to nutrition (Walker at al., 2009). Due to the reported prevalence of nutritional deficiencies, particularly among black South Africans, and resulting from multidimensional poverty, there is an inadequate dietary intake of vitamins B12 due to lack of access of food containing these vitamins, and lack of access to medical care for vitamin supplementation (Gebremedhin, 2021). The Centre of Excellence in Food Security reported that South Africans commonly consume high-energy foods that are nutrient poor, such as carbohydrates and sugar (Makwela, 2017). Nutritional food for a well-balanced diet may often not be affordable; causing fast foods and carbohydrate diets to be favoured in South Africa, due both to their affordability and their accessibility (Makwela, 2017). Of course, it should be acknowledged that high energy, “fast food,” is often also preferred by South Africans over healthier, more nutritional options (Makwela, 2017). High-energy diets have been associated with obesity, which is currently on the rise in South Africa, particularly among black South African females (Micklesfield et al., 2013; Makwela, 2017). Vitamin B12 is required for the metabolism of carbohydrates; hence, diets rich in carbohydrates can result in a rapid depletion of vitamin B12 stores (Ling and Chow, 1953). Therefore, even with an adequate intake of vitamin B12, the body is unable to effectively absorb and use the nutrient in the case of carbohydrate-rich diets (Ling and Chow,1953). Individuals consuming a carbohydrate-rich diet may possibly be at risk for megaloblastic anaemia resulting in the development of porotic hyperostosis. Additionally, mothers who are vitamin B12 deficient can produce breast milk with inadequate vitamin B12 content, which can affect the nutrition of the infant (Eglash, 2020). With regards to this sample and their

recorded birth dates, many individuals from the Pretoria Bone Collection were living in the apartheid timeframe, and as such are assumed to have been impacted negatively due to their living conditions in those times. Hence, the high occurrence of porotic hyperostosis in the black South African sample can potentially be due to vitamin B12 deficiency or diets conducive to rapid B12 depletion (e.g., carbohydrate or fat rich diets). Similar findings were noted by Alblas (2019) and Zakai et al. (2009), as it was found that black South Africans showed a high prevalence of megaloblastic anaemia owing to malnutrition, parasite pathogens and poor socioeconomic status, particularly in rural areas in South Africa (Limpopo, Mpumalanga, and KwaZulu-Natal) that are endemic for malaria. A large proportion of black South African children and adults live in these areas due to apartheid assigned homelands forcing families to settle in these areas. Hence, individuals living in these regions are more prone to be affected by malaria. Research by Pradhan (2009) and Aggarwal et al., (2011) noted that malaria is linked to dyserythropoiesis caused by cytokines and growth factors, where the concentration levels will increase depending on the severity of the disease. These cytokines can induce the production for nitric oxide (NO) which decreases human erythropoiesis and can inhibit methionine synthase (Aggarwal et al., 2011). This in turn results in a functional vitamin B12 deficiency, which can lead to megaloblastic anaemia (Aggarwal et al., 2011). As such, parasite pathogens may have an influence on the prevalence of porotic hyperostosis, particularly in the black South African sample.

Additionally, vitamin B12 and folic acid deficiencies have shown to be caused by alcoholism as it decreases the absorption of these vitamins and causes inflammation and disruption of normal stomach functioning (Walker at al., 2009). In South Africa, there is a high consumption of alcohol. Statistical data has shown that 65,8% males consume alcohol and are from low socio-economic status (Frankenstein et al., 2018). Another reason for this trend may be due to the effects of migrant labour practice. In 2011, it was estimated that 60% of migrants in South Africa are male, of which 71,6% are black Africans (Ferraro and Weideman, 2020). Migrant labourers have poor living conditions in overcrowded areas far from their families, are highly exploited, and experiencing undernutrition and crime (Mazibuko, 2000). This may potentially explain the higher prevalence of porotic hyperostosis seen among black South African males. This has also been found in studies done by Alblas (2019) and Hens et al. (2019), in which men showed a significant higher prevalence of porotic hyperostosis and cribra

orbitalia than females. However, even if the reason for this is still unclear, it was theorised that it could explain the fact that males are shown to be more susceptible to disease and stressors (Alblas, 2019). This is in part due to the roles played by sex hormones. High levels of testosterone have shown to decrease immune function, thus increase susceptibility of illness and infection, which may play a role in the development of megaloblastic anaemia and increase porotic lesions in the male crania (Graham and Özener, 2016).

However, it should be noted that, while porotic hyperostosis had a higher frequency in males, cribra orbitalia and its correlation to porotic hyperostosis had a significant correlation in black South African females of this study. This was suspected, as previous studies have noted that black South African females are predisposed to megaloblastic anaemia, which is often due to a lack of access to health care, undernourishment, poor living conditions and teenage pregnancy. All these factors contributes to a high rate of vitamin B12 deficiency in females, which is linked to the pathogenesis of both cribra orbitalia and porotic hyperostosis (Rosso and Lederman, 1982; Alblas, 2019). Subsequently, the high rate of vitamin B12 deficiency in black South African females may be attributed to the excessive intake of energy rich foods, which have led up to a surge of obesity in this cohort (Micklesfield et al, 2013). Interestingly, studies have shown that vitamin B12 deficiencies are commonly observed in individuals suffering from obesity (Pinhas-Hamiel et al., 2006; Sun et al., 2019). Although black females did not show a significant frequency for cribra orbitalia or porotic hyperostosis like their male counterparts, females did show a significant correlation for having both cribra orbitalia and porotic hyperostosis, which might be due to their genetic predisposition to megaloblastic anaemia.

Similar to porotic hyperostosis, enamel hypoplasia was frequently seen in this sample. Enamel hypoplasia is linked to nutritional stress, infection, disease, and endocrine dysfunction during ontogeny (Waldron, 2003). The multifactorial cause of enamel hypoplasia can interrupt the normal formation of enamel resulting in defects, such as pits and lines on the enamel surface. Children raised in areas of low socioeconomic status are likely to show signs of enamel hypoplasia as a result of nutritional deficiencies and their living conditions. Enamel hypoplasia also has longevity into adulthood, as enamel cannot be replaced or remodelled once it has

formed (Hagg et al., 2017). Consequently, given the population history and possible living conditions of this sample during apartheid, black South Africans showed a high prevalence of enamel hypoplasia, as expected.

Lastly, as noted previously, a significant correlation between periostitis and cribra orbitalia was detected, particularly in black South Africans of this study. A possible aetiology for this occurrence may be scurvy. Indeed, scurvy is caused by a vitamin C deficiency, undernutrition, deficiency in folate and iron, or famine conditions (Cheung et al., 2003; Pimentel, 2003). In South Africa, this disease has mainly been linked to migrant workers, which, as mentioned previously, may form part of this sample (Van Der Merwe et al., 2010) . In scurvy, pathological pitting can also be seen on the lateral roofs of the orbits, the body of the sphenoid, the ethmoids as well as on the scapula; ossified haematomas and some periostitis may also be observed on the long bones (Snoddy et al., 2018). Alternatively, the link between cribra orbitalia and periostitis may be due to certain types of cancers, chronic infection or because an individual experienced poor living conditions in conjunction with bone traumas, such as fractures (Waldron, 2003; Hagg et al., 2017). However, a myriad of factors maybe be influencing this correlation and as such more research needs to be done to better understand this relationship.

Even though asymmetry has shown no significant correlation to pathological lesions, it should be acknowledged that lesions relating to cribra orbitalia, porotic hyperostosis and periostitis can often heal due to the plasticity and remodelling of bone, and thus not being observable in individuals who have a high FA index. Other explanations include the fact that signs of nutritional deficits may not produce skeletal lesion, or that individuals could have passed on before skeletal signs of stress were able to develop. Enamel hypoplasia on the other hand has shown to last into adulthood, as enamel cannot remodel or reform after permanent teeth have erupted (Hagg et al., 2017). Therefore, enamel hypoplasia may be a good indicator for stress in the South African population and should also be considered in future studies relating to fluctuating asymmetry.

In conclusion, this study has shown that both population history and sex may have a link to the expression of diseases. As such, future studies should take into consideration population history, and more importantly sex of the individuals, to better

understand the process and expression of diseases. Future research should also explore more in-depth correlations between pathological lesions, using other skeletal elements such as the pelvis or scapula to better understand patterns of lesions and their possible links to disease such as scurvy or types of cancers. While this study only found one link to pathological lesions and fluctuating asymmetry, future studies should still examine fluctuating asymmetry and its correlation to pathological lesions as stressors, and the ability to buffer stressors that can differ between populations and sex cohorts, as well as between traits. When possible, future studies should take into consideration the medical history and background of individuals to further explore this relationship.

5.6. References

Aggarwal, V., Maheshwari, A., Rath, B., Kumar, P., Basu, S., 2011. Refractory Pancytopenia and Megaloblastic Anaemia due to Falciparum Malaria. Journal of Tropical Pediatrics. 57, 283–285. https://doi.org/10.1093/tropej/fmq090

Alblas, A., 2019. Assessment of health status in a 20th century skeletal collection from the Western Cape 259. PhD thesis. Stellenbosch University. Available from: https://scholar.sun.ac.za/handle/10019.1/106020

Bernitz, H., Kenyhercz, M., Kloppers, B., Nöelle L'Abbé, E., Nicholas Labuschagne, G., Olckers, A., Myburgh, J., Saayman, G., Steyn, M., Stull, K., 2015. The History and Current Status of Forensic Science in South Africa, in: The Global Practice of Forensic Science. John Wiley & Sons, Ltd, pp. 241–259. https://doi.org/10.1002/9781118724248.ch23

Brook, A. 2009. Multilevel Complex Interactions Between Genetic, Epigenetic and Environmental Factors in the Aetiology of Anomalies of Dental Development. Archives of Oral Biology. 54s:s3-s17. https://doi.org/10.1016/j.archoralbio.2009.09.005

Casna, M., Schrader, S., 2022. Urban Beings: A Bioarchaeological Approach to Socioeconomic Status, Cribra Orbitalia, Porotic Hyperostosis, Linear Enamel Hypoplasia, and Sinusitis in the Early-Modern Northern Low Countries (A.D. 1626–1850). Bioarchaeology International https://doi.org/10.5744/bi.2022.0001

Cheung, E., Mutahar, R., Assefa, F., Ververs, M.-T., Nasiri, S.M., Borrel, A., Salama, P., 2003. An Epidemic of Scurvy in Afghanistan: Assessment and Response. Food Nutrition Bulletin 24, 247–255. https://doi.org/10.1177/156482650302400302

Coolidge, R., 2015. The Relationship of Childhood Stress to Adult Health and Mortality Among Individuals from Two U.S. Documented Skeletal Collections, Late 19th to Early 20th Centuries. Graduate Theses and Dissertations. Available from: https://scholarcommons.usf.edu/etd/5929 (accessed 2.10.21)

Daniel, L., 2020. One In Five South Africans Now Lives on Less Than R28 a Day, The UN Finds, Business insider. Available from: https://www.businessinsider.co.za/heres-how-many-south-africans-live-on-less-than-r28-a-day-and-why-its-getting-worse-2020-12 (accessed 7.24.22)

Eglash, A., 2020. Breastfeeding and Maternal/Child Vitamin B12 Deficiency. The Institute for Advancement of Breastfeeding and Lactation Education IABLE. Available from: https://lacted.org/questions/0197-vitamin-b12-deficiency-breastfeeding/ (accessed 11.24.22)

Ferraro, F., Weideman, M., 2020. Labour-Related Experience of Migrants and Refugees in South Africa. The Future of Work Labour and Migration in the 21st Century. Available from: https://icmc.net/future-of-work/report/04-south-africa (accessed 11.24.22)

Fogel, R., 2019. Informal Housing, Poverty, and Legacies of Apartheid in South Africa | Urban@UW. Available from: https://urban.uw.edu/news/informal-housing-poverty-and-legacies-of-apartheid-in-south-africa/ (accessed 10.14.22).

Gawlikowska, A., Szczurowski, J., Czerwiński, F., Miklaszewska, D., Adamiec, E., Dzieciołowska, E., 2007. The Fluctuating Asymmetry of Medieval and Modern Human Skulls. Journal of Comparative Human Biology 58, 159–172. https://doi.org/10.1016/j.jchb.2006.10.001

Gebremedhin, S., 2021. Trends in Vitamin B12 Supply and Prevalence of Inadequate Intake in Africa: Regional and Country-Specific Estimates. Food Nutrition Bulletin 42, 467–479. https://doi.org/10.1177/03795721211043353

Graham, J., Özener, B., 2016. Fluctuating Asymmetry of Human Populations: A Review. Symmetry 8, 154.https://doi.org/10.3390/sym8120154

Goodman, A., Rose, J. 1990. Assessment of Systemic Physiological Perturbations from Dental Enamel Hypoplasias and Associated Histologial Structures. Year of Physical Anthropology. 33:59-110. https://doi.org/10.1002/ajpa.1330330506

Hagg, A.C., 2016. Assessment of Skeletal and Dental Fluctuating Asymmetry in Two Historic Dutch Populations. MSc Thesis, University of Pretoria, South Africa.226. Available from: http://hdl.handle.net/2263/56936 (accessed 7.7.20)

Hagg, A.C., Van der Merwe, A.E., Steyn, M., 2017. Developmental instability and its relationship to mental health in two historic Dutch populations. International Journal of Paleopathology. 17, 42–51. https://doi.org/10.1016/j.ijpp.2017.04.001

Harris, E.F., Nweeia, M.T., 1980. Dental Asymmetry as a Measure of Environmental Stress in the Ticuna Indians of Colombia. American Journal of Physical Anthropology 53, 133–142. https://doi.org/10.1002/ajpa.1330530118

Hens, S.M., Godde, K., Macak, K.M., 2019. Iron Deficiency Anaemia, Population Health, and Frailty in a Modern Portuguese Skeletal Sample. PLOS One 14, e0213369. https://doi.org/10.1371/journal.pone.0213369

Kim, J., Lee, J., Shin, J.-Y., Park, B.-J., 2015. Socioeconomic Disparities in Osteoporosis Prevalence: Different Results in the Overall Korean Adult Population and Single-person Households. Journal of Preventive Medicine and Public Health 48, 84–93. https://doi.org/10.3961/jpmph.14.047

Krüger, G.C., L'Abbé, E.N., Stull, K.E., Kenyhercz, M.W., 2015. Sexual Dimorphism in Cranial Morphology Among Modern South Africans. International Journal of Legal Medicine 129, 869–875. https://doi.org/10.1007/s00414-014-1111-0

L'Abbé, E.N., Krüger, G.C., Theye, C.E.G., Hagg, A.C., Sapo, O., 2021. The Pretoria Bone Collection: A 21st Century Skeletal Collection in South Africa. Forensic Science 1, 220–227. https://doi.org/10.3390/forensicsci1030020

L'Abbé, E.N., Loots, M., Meiring, J.H., 2005. The Pretoria Bone Collection: A Modern South African Skeletal Sample. HOMO 56, 197–205. https://doi.org/10.1016/j.jchb.2004.10.004

Liebenberg, L., Krüger, G.C., L'Abbé, E.N., Stull, K.E., 2019. Postcraniometric Sex and Ancestry Estimation in South Africa: A Validation Study. International Journal of Legal Medicine 133, 289–296. https://doi.org/10.1007/s00414-018-1865-x

Liljequist, D., Elfving, B., Roaldsen, K.S., 2019. Intraclass Correlation – A Discussion and Demonstration of Basic Features. PLOS ONE 14, 1–35. https://doi.org/10.1371/journal.pone.0219854

Linford, A., 2017. Inequality Trends in South Africa. GeoCurrents. Available from: https://www.geocurrents.info/economic-geography/inequality-trends-in-south-africa (accessed 10.14.22)

Ling, C.T., Chow, B.F., 1953. Effect of Vitamin B12 on the Levels of Soluble Sulfhydryl Compounds in Blood. Journal of Biological Chemistry 202, 445–456.

Livshits, G., Davidi, L., Kobyliansky, E., Ben-Amitai, D., Levi, Y., Merlob, P., Optiz, J.M., Reynolds, J.F., 1988. Decreased Developmental Stability as Assessed by Fluctuating Asymmetry of Morphometric Traits in Preterm Infants. American Journal of Medical Genetics 29, 793–805. https://doi.org/10.1002/ajmg.1320290409

Makwela, M., 2017. Too much sugar and carbs in South African Diet. Centre of Excellence. Available from: https://foodsecurity.ac.za/news/too-much-sugar-and-carbs-in-south-african-diet/ (accessed 11.24.22).

Mazibuko, R.P., 2000. The Effects of Migrant Labour on The Family System.

McFadden, C., Oxenham, M.F., 2020. A Paleoepidemiological Approach to The Osteological Paradox: Investigating Stress, Frailty and Resilience Through Cribra Orbitalia. American Journal of Physical Anthropology 173, 205–217. https://doi.org/10.1002/ajpa.24091

Micklesfield, L.K., Lambert, E.V., Hume, D.J., Chantler, S., Pienaar, P.R., Dickie, K., Puoane, T., Goedecke, J.H., 2013. Socio-Cultural, Environmental and Behavioural Determinants of Obesity in Black South African Women. The Cardiovascular Journal of Africa 24, 369–375. https://doi.org/10.5830/CVJA-2013-069

Miszkiewicz, J.J., Cooke, K.M., 2019. Socio-economic Determinants of Bone Health from Past to Present. Clinical Reviews in Bone and Mineral Metabolism 17, 109–122. https://doi.org/10.1007/s12018-019-09263-1

Ng, J.-S., Chin, K.-Y., 2021. Potential Mechanisms Linking Psychological Stress to Bone Health. International Journal of Medical Science 18, 604–614. https://doi.org/10.7150/ijms.50680

Ortner, D.J., 2003. Identification of Pathological Conditions in Human Skeletal Remains. London: Academic Press. ISBN: 9780128097380

Ortner, D.J., 2019. Ortner's identification of pathological conditions in human skeletal remains, 2nd edition. ed, Smithsonian contributions to anthropology. Academic Press, London, England.

Palmer, A., Strobeck, C., 2003. Fluctuating Asymmetry and Developmental Stability: Heritability of Observable Variation vs. Heritability of Inferred Cause. Journal of Evolutionary Biology 10, 39–49. https://doi.org/10.1046/j.1420-9101.1997.10010039.x

Perini, T.A., de Oliveira, G.L., 2005. Technical Error of Measurement in Anthropometry. Revista Brasileira de Medicina do Esporte 11,5. https://doi.org/10.1590/S1517-86922005000100009

Pimentel, L., 2003. Scurvy: Historical Review and Current Diagnostic Approach. American Journal of Emergency Medicine 21, 328–332. https://doi.org/10.1016/s0735-6757(03)00083-4

Pinhas-Hamiel, O., Doron-Panush, N., Reichman, B., Nitzan-Kaluski, D., Shalitin, S., Geva-Lerner, L., 2006. Obese Children and Adolescents: A Risk Group for Low Vitamin B12 Concentration. The Archives of Paediatrics & Adolescent Medicine160, 933–936. https://doi.org/10.1001/archpedi.160.9.933

Pradhan, P., 2009. Malarial Anaemia and Nitric Oxide Induced Megaloblastic Anaemia: A Review on The Causes of Malarial Anaemia. Journal of Vector Borne Diseases 46, 100–108.

R Core Team. 2016. R: A Language and Environment for Statistical Computing. R Foundation for Statistical Computing, Vienna, Austria. Available from: https://www.R-project.org/ (accessed 11.4.2020)

Rinaldo, N., 2018. How Reliable is the Assessment of Porotic Hyperostosis and Cribra Orbitalia in Skeletal Human Remains?

A Methodological Approach for Quantitative Verification by Means of a New Evaluation Form. Archaeological and Anthropological Sciences 11. https://doi.org/10.3390/sym10070232

Rosso, P., Lederman, S.A., 1982. Nutrition in The Pregnant Adolescent. Current Concepts of Maternal Nutrition 11, 47–62.

Salvadei, L., Ricci, F., Manzi, G., 2001. Porotic Hyperostosis as a Marker of Health and Nutritional Conditions During Childhood: Studies at the Transition Between Imperial Rome and the Early Middle Ages. American Journal of Human Biology 13, 709–717. https://doi.org/10.1002/ajhb.1115

Schoonjans, F., 2020. Intraclass Correlation Coefficient. MedCalc. Available from: https://www.medcalc.org/manual/intraclasscorrelation.php (accessed 3.31.20).

Schuurs, A. 2013. Pathology of the Hard Dental Tissues. West Sussex: John Wiley & Sons.

Snoddy, A.M.E., Buckley, H.R., Elliott, G.E., Standen, V.G., Arriaza, B.T., Halcrow, S.E., 2018. Macroscopic Features of Scurvy in Human Skeletal Remains: A Literature Synthesis and Diagnostic Guide. American Journal of Physical Anthropology 167, 876–895. https://doi.org/10.1002/ajpa.23699

Steyn, M., L'Abbé, E.N., Myburgh, and J., 2016. Forensic Anthropology as Practiced in South Africa, in: Handbook of Forensic Anthropology and Archaeology. Routledge.

Stoddard, E., 2022. Dismal ascent: South African Unemployment Rate Hits Record 35.3% In Q4 2021. Daily Maverick. Available from:

https://www.dailymaverick.co.za/article/2022-03-29-south-african-unemployment-rate-hits-record-35-3-in-q4-2021/ (accessed 7.24.22)

Storm, R.A., 2009. Human Skeletal Asymmetry. A Study of Directional and Fluctuating Asymmetry in Assessing Health, Environmental Conditions, and Social Status in English Populations from the 7th to the 19th Centuries. Doctor of Philosophy. University of Bradford. Available from: http://hdl.handle.net/10454/4325 (accessed 2.9.21)

Sun, Y., Sun, M., Liu, B., Du, Y., Rong, S., Xu, G., Snetselaar, L.G., Bao, W., 2019. Inverse Association Between Serum Vitamin B12 Concentration and Obesity Among Adults in the United States. Front. Endocrinol. 10.

Frankenstein, P.J., Majorelle, N.K., Lombard, C., Jernigan, D.H., Parry, C.D.H., 2018. Heavy Drinking And Contextual Risk Factors Among Adults In South Africa : Findings From the International Alcohol Control Study. Substance Abuse Treatment, Prevention, And Policy 13, 43. https://doi.org/10.1186/s13011-018-0182-1

Upex, B., Dobney, K., 2012. Dental Enamel Hypoplasia as Indicators of Seasonal Environmental and Physiological Impacts in Modern Sheep Populations: A Model for Interpreting the Zooarchaeological Record. Journal of Zoology 287, 259–268. https://doi.org/10.1111/j.1469-7998.2012.00912.x

Van Der Merwe, A.E., Ribot, I., Morris, D., Steyn, M., Maat, G.J.R., 2010. The Origins of Late Nineteenth-Century Migrant Diamond Miners Uncovered in a Salvage Excavation in Kimberley, South Africa. South African Archaeological Bulletin 65, 175–184.

Walker, P., Bathurst, R., Richman, R., Gjerdrum, T., Andrushko, V., 2009. The Cause of Porotic Hyperostosis and Cribra Orbitalia: A Reappraisal of the Iron-Deficiency-Anemia Hypothesis. American Journal of Physical Anthropology. 139, 109-125. https://doi.org/10.1002/ajpa.21031

Wippert, P.-M., Rector, M., Kuhn, G., Wuertz-Kozak, K., 2017. Stress and Alterations in Bones: An Interdisciplinary Perspective. Frontiers in Endocrinology 8, 96. https://doi.org/10.3389/fendo.2017.00096

Zakai, N.A., McClure, L.A., Prineas, R., Howard, G., McClellan, W., Holmes, C.E., Newsome, B.B., Warnock, D.G., Audhya, P., Cushman, M., 2009. Correlates of Anemia in American Blacks and Whites. American Journal of Epidemiology 169, 355–364. https://doi.org/10.1093/aje/kwn355

Zariņa, G., Sholts, S.B., Tichinin, A., Rudovica, V., Vīksna, A., Engīzere, A., Muižnieks, V., Bartelink, E.J., Wärmländer, S.K.T.S., 2016. Cribra Orbitalia as a Potential Indicator of Childhood Stress: Evidence from Paleopathology, Stable C, N, And O Isotopes, and Trace Element Concentrations in Children from A 17th -18th Century Cemetery in Jl·kabpils, Latvia. Journal of Trace Elements in Medicine and Biology 38, 131–137. https://doi.org/10.1016/j.jtemb.2016.05.008

Chapter 6 - Discussion and Conclusion

Biological anthropologists study health and diseases to better understand the implications and impacts of these diseases on skeletal health, formation, and variation. By measuring fluctuating asymmetry (an indicator of developmental stress) within and between populations, anthropologists can understand the overall impact stressors, such as a disease, can have on skeletal remains (Graham and Özener, 2016). While living conditions in certain regions of South Africa have improved, the long-lasting effects of apartheid are still apparent on a socio-economic level (Bernitz et al., 2015; Steyn et al., 2016). Currently, many South Africans are in a state of multidimensional poverty, resulting in a lack of basic needs and resources, as well as high rates of unemployment. Stressful and poor living conditions can, therefore, negatively impact these individuals, and thus have implications on skeletal growth, health, and formation (Daniel, 2020; Stoddard, 2022). This is the first research project using a combination of skeletal material and micro-XCT scans to explore skeletal asymmetry and its association with the development of osteopathological lesions in a modern South African sample. The overall aim of this study was to assess skeletal asymmetry and indicators of developmental stress in a South African sample.

The results indicated that significant asymmetrical patterns were frequently observed in the orbital, nasal and temporal regions of the cranium. This was seen for both inter-landmark distances and GMM. Asymmetry in the temporal bones and orbits was consistent with findings in the literature (Storm and Knusel, 2005; Gawlikowaka et al., 2007; DeLeon, 2007; Hagg et al., 2017). The temporal regions are often influenced by the environment and has no genetic constraints, while craniofacial traits, often thought to be under strict genetic control, may exhibit genetic variation pertaining to factors such a sex, population, environment, and growth and development (von Cramon-Taubadel, 2014). Therefore, the results of the present study correspond with the literature, showing that the expression of FA fluctuates across traits and matrices (Møller and Swaddle, 1997; Storm, 2009; Blackburn, 2011; Hagg et al., 2017). Due to the population history and environmental conditions of the South African population, a high prevalence of asymmetry and its influence in different regions of the crania is expected.

In this study, it was important to note the cranial regions that are highly affected by asymmetry. Measurements or scoring done in these asymmetrical regions can be used in biological profile estimations and thus high levels of asymmetry in these areas can affect classification accuracies. For example, Walker's (2008) traits for sex estimation employ the orbits and mastoids on the temporal bones for scoring; similarly, Hefner (2009) scores the shape of the orbits for population affinity estimation. Measurements from these regions are often used for sex and population affinity estimations. While the potential influence of asymmetry on biological profile estimates may be minimal when taking measurements, anthropologists should be mindful and conservative with the sides and elements being used individually. In terms of morphological scoring, both left and right sides should be included in the scores, especially when scoring the orbits and mastoids, as this may potentially influence estimates in the South African population due to the prevalence of asymmetry observed in these specific areas. Additionally, medical doctors should consider the large variation and asymmetry seen in the South African sample, especially when drawing up their craniofacial treatment plan.

To assess the correlation between asymmetry and pathological lesions, FA17 indices were calculated. Twenty-six individuals from the sample were found to be significantly asymmetrical (FA17>0.05). Amongst these 26 individuals, periostitis was the most frequently observed lesions. This is not particularly surprising, given the multitude of causes that may lead to the formation of this type of lesion. Periostitis is predominantly observed in populations faced with stressful and poor living conditions. Periostitis can also be present in cases where an individual suffered from a chronic disease (e.g., cancer) or trauma (e.g., fractures) (Waldron, 2003; Hagg et al., 2017). These factors may all play a role in the inflammation of the periosteum, causing the stripping away of bone (Waldron, 2003; Hagg et al., 2017). A significant but weak correlation (r=0.363) was observed in the white South African population between periostitis and asymmetry. However, this relationship is only partially understood. Ultimately, the presence of periostitis did not provide much information pertaining to developmental stress for this sample.

While the statistical analysis detected little to no correlation between asymmetry and stress indicators, it is worth noting that in this sample, black South African individuals

had the most pronounced craniofacial asymmetry for the majority of the cranial traits, and the highest prevalence of disease, particularly porotic hyperostosis and enamel hypoplasia. In this sample, Black South Africans have experienced developmental stressors, especially since many individuals lived during apartheid (according to their birth dates) and may have been impacted negatively due to their living conditions. While cranial asymmetry is likely a consequence of population history and low-socioeconomic status, pathological lesions are likely a sign of nutritional deficiency brought on by low-socioeconomic status. Porotic hyperostosis has been largely attributed to megaloblastic anaemia which is commonly linked to vitamin B9 or B12 deficiencies (Walker at al., 2009). In South African, the possible causes for an inadequate intake of B12 can largely be linked to diets conducive to rapid vitamin B12 depletion (e.g., carbohydrates or fat-rich diets) or a predisposed deficiency to vitamin B12. Enamel hypoplasia, linked to nutritional stress may also occur due to infection, disease, or stressful living conditions. As such, South African children raised in areas of low socioeconomic status are likely to show signs of enamel hypoplasia as a result of nutritional deficiencies and their living conditions. Consequently, enamel hypoplasia, which has longevity into adulthood as enamel cannot be replaced or remodelled once it has formed, will therefore be observable in South African adults (Hagg et al., 2017). Given the following results, and even though no statistically significant relationship exists between asymmetry and developmental stressors, the high presence of asymmetry and disease in the black South African cohort may be insightful on the role of health and disease and their implications on skeletal formation.

To conclude, even though asymmetry has shown no statistical significance to pathological lesions and asymmetry – lesions relating to cribra orbitalia, porotic hyperostosis, and periostitis – can often heal due to the plasticity and remodelling of bone. As a result, these lesions may not be present in individuals who have a high FA index. Other explanations include the fact that signs of nutritional deficits may not produce skeletal lesion, or that individuals could have passed on before skeletal signs of stress were able to develop. On the other hand, enamel hypoplasia has been shown to remain into adulthood and thus may be a useful tool for assessing asymmetry (Hagg et al., 2017).

Overall, this study, using a combination of virtual and traditional methods, has shown that craniofacial asymmetry is prevalent in the South African population and that asymmetrical differences exist between sexes and populations. It was also found that sex and population affinity play an essential role in the expression of the four types of disease assessed in this study. The cranium was highly informative for the assessment of fluctuating asymmetry, especially when using geometric morphometric methods. Furthermore, asymmetrical differences were observed to be more important in shape than in size.

Future research could benefit from using dentition to assess fluctuating asymmetry and its relationship to enamel hypoplasia. Furthermore, future studies should examine fluctuating asymmetry and its correlation to pathological lesions, as stressors and the ability to buffer stressors can differ between populations, sexes, and traits. These studies should also consider using living samples with known medical information and backgrounds.

Chapter 7- REFERENCES

Aggarwal, V., Maheshwari, A., Rath, B., Kumar, P., Basu, S., 2011. Refractory Pancytopenia and Megaloblastic Anaemia due to Falciparum Malaria. Journal of Tropical Pediatrics. 57, 283–285. https://doi.org/10.1093/tropej/fmq090

Akhil, G., Senthil Kumar, K.P., Raja, S., Janardhanan, K., 2015. Three-Dimensional Assessment of Facial Asymmetry: A Systematic Review. Journal of Pharmacy Bioallied Science 7, S433–S437. https://doi.org/10.4103/0975-7406.163491

Alblas, A., 2019. Assessment of health status in a 20th century skeletal collection from the Western Cape 259. PhD thesis. Stellenbosch University. Available from: https://scholar.sun.ac.za/handle/10019.1/106020

Andronowski, J.M., Crowder, C. and Soto Martinez, M. 2018. Recent Advancements in the Analysis of Bone Microstructure: New Dimensions in Forensic Anthropology. Forensic Sciences Research 3(4),294–309. https://doi.org/10.1080/20961790.2018.1483294

Anison, J.J., Rajasekar, L., Ragavendra, B., 2015. Understanding Asymmetry – A Review. Biomedical and Pharmacology Journal 8, 659–668. https://dx.doi.org/10.13005/bpj/764

Auerbach, B.M., Ruff, C.B., 2006. Limb Bone Bilateral Asymmetry: Variability and Commonality Among Modern Humans. Journal of Human Evolution 50, 203–218. https://doi.org/10.1016/j.jhevol.2005.09.004

Barrett, C.K.; Guatelli-Steinberg, D.; Sciulli, P.W., 2012. Revisiting Dental Fluctuating Asymmetry in Neanderthals and Modern Humans. American Journal of Physical Anthropology 149, 193–204. https://doi.org/10.1002/ajpa.22107

Blackburn, A., 2011. Bilateral Asymmetry of the Humerus During Growth and Development. American Journal of Physical Anthropology 145, 639–646. https://doi.org/10.1002/ajpa.21555

Benítez, H.A., Lemic, D., Villalobos-Leiva, A., Bažok, R., Órdenes-Claveria, R., Pajač Živković, I., Mikac, K.M., 2020. Breaking Symmetry: Fluctuating Asymmetry and Geometric Morphometrics as Tools for Evaluating Developmental Instability under Diverse Agroecosystems. Symmetry 12, 1789. https://doi.org/10.3390/sym12111789

Benazzi, S., Coquerelle, M., Fiorenza, L., Bookstein, F., Katina, S., Kullmer, O., 2011. Comparison of Dental Measurement Systems for Taxonomic Assignment of First Molars. American Journal of Physical Anthropology 144:342–354. https://doi.org/10.1002/ajpa.21409

Bernitz, H., Kenyhercz, M., Kloppers, B., Nöelle L'Abbé, E., Nicholas Labuschagne, G., Olckers, A., Myburgh, J., Saayman, G., Steyn, M., Stull, K., 2015. The History and Current Status of Forensic Science in South Africa, in: The Global Practice of Forensic Science. John Wiley & Sons, Ltd, pp. 241–259. https://doi.org/10.1002/9781118724248.ch23

Bigoni, L., Krajíček, V., Sládek, V., Velemínský, P., Velemínská, J., 2013. Skull Shape Asymmetry and the Socioeconomic Structure of an Early Medieval Central European Society. American Journal of Physical Anthropology 150, 349–364. https://doi.org/10.1002/ajpa.22210

Brook, A. 2009. Multilevel Complex Interactions Between Genetic, Epigenetic and Environmental Factors in the Aetiology of Anomalies of Dental Development. Archives of Oral Biology. 54s:s3-s17. https://doi.org/10.1016/j.archoralbio.2009.09.005

Caple, J., Stephan, C.N., 2016. A Standardized Nomenclature for Craniofacial and Facial Anthropometry. International Journal of Legal Medicine 130, 863–879. https://doi.org/10.1007/s00414-015-1292-1

Casna, M., Schrader, S., 2022. Urban Beings: A Bioarchaeological Approach to Socioeconomic Status, Cribra Orbitalia, Porotic Hyperostosis, Linear Enamel Hypoplasia, and Sinusitis in the Early-Modern Northern Low Countries (A.D. 1626–1850). Bioarchaeology International https://doi.org/10.5744/bi.2022.0001

Cavalcanti, M., Rocha, S., Vannier, M., 2004. Craniofacial measurements based on 3D-CT volume rendering: implications for clinical applications. Dentomaxillofacial Radiology 33, 170–176. https://doi.org/10.1259/dmfr/13603271

Cheong, Y.-W., Lo, L.-J., 2011. Facial Asymmetry: Etiology, Evaluation, and Management 34, 11. PMID: 21880188

Cheung, E., Mutahar, R., Assefa, F., Ververs, M.-T., Nasiri, S.M., Borrel, A., Salama, P., 2003. An Epidemic of Scurvy in Afghanistan: Assessment and Response. Food Nutrition Bulletin 24, 247–255. https://doi.org/10.1177/156482650302400302

Cohen, J.M., 2005. Comparing Digital and Conventional Cephalometric Radiographs. American Journal of Orthodontics and Dentofacial Orthopedics 128, 157–160. https://doi.org/10.1016/j.ajodo.2005.03.017

Cole, S.J., Hulse, C.N., Stull, K.E., 2020. The Effects of Skeletal Asymmetry on Accurate Sex Classification, in A.R. Klales (Ed.): Sex Estimation of the Human Skeleton: History, Methods, and Emerging Techniques. Elsevier, pp. 307–325. https://doi.org/10.1016/B978-0-12-815767-1.00019-5

Coolidge, R., 2015. The Relationship of Childhood Stress to Adult Health and Mortality Among Individuals from Two U.S. Documented Skeletal Collections, Late 19th to Early 20th Centuries. Graduate Theses and Dissertations. Available from: https://scholarcommons.usf.edu/etd/5929 (accessed 2.10.21)

Corron, L., Stull, K., 2017. The Effects of Epiphyseal Fusion Asymmetry on Juvenile Age Estimation. 86th Annual meeting of the American Association of Physical Anthropologists, Nouvelle-Orléans, United States. Available from: https://hal.archives-ouvertes.fr/hal-01819886 (accessed 3.7.2021)

Costa, R.L., 1986. Asymmetry of the Mandibular Condyle in Haida Indians. American Journal of Physical Anthropology 70, 119–123. https://doi.org/10.1002/ajpa.1330700116

Cuk T, Leben-Seljak P, Stefancic M., 2001. Lateral Asymmetry of Human Long Bones. Variability and Evolution 9,19-32. Available from: https://nanopdf.com/queue/lateral-asymmetry-of-human-long-bones_pdf?queue_id=-1&x=1622567890&z=MTk3LjIzNC4xODkuMjEw (accessed 4.12.21)

Daniel, L., 2020. One in Five South Africans Now Lives on Less Than R28 a Day, The UN Finds. Business insider. Available from: https://www.businessinsider.co.za/heres-how-many-south-africans-live-on-less-than-r28-a-day-and-why-its-getting-worse-2020-12 (accessed 7.24.22).

De Coster, G., Van Dongen, S., Malaki, P., Muchane, M., Alcantara, A., Matheve, H., Lens, L., 2013. Fluctuating Asymmetry and Environmental Stress: Understanding the Role of Trait History. PLOS ONE 8, e57966. https://doi.org/10.1371/journal.pone.0057966

DeLeon, V., 2007. Fluctuating asymmetry and stress in a Medieval Nubian population. American Journal of Physical Anthropology, 132, 520–534. https://doi.org/10.1002/ajpa.20549

de Moraes, M.E.L., Hollender, L.G., Chen, C.S.K., Moraes, L.C., Balducci, I., 2011. Evaluating Craniofacial Asymmetry with Digital Cephalometric Images and Cone-Beam Computed Tomography. American Journal of Orthodontics and Dentofacial Orthopedics 139, e523–e531. https://doi.org/10.1016/j.ajodo.2010.10.020

Dryden. Ian. L, Mardia, K.V., 2016. Procrustes analysis, in: Statistical Shape Analysis, with Applications in R. John Wiley & Sons, Ltd, pp. 125–173. https://doi.org/10.1002/9781119072492.ch7

Ducos, M.B., Tabugo, S.R., 2015. Fluctuating Asymmetry as Bioindicator of Stress and Developmental Instability in Gafrarium Tumidum (Ribbed Venus Clam) From Coastal Areas of Iligan Bay, Mindanao, Philippines. AACL Bioflux 8, 292–300

Eglash, A., 2020. Breastfeeding and Maternal/Child Vitamin B12 Deficiency. The Institute for Advancement of Breastfeeding and Lactation Education IABLE. Available from: https://lacted.org/questions/0197-vitamin-b12-deficiency-breastfeeding/ (accessed 11.24.22)

Ferraro, F., Weideman, M., 2020. Labour-Related Experience of Migrants and Refugees in South Africa. The Future of Work Labour and Migration in the 21st Century. Available from: https://icmc.net/future-of-work/report/04-south-africa (accessed 11.24.22)

Fink, B., Manning, J.T., Neave, N., Grammer, K., 2004. Second to Fourth Digit Ratio and Facial Asymmetry. Evolution and Human Behavior 25, 125–132. https://doi.org/10.1016/S1090-5138(03)00084-9

Fogel, R., 2019. Informal Housing, Poverty, and Legacies of Apartheid in South Africa | Urban@UW. Available from: https://urban.uw.edu/news/informal-housing-poverty-and-legacies-of-apartheid-in-south-africa/ (accessed 10.14.22)

Franks, E.M., Cabo, L.L., 2014. Quantifying asymmetry: Ratios and alternatives. American Journal of Physical Anthropology 154, 498–511. https://doi.org/10.1002/ajpa.22539

Franklin, D., Cardini, A., Flavel, A., Kuliukas, A., 2012. The Application of Traditional and Geometric Morphometric Analyses for Forensic Quantification of Sexual Dimorphism: Preliminary Investigations in A Western Australian Population.

International Journal of Legal Medicine 126, 549–558. https://doi.org/10.1007/s00414-012-0684-8

Friess, M., 2012. Scratching the Surface? The use of surface scanning in physical and paleoanthropology. Journal of Anthropological Science, 1–26. https://doi.org/10.4436/jass.90004

Gangestad, S.W., Thornhill, R., Yeo, R.A., 1994. Facial Attractiveness, Developmental Stability, and Fluctuating Asymmetry. Ethology and Socio-biology 15, 73–85. https://doi.org/10.1016/0162-3095(94)90018-3

Gawlikowska, A., Szczurowski, J., Czerwiński, F., Miklaszewska, D., Adamiec, E., Dzieciołowska, E., 2007. The Fluctuating Asymmetry of Medieval and Modern Human Skulls. Journal of Comparative Human Biology 58, 159–172. https://doi.org/10.1016/j.jchb.2006.10.001

Garvin, H.M., Stock, M.K., 2016. The Utility of Advanced Imaging in Forensic Anthropology. Academic Forensic Pathology 6, 499–516. https://www.ncbi.nlm.nih.gov/pmc/articles/PMC6474549/

Gebremedhin, S., 2021. Trends in Vitamin B12 Supply and Prevalence of Inadequate Intake in Africa: Regional and Country-Specific Estimates. Food Nutrition Bulletin 42, 467–479. https://doi.org/10.1177/03795721211043353

Goodall, C., 1991. Procrustes Methods in the Statistical Analysis of Shape. Journal of the Royal Statistical Society: Series B (Methodological) 53, 285–321. https://doi.org/10.1111/j.2517-6161.1991.tb01825.x

Goodman, A., Rose, J. 1990. Assessment of Systemic Physiological Perturbations from Dental Enamel Hypoplasias and Associated Histologial Structures. Year of Physical Anthropology. 33:59-110. https://doi.org/10.1002/ajpa.1330330506

Government Gazette, 2021. Final Report. South Africa. Available from: https://www.gov.za/sites/default/files/gcis_document/201409/report0.pdf

Graham, J., Özener, B., 2016. Fluctuating Asymmetry of Human Populations: A Review. Symmetry 8, 154.https://doi.org/10.3390/sym8120154

Gribel, B., Gribel, M., Frazäo, D., McNamara, J., Manzi, F., 2011. Accuracy and reliability of craniometric measurements on lateral cephalometry and 3D measurements on CBCT scans. The Angle orthodontist 81, 26–35. https://doi.org/10.2319/032210-166.1

Grünheid, T., Patel, N., De Felippe, N.L., Wey, A., Gaillard, P.R., Larson, B.E., 2014. Accuracy, Reproducibility, and Time Efficiency of Dental Measurements Using

Different Technologies. American Journal of Orthodontics and Dentofacial Orthopedics 145,157–164. https://doi.org/10.1016/j.ajodo.2013.10.012

Guatelli-Steinberg, D., Sciulli, P.W., Edgar, H.H.J., 2006. Dental Fluctuating Asymmetry in the Gullah: Tests of Hypotheses Regarding Developmental Stability in Deciduous Vs. Permanent and Male Vs. Female Teeth. American Journal of Physical Anthropology 129, 427–434. https://doi.org/10.1002/ajpa.20237

Hagg, A.C., Van der Merwe, A.E., Steyn, M., 2017. Developmental instability and its relationship to mental health in two historic Dutch populations. International Journal of Paleopathology. 17, 42–51. https://doi.org/10.1016/j.ijpp.2017.04.001

Hallgrimsson, B., 1999. Ontogenetic Patterning of Skeletal Fluctuating Asymmetry in Rhesus Macaques and Humans: Evolutionary and Developmental Implications. International Journal of Primatology 20, 121–151. https://doi.org/10.1023/A:1020540418554Harris, E.F., Nweeia, M.T., 1980. Dental Asymmetry as a Measure of Environmental Stress in the Ticuna Indians of Colombia. American Journal of Physical Anthropology 53, 133–142. https://doi.org/10.1002/ajpa.1330530118

Harris, E.F., Nweeia, M.T., 1980. Dental Asymmetry as a Measure of Environmental Stress in the Ticuna Indians of Colombia. American Journal of Physical Anthropology 53, 133–142. https://doi.org/10.1002/ajpa.1330530118

Hefner, J.T., 2009. Cranial Nonmetric Variation and Estimating Ancestry. Journal of Forensic Sciences 54, 985–995. https://doi.org/10.1111/j.1556-4029.2009.01118.x

Hens, S.M., Godde, K., Macak, K.M., 2019. Iron Deficiency Anaemia, Population Health, and Frailty in a Modern Portuguese Skeletal Sample. PLOS One 14, e0213369. https://doi.org/10.1371/journal.pone.0213369

Hillson, S., FitzGerald, C., Flinn, H., 2005. Alternative Dental Measurements: Proposals and Relationships with Other Measurements. American Journal of Physical Anthropology 126,413–426. https://doi.org/10.1002/ajpa.10430

Hiramoto, Y., 1993. Right-Left Differences in the Lengths of Human Arm and Leg Bones. Kaibogaku Zasshi 68, 536–543. PMID: 8279264.

Hoffman, J.W. and De Beer, F.C. 2012. Characteristics of the Micro-Focus X-ray Tomography Facility (MIXRAD) at Necsa in South Africa. 18th World Conference on Non-Destructive Testing. Durban, South Africa.

Holland, A.J., 2016. Assessment of fluctuating asymmetry as an indicator of water quality stress in South Africa. PhD thesis, Rhodes University, South Africa. Available from: http://vital.seals.ac.za:8080/vital/access/services/Download/vital:19958/SOURCE1

Howell, B.R., McMurray, M.S., Guzman, D.B., Nair, G., Shi, Y., McCormack, K.M., Hu, X., Styner, M.A., Sanchez, M.M., 2017. Maternal Buffering Beyond Glucocorticoids: Impact of Early Life Stress on Corticolimbic Circuits That Control Infant Responses to Novelty. Social Neuroscience 12, 50–64. https://doi.org/10.1080/17470919.2016.1200481

Hoover, K., 2007. Fluctuating Asymmetry as a Measure of Developmental Stress at the Mohr Site. Journal of Middle Atlantic Archaeology 23, 123–33. https://doi.org/10.1177/000134550805700201

Howell, B.R., McMurray, M.S., Guzman, D.B., Nair, G., Shi, Y., McCormack, K.M., Hu, X., Styner, M.A., Sanchez, M.M., 2017. Maternal Buffering Beyond Glucocorticoids: Impact of Early Life Stress on Corticolimbic Circuits That Control Infant Responses to Novelty. Social Neuroscience 12, 50–64. https://doi.org/10.1080/17470919.2016.1200481

Kanchan, T., Kumar, T.S.M., Kumar, G.P., Yoganarasimha, K., 2008. Skeletal Asymmetry. Journal of Forensic and Legal Medicine 15, 177–179. https://doi.org/10.1016/j.jflm.2007.05.009

Kieser, J.A., Groeneveld, H.T., 1988. Fluctuating Odontometric Asymmetry in an Urban South African Black Population. Journal of Dental Research 67, 1200–1205. https://doi.org/10.1177/00220345880670091001

Kieser, J.A., Groeneveld, H.T., Preston, C.B., 1986. Fluctuating Dental Asymmetry as a Measure of Odontogenic Canalization in Man. American Journal of Physical Anthropology 71, 437–444. https://doi.org/10.1002/ajpa.1330710407

Kim, J., Lee, J., Shin, J.-Y., Park, B.-J., 2015. Socioeconomic Disparities in Osteoporosis Prevalence: Different Results in the Overall Korean Adult Population and Single-person Households. Journal of Preventive Medicine and Public Health 48, 84–93. https://doi.org/10.3961/jpmph.14.047

Kim, S.G., 2011. Clinical Complications of Dental Implants. Implant Dentistry - A Rapidly Evolving Practice. https://doi.org/10.5772/17262

Klingenberg, C., 2015. Analyzing Fluctuating Asymmetry with Geometric Morphometrics: Concepts, Methods, and Applications. Symmetry 7, 843–934. https://doi.org/10.3390/sym7020843

Klingenberg, C.P., Barluenga, M., Meyer, A., 2002. Shape Analysis of Symmetric Structures: Quantifying Variation among Individuals and Asymmetry. Evolution 56, 1909–1920

Krishan, K., Kanchan, T., DiMaggio, J.A., 2010. A Study of Limb Asymmetry and Its Effect on Estimation of Stature in Forensic Case Work. Forensic Science International 200, 181.e1–5. https://doi.org/10.1016/j.forsciint.2010.04.015

Krüger, G.C., L'Abbé, E.N., Stull, K.E., Kenyhercz, M.W., 2015. Sexual Dimorphism in Cranial Morphology Among Modern South Africans. International Journal of Legal Medicine 129, 869–875. https://doi.org/10.1007/s00414-014-1111-0

Kujanová, M., Bigoni, L., Velemínská, J., Veleminsky, P., 2008. Limb Bones Asymmetry and Stress in Medieval and Recent Populations of Central Europe. International Journal of Osteoarchaeology 18, 476–491. https://doi.org/10.1002/oa.958

L'Abbé, E.N., Krüger, G.C., Theye, C.E.G., Hagg, A.C., Sapo, O., 2021. The Pretoria Bone Collection: A 21st Century Skeletal Collection in South Africa. Forensic Science 1, 220–227. https://doi.org/10.3390/forensicsci1030020

L'Abbé, E.N., Loots, M., Meiring, J.H., 2005. The Pretoria Bone Collection: A Modern South African Skeletal Sample. HOMO 56, 197–205. https://doi.org/10.1016/j.jchb.2004.10.004

Langley, N.R., Jantz, L.M., Ousley, S.D., Jantz, R.L., Milner, G., 2016. Data Collection Procedures for Forensic Skeletal Material 2.0. University of Tennessee and Lincoln Memorial University.

Latimer, H.B., Lowrance, E.W., 1965. Bilateral Asymmetry in Weight and in Length of Human Bones. The Anatomical Record 152, 217–224. https://doi.org/10.1002/ar.1091520213

Letzer, G.M., Kronman, J.H., 1967. A Posteroanterior Cephalometric Evaluation of Craniofacial Asymmetry. Angle Orthodontist 37, 205–211. https://doi.org/10.1043/0003-3219(1967)037<0205:APCEOC>2.0.CO;2

Liebenberg, L., Krüger, G.C., L'Abbé, E.N., Stull, K.E., 2019. Postcraniometric Sex and Ancestry Estimation in South Africa: A Validation Study. International Journal of Legal Medicine 133, 289–296. https://doi.org/10.1007/s00414-018-1865-x

Liebenberg, L., L'Abbé, E.N., Stull, K.E., 2015. Population Differences in The Postcrania of Modern South Africans and the Implications for Ancestry Estimation. Forensic Science International 257, 522–529. https://doi.org/10.1016/j.forsciint.2015.10.015

Liljequist, D., Elfving, B., Roaldsen, K.S., 2019. Intraclass Correlation – A Discussion and Demonstration of Basic Features. PLOS ONE 14, 1–35. https://doi.org/10.1371/journal.pone.0219854

Linford, A., 2017. Inequality Trends in South Africa. GeoCurrents. Available from: https://www.geocurrents.info/economic-geography/inequality-trends-in-south-africa (accessed 10.14.22)

Ling, C.T., Chow, B.F., 1953. Effect of Vitamin B12 on the Levels of Soluble Sulfhydryl Compounds in Blood. Journal of Biological Chemistry 202, 445–456.

Livshits, G., Davidi, L., Kobyliansky, E., Ben-Amitai, D., Levi, Y., Merlob, P., Optiz, J.M., Reynolds, J.F., 1988. Decreased Developmental Stability as Assessed by Fluctuating Asymmetry of Morphometric Traits in Preterm Infants. American Journal of Medical Genetics 29, 793–805. https://doi.org/10.1002/ajmg.1320290409

Makwela, M., 2017. Too much sugar and carbs in South African Diet. Centre of Excellence. Available from: https://foodsecurity.ac.za/news/too-much-sugar-and-carbs-in-south-african-diet/ (accessed 11.24.22).

Manning, J.T., Scutt, D., Whitehouse, G.H., Leinster, S.J., 1997. Breast Asymmetry and Phenotypic Quality in Women. Evolution and Human Behavior 18, 223–236. https://doi.org/10.1016/S0162-3095(97)00002-0

Marciano, M.A., Duarte, M.A.H., Ordinola-Zapata, R., Del Carpio Perochena, A., Cavenago, B.C., Villas-Bôas, M.H., Minotti, P.G., Bramante, C.M. and Moraes, I.G. 2012. Applications of Micro-Computed Tomography in Endodontic Research. In: Méndez-Vilas (ed.). Current Microscopy Contributions to Advances in Science and Technology. pp. 782–788. ISBN: 8493984361, 9788493984366

Mardia, K.V., Bookstein, F.L., Moreton, I.J., 2000. Statistical Assessment of Bilateral Symmetry of Shapes. Biometrika 87, 285–300

Martínez-Abadías, N., Esparza, M., Sjøvold, T., Gonzalez-Jose, R., Santos, M., Hernández, M., 2009. Heritability of Human Cranial Dimensions: Comparing the Evolvability of Different Cranial Regions. Journal of Anatomy 214, 19–35. https://doi.org/10.1111/j.1469-7580.2008.01015.x

Mazibuko, R.P., 2000. The Effects of Migrant Labour on The Family System.

McFadden, C., Oxenham, M.F., 2020. A Paleoepidemiological Approach to The Osteological Paradox: Investigating Stress, Frailty and Resilience Through Cribra Orbitalia. American Journal of Physical Anthropology 173, 205–217. https://doi.org/10.1002/ajpa.24091

Micklesfield, L.K., Lambert, E.V., Hume, D.J., Chantler, S., Pienaar, P.R., Dickie, K., Puoane, T., Goedecke, J.H., 2013. Socio-Cultural, Environmental and Behavioural Determinants of Obesity in Black South African Women. The Cardiovascular Journal of Africa 24, 369–375. https://doi.org/10.5830/CVJA-2013-069

Miszkiewicz, J.J., Cooke, K.M., 2019. Socio-economic Determinants of Bone Health from Past to Present. Clinical Reviews in Bone and Mineral Metabolism 17, 109–122. https://doi.org/10.1007/s12018-019-09263-1

Meyer, A., Steyn, M., Morris, A., 2013. Chinese Indentured Labour on the Witwatersrand Mines, South Africa (AD 1904–1910): A Bioarchaeological Analysis of the Skeletal Remains Of 36 Chinese Miners. South African Archaeological Society Goodwin Series 11, 39–51. Available from: https://www.jstor.org/stable/43997028 (accessed 3.11.21)

Mitteroecker, P., Gunz, P., 2009. Advances in Geometric Morphometrics. Evolutionary Biology 36, 235–247. https://doi.org/10.1007/s11692-009-9055-x

Møller, A.P., Swaddle, J.P., 1997. Asymmetry, Developmental Stability, and Evolution. Oxford University Press

Nandi, M.E., Olabiyi, O.A., Okubike, E.A., Iheaza, E.C., 2018. A Study of Bilateral Asymmetry of Upper Extremities and Its Effects on Stature Reconstruction Amongst Nigerians. AJFSFM 1, 978–988. https://doi.org/10.26735/16586794.2018.023

Ng, J.-S., Chin, K.-Y., 2021. Potential Mechanisms Linking Psychological Stress to Bone Health. International Journal of Medical Science 18, 604–614. https://doi.org/10.7150/ijms.50680

Olejniczak, A.J., Tafforeau, P., Smith, T.M., Temming, H., Hublin, J.-J., 2007. Technical Note: Compatibility of Microtomographic Imaging Systems for Dental Measurements. American Journal of Physical Anthropology 134, 130–134. https://doi.org/10.1002/ajpa.20615

Ortner, D.J., 2019. Ortner's identification of pathological conditions in human skeletal remains, 2nd edition. ed, Smithsonian contributions to anthropology. Academic Press, London, England.

Ortner, D. 2003. Identification of Pathological Conditions in Human Skeletal Remains. London: Academic Press. ISBN: 9780128097380

Özener, B., Fink, B., 2010. Facial Symmetry in Young Girls and Boys from a Slum and a Control Area of Ankara, Turkey. Evolution and Human Behaviour 31, 436–441. https://doi.org/10.1016/j.evolhumbehav.2010.06.003

Palmer, A., Strobeck, C., 2003. Fluctuating Asymmetry and Developmental Stability: Heritability of Observable Variation vs. Heritability of Inferred Cause. Journal of Evolutionary Biology 10, 39–49. https://doi.org/10.1046/j.1420-9101.1997.10010039.x

Palmer, A. R.,1996. Waltzing with asymmetry. Is fluctuating asymmetry a powerful new tool for biologists or just an alluring new dance step? Bioscience, 46 : 518–532. https://doi.org/10.2307/1312930

Palmer, A.R., 1994. Fluctuating Asymmetry Analyses: A Primer, in: Markow, T.A. (Ed.), Developmental Instability: Its Origins and Evolutionary Implications, Contemporary Issues in Genetics and Evolution. Springer Netherlands, Dordrecht, pp. 335–364. https://doi.org/10.1007/978-94-011-0830-0_26

Perini, T.A., de Oliveira, G.L., 2005. Technical Error of Measurement in Anthropometry. Revista Brasileira de Medicina do Esporte 11,5. https://doi.org/10.1590/S1517-86922005000100009

Perzigian, A.J., 1977. Fluctuating Dental Asymmetry: Variation Among Skeletal Populations. American Journal of Physical Anthropology 47, 81–88. https://doi.org/10.1002/ajpa.1330470114

Pimentel, L., 2003. Scurvy: Historical Review and Current Diagnostic Approach. American Journal of Emergency Medicine 21, 328–332. https://doi.org/10.1016/s0735-6757(03)00083-4

Pinhas-Hamiel, O., Doron-Panush, N., Reichman, B., Nitzan-Kaluski, D., Shalitin, S., Geva-Lerner, L., 2006. Obese Children and Adolescents: A Risk Group for Low

Vitamin B12 Concentration. The Archives of Paediatrics & Adolescent Medicine160, 933–936. https://doi.org/10.1001/archpedi.160.9.933

Pradhan, P., 2009. Malarial Anaemia and Nitric Oxide Induced Megaloblastic Anaemia: A Review on The Causes of Malarial Anaemia. Journal of Vector Borne Diseases 46, 100–108.

Profico et al., 2019. Virtual Anthropology and its Application in Cultural Heritage Studies. Studies in Conservation 64, 323–336. https://doi.org/10.1080/00393630.2018.1507705

R Core Team. 2016. R: A Language and Environment for Statistical Computing. R Foundation for Statistical Computing, Vienna, Austria. Available from: https://www.R-project.org/ (accessed 11.4.2020)

Reck, C., Zietlow, A.-L., Müller, M., Dubber, S., 2016. Perceived Parenting Stress in the Course of Postpartum Depression: The Buffering Effect of Maternal Bonding. Archives of Women's Mental Health 19, 473–482. https://doi.org/10.1007/s00737-015-0590-4

Ridel, A.F., Demeter, F.P., L'Abbé, E.N., Vandermeulen, D., Oettlé, A.C., 2020. Nose Approximation Among South African Groups from Cone-Beam Computed Tomography (CBCT) Using a New Computer-Assisted Method Based on Automatic Landmarking. Forensic Science International 313, 110357–110357. https://doi.org/10.1016/j.forsciint.2020.110357

Rinaldo, N., 2018. How Reliable is the Assessment of Porotic Hyperostosis and Cribra Orbitalia in Skeletal Human Remains? A Methodological Approach for Quantitative Verification by Means of a New Evaluation Form. Archaeological and Anthropological Sciences 11. https://doi.org/10.3390/sym10070232

Rossi, M., Ribeiro, E., Smith, R., 2003. Craniofacial Asymmetry in Development: An Anatomical Study. The Angle Orthodontist 73, 381–5. https://doi.org/10.1043/0003-3219(2003)073%3C0381:caidaa%3E2.0.co;2

Rosso, P., Lederman, S.A., 1982. Nutrition in The Pregnant Adolescent. Current Concepts of Maternal Nutrition 11, 47–62

Sajid, M., Shafique, T., Riaz, I., Imran, M., Baig, M., Baig, S., Manzoor, S., 2018. Facial Asymmetry-Based Anthropometric Differences between Gender and Ethnicity. Symmetry 10, 232. https://doi.org/10.3390/sym10070232

Salvadei, L., Ricci, F., Manzi, G., 2001. Porotic Hyperostosis as a Marker of Health and Nutritional Conditions During Childhood: Studies at the Transition Between

Imperial Rome and the Early Middle Ages. American Journal of Human Biology 13, 709–717. https://doi.org/10.1002/ajhb.1115

Saunders, S.R., Mayhall, J.T., 982. Fluctuating Asymmetry of Dental Morphological Traits: New Interpretations. Human Biology 54, 789–799. Available from: https://www.jstor.org/stable/41464652 (accessed 2.6.21)

Schlager S. 2013. Soft-Tissue Reconstruction of the Human Nose: Population Differences and Sexual Dimorphism. PhD thesis, Universitatsbibliothek Freiburg. http://dx.doi.org/10.13140/RG.2.1.2564.5528

Schoonjans, F., 2020. Intraclass Correlation Coefficient. MedCalc. Available from: https://www.medcalc.org/manual/intraclasscorrelation.php (accessed 3.31.20).

Schuurs, A. 2013. Pathology of the Hard Dental Tissues. West Sussex: John Wiley & Sons.

Sciulli, P.W., 2002. Dental Asymmetry in a Late Archaic and Late Prehistoric Skeletal Sample of the Ohio Valley Area. Dental Anthropology 16, 33–44. http://dx.doi.org/10.26575/daj.v16i2.158

Scrucca, L., 2000. Assessing Multivariate Normality through Interactive Dynamic Graphics. Semantic Scholar. Available form: https://www.semanticscholar.org/paper/Assessing-Multivariate-Normality-through-Dynamic-Scrucca/db83b656fa6d07c8ec9bae03c6affd00ae80247c (accessed 4.16.21)

Shah, S.M., Joshi, M.R., 1978. An Assessment of Asymmetry in the Normal Craniofacial Complex. Angle Orthodontist 48, 141–148. https://doi.org/10.1043/0003-3219(1978)048<0141:AAOAIT>2.0.CO;2

Siebert, J.R., Swindler, D.R., 2002. Evolutionary Changes in the Midface and Mandible: Establishing the Primate Form, in: Understanding Craniofacial Anomalies. John Wiley & Sons, Ltd, pp. 343–378. https://doi.org/10.1002/0471221953.ch15

Simmons, L.W., Rhodes, G., Peters, M., Koehler, N., 2004. Are Human Preferences for Facial Symmetry Focused on Signals of Developmental Instability? Behavioral Ecology 15, 864–871. https://doi.org/10.1093/beheco/arh099

Slice, D., 2007. Geometric Morphometrics. Annual Review of Anthropology 36, 261-281. https://doi.org/10.1146/annurev.anthro.34.081804.120613

Smith, C.E.L., Poulter, J.A., Antanaviciute, A., Kirkham, J., Brookes, S.J., Inglehearn, C.F., Mighell, A.J., 2017. Amelogenesis Imperfecta; Genes, Proteins, and Pathways. Frontiers in Physiology. 8. https://doi.org/10.3389/fphys.2017.00435

Snoddy, A.M.E., Buckley, H.R., Elliott, G.E., Standen, V.G., Arriaza, B.T., Halcrow, S.E., 2018. Macroscopic Features of Scurvy in Human Skeletal Remains: A Literature Synthesis and Diagnostic Guide. American Journal of Physical Anthropology 167, 876–895. https://doi.org/10.1002/ajpa.23699

Srivastava, D., Singh, H., Mishra, S., Sharma, P., Kapoor, P., Chandra, L., 2018. Facial Asymmetry Revisited: Part I- Diagnosis and Treatment Planning. Journal of Oral Biology and Craniofacial Research 8, 7–14. https://doi.org/10.1016/j.jobcr.2017.04.010

Steyn, M., L'Abbé, E.N., Myburgh, and J., 2016. Forensic Anthropology as Practiced in South Africa, in: Handbook of Forensic Anthropology and Archaeology. Routledge

Stoddard, E., 2022. DISMAL ASCENT: South African Unemployment Rate Hits Record 35.3% In Q4 2021. Daily Maverick. Available from: https://www.dailymaverick.co.za/article/2022-03-29-south-african-unemployment-rate-hits-record-35-3-in-q4-2021/ (accessed 7.24.22)

Storm, R.A., 2009. Human Skeletal Asymmetry. A Study of Directional and Fluctuating Asymmetry in Assessing Health, Environmental Conditions, and Social Status in English Populations from the 7th to the 19th Centuries. Doctor of Philosophy. University of Bradford. Available from: http://hdl.handle.net/10454/4325 (accessed 2.9.21)

Storm, R., & Knüsel, C., 2005. Fluctuating Asymmetry: A Potential Osteological Application. Paper presented at proceedings of the fifth annual conference of the British Association for Biological Anthropology and Osteoarchaeology, Southampton, England

Sun, Y., Sun, M., Liu, B., Du, Y., Rong, S., Xu, G., Snetselaar, L.G., Bao, W., 2019. Inverse Association Between Serum Vitamin B12 Concentration and Obesity Among Adults in the United States. Front. Endocrinol. 10

Suwa, G., Kono, R., 2005. A Micro-CT Based Study of Linear Enamel Thickness in the Mesial Cusp Section of Human Molars: Re-Evaluation of Methodology and Assessment of Within-Tooth, Serial, and Individual Variation. Anthropological Science 113,273–289. https://doi.org/10.1537/ase.050118

Theye, 2022. The Effects of Aging and Tooth Loss on the Microstructure of the Mandible in South Africans, PhD thesis, University of Pretoria, South Africa.

Thompson, R.A., 2014. Stress and Child Development. Future Child 24, 41–59. https://doi.org/10.1353/foc.2014.0004

Townsend, G., Brown, T., 1980. Dental asymmetry in Australian Aboriginals. Human biology 52, 661-673. PMID: 7203440

Townsend, G.C., Garcia-Godoy, F., 1984. Fluctuating Asymmetry in the Deciduous Dentition of Dominican Mulatto Children. Archives of Oral Biology 29, 483–486. https://doi.org/10.1016/0003-9969(84)90067-0

Trangenstein, P.J., Morojele, N.K., Lombard, C., Jernigan, D.H., Parry, C.D.H., 2018. Heavy Drinking And Contextual Risk Factors Among Adults in South Africa : Findings From the International Alcohol Control Study. Substance Abuse Treatment, Prevention, and Policy 13, 43. https://doi.org/10.1186/s13011-018-0182-1

Trochim, W.M.K., 2020. The Research Methods Knowledge Base. Available from : https://conjointly.com/kb/cite-kb/(accessed 11.03.21.)

Upex, B., Dobney, K., 2012. Dental Enamel Hypoplasia as Indicators of Seasonal Environmental and Physiological Impacts in Modern Sheep Populations: A Model for Interpreting the Zooarchaeological Record. Journal of Zoology 287, 259–268. https://doi.org/10.1111/j.1469-7998.2012.00912.x

von Cramon-Taubadel, N., 2014. Evolutionary Insights into Global Patterns of Human Cranial Diversity: Population History, Climatic and Dietary Effects. Journal of Anthropological Science 92, 43–77. https://doi.org/10.4436/jass.91010

Van Der Merwe, A.E., Ribot, I., Morris, D., Steyn, M., Maat, G.J.R., 2010. The Origins of Late Nineteenth-Century Migrant Diamond Miners Uncovered in a Salvage Excavation in Kimberley, South Africa. South African Archaeological Bulletin 65, 175–184

Van Valen, L.,1962. A Study of Fluctuating Asymmetry. Evolution 16, 125–142. https://doi.org/10.1111/j.1558-5646.1962.tb03206.x

Varner, T.B., 2015. Landmark-Based Approach to Examining Changes in Arch Shape: A Longitudinal Study. MSc, University of Iowa. https://doi.org/10.17077/etd.9loii46z

Wade, T.J., 2010. The Relationships between Symmetry and Attractiveness and Mating Relevant Decisions and Behavior: A Review. Symmetry 2, 1081–1098. https://doi.org/10.3390/sym2021081

Waldron, T., 2009. Palaeopathology. (Cambridge Manuals in Archaeology). Cambridge University Press. ISBN-13: 978-0-521-86137-3

Walker, P.L., 2008. Sexing Skulls Using Discriminant Function Analysis of Visually Assessed Traits. American Journal of Forensic Anthropology 136. https://doi.org/10.1002/ajpa.20776

Walker, P., Bathurst, R., Richman, R., Gjerdrum, T., Andrushko, V., 2009. The Cause of Porotic Hyperostosis and Cribra Orbitalia: A Reappraisal of the Iron-Deficiency-Anemia Hypothesis. American Journal of Physical Anthropology. 139, 109-125. https://doi.org/10.1002/ajpa.21031

Weisensee, K., 2013. Assessing the Relationship Between Fluctuating Asymmetry and Cause of Death in Skeletal Remains: A Test of the Developmental Origins of Health and Disease Hypothesis. American Journal of Human Biology 25, 411–417. https://doi.org/10.1002/ajhb.22390

Wilson, J.M., Manning, J.T., 1996. Fluctuating Asymmetry and Age in Children: Evolutionary Implications for the Control of Developmental Stability. Journal of Human Evolution 30, 529–537. https://doi.org/10.1006/jhev.1996.0041

Wippert, P.-M., Rector, M., Kuhn, G., Wuertz-Kozak, K., 2017. Stress and Alterations in Bones: An Interdisciplinary Perspective. Frontiers in Endocrinology 8, 96. https://doi.org/10.3389/fendo.2017.00096

Zakai, N.A., McClure, L.A., Prineas, R., Howard, G., McClellan, W., Holmes, C.E., Newsome, B.B., Warnock, D.G., Audhya, P., Cushman, M., 2009. Correlates of Anemia in American Blacks and Whites. American Journal of Epidemiology 169, 355–364. https://doi.org/10.1093/aje/kwn355

Zariņa, G., Sholts, S.B., Tichinin, A., Rudovica, V., Vīksna, A., Engīzere, A., Muižnieks, V., Bartelink, E.J., Wärmländer, S.K.T.S., 2016. Cribra Orbitalia as a Potential Indicator of Childhood Stress: Evidence from Paleopathology, Stable C, N, And O Isotopes, and Trace Element Concentrations in Children from A 17th -18th Century Cemetery in Jl·kabpils, Latvia. Journal of Trace Elements in Medicine and Biology 38, 131–137. https://doi.org/10.1016/j.jtemb.2016.05.008

Zivanović, S., 1983. A note on the effect of asymmetry in suture closure in mature human skulls. American Journal of Physical Anthropology 60, 431–435. https://doi.org/10.1002/ajpa.1330600404

Zukeran, C., Fukumine, T., Doi, N., Sensui, N., Ishida, H., Kanaya, F., Shimabukuro, A., 2002. Preliminary Observations of Some Paleopathological Conditions in Historic and Modern Human Skeletal Remains from Ishigaki Island, Ryukyu Islands, Japan. Anthropological Science 110, 421–436. https://doi.org/10.1537/ase.110.421

Appendix A

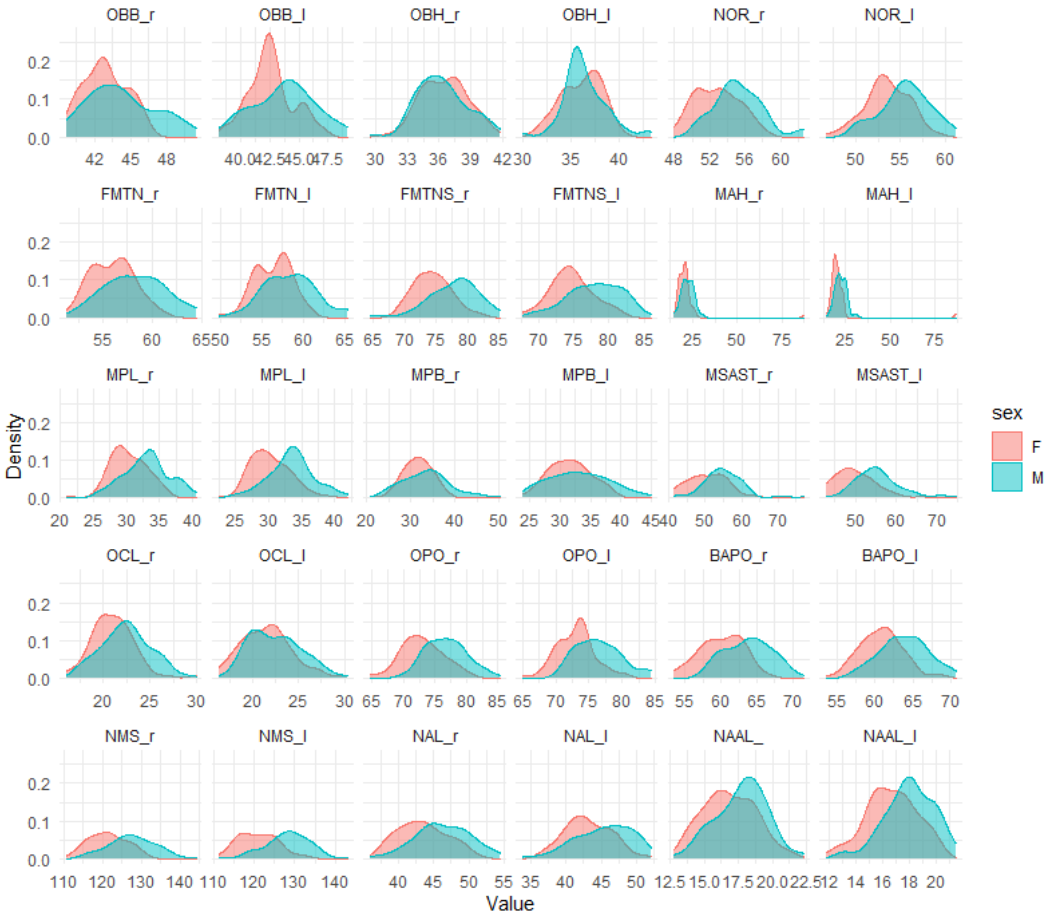

Figure A.1 *- Kernel density plots of the left and right inter-landmark distances in females (F) and males (M)*

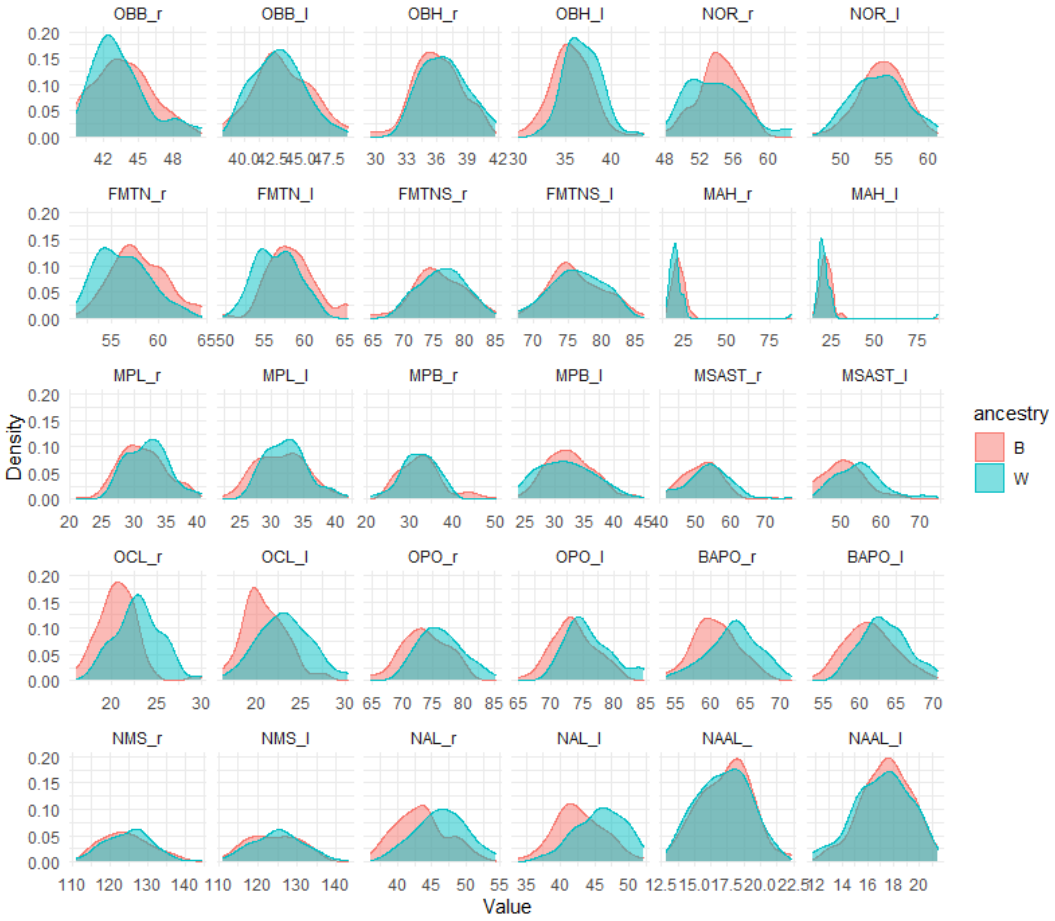

Figure A.2 *- Kernel density plots of the left and right inter-landmark distances in black (B) and white (W) South Africans*

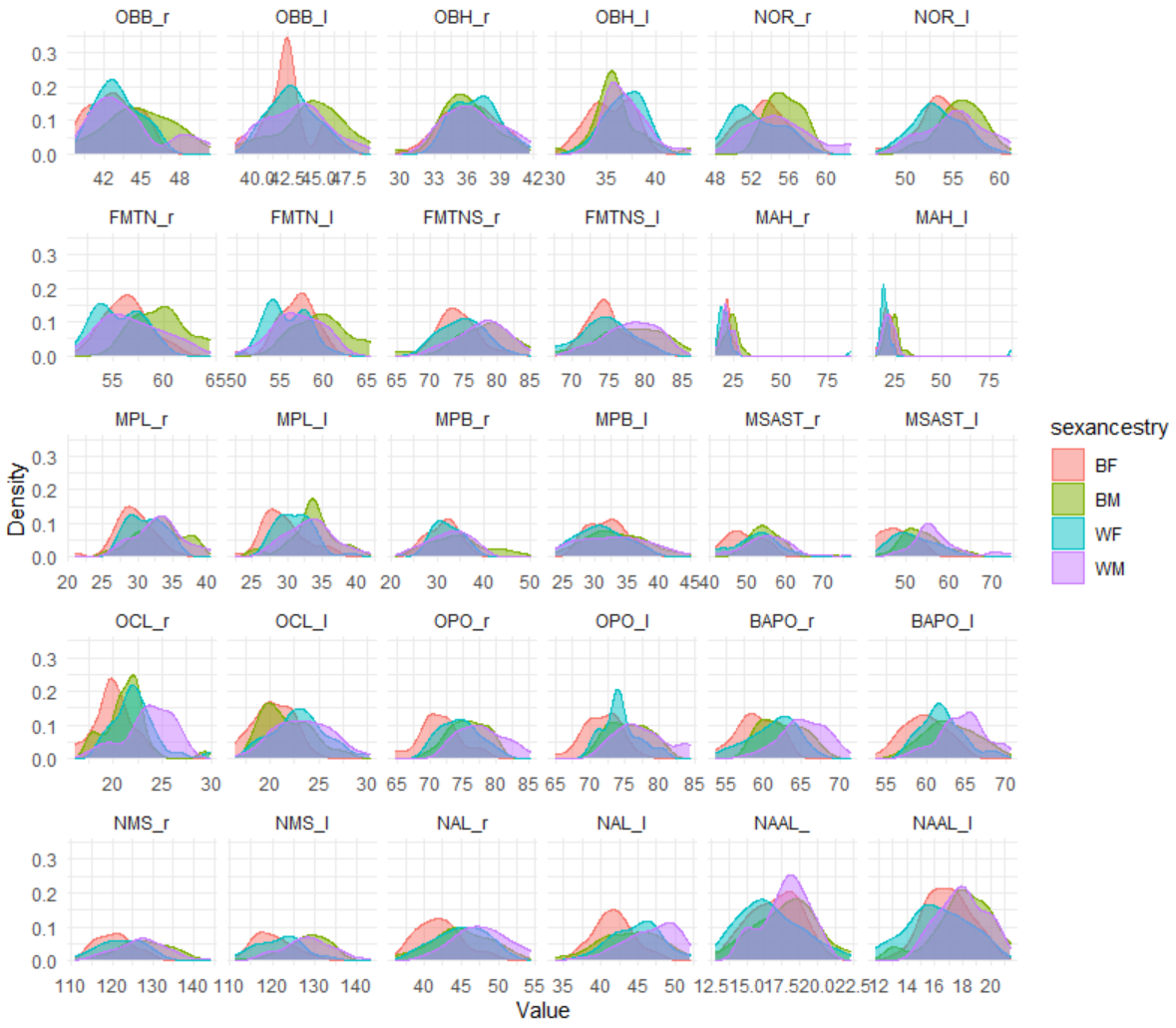

Figure A.3 *- Kernel density plots of theleft and right inter-landmark distances in sex and population simultaneously*

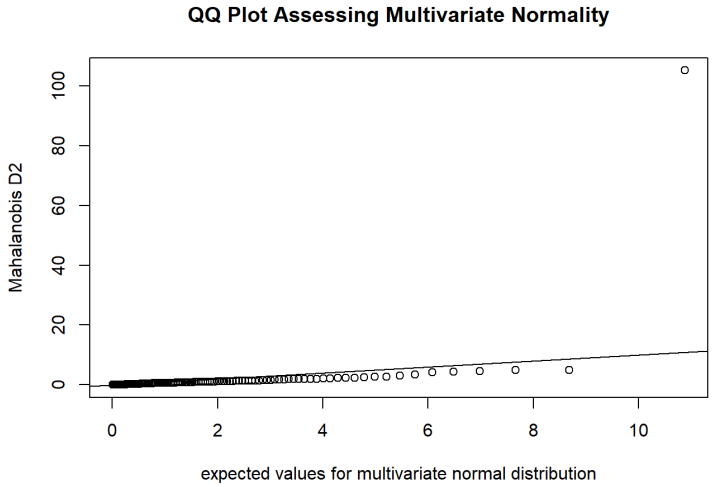

Figure A.4 *- QQ plot representing normal distribution for sex*

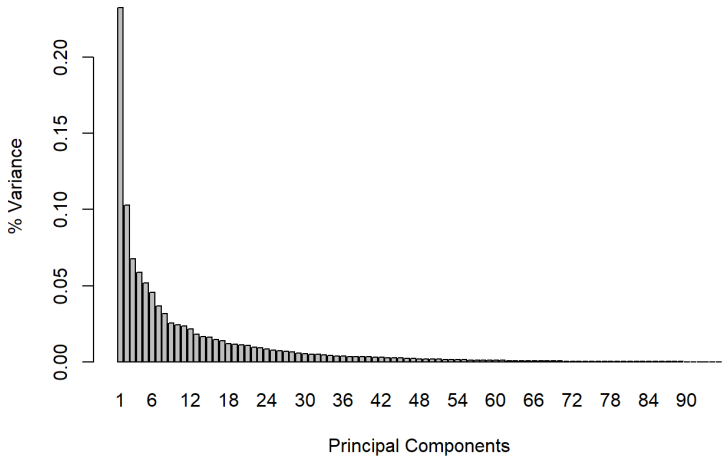

Figure A.5 *- PCA graph indicating variance distribution for sex*

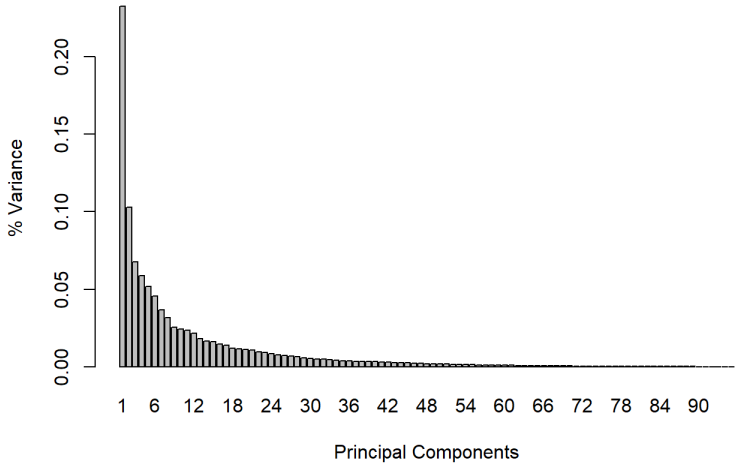

Figure A.6 *- PCA graph indicating variance distribution for population affinity*

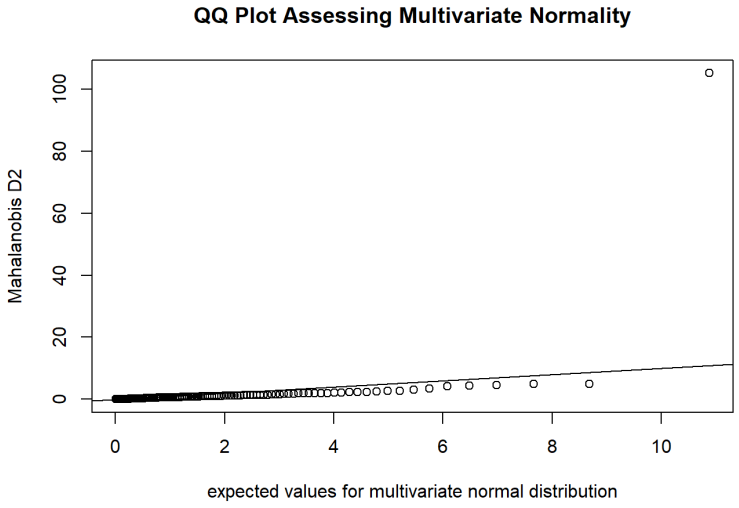

Figure A.7 *- QQ plot showing normal distribution for population affinity*

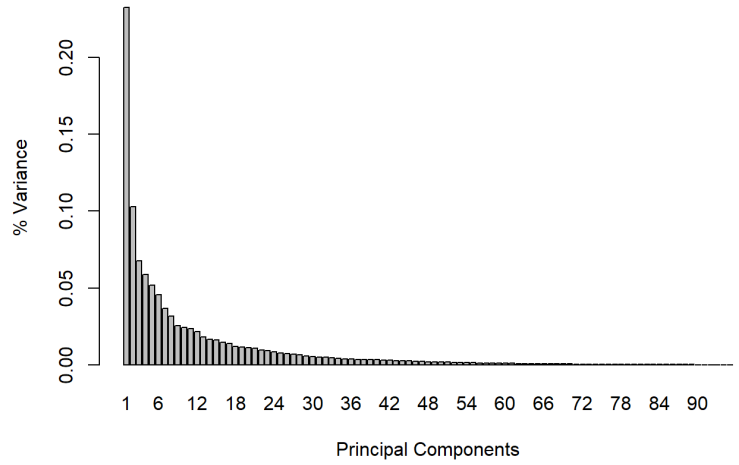

Figure A.8 *- PCA graph indicating variance distribution for sex and population simultaneously*

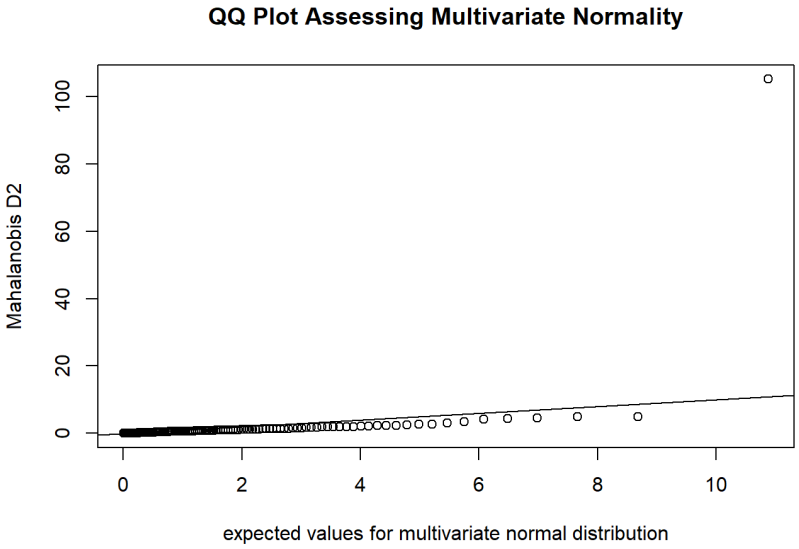

Figure A.9 *- QQ plot representing a normal distribution for sex and population simultaneously*

Table A.1 *- Asymmetrical individuals in the sample(FA17>0.05) with pathological lesions (A- absent; P- present)*

Individual	Sexpopulation	Ancestry	Sex	FA17	Cribra Orbitalia	Porotic Hyperostosis	Enamel Hypoplasia	Periostitis
1	BM	M	B	0,054	P	P	A	A
2	WM	M	W	0,058	P	A	A	P
3	WM	M	W	0,051	A	A	A	P
4	WF	F	W	0,051	A	A	P	P
5	BM	M	B	0,053	A	A	A	P
6	WM	M	W	0,071	A	A	P	A
7	BM	M	B	0,056	P	A	A	P
8	WF	F	W	0,055	A	A	A	A
9	BM	M	B	0,053	A	P	A	P
10	BM	M	B	0,073	A	P	P	A
11	WM	M	W	0,052	A	A	A	A
12	WM	M	W	0,060	A	A	A	P
13	BF	F	B	0,051	A	A	P	A
14	WF	F	W	0,065	A	P	A	P
15	WF	F	W	0,052	A	A	A	P
16	WM	M	W	0,064	P	P	P	A
17	WM	M	W	0,060	A	A	A	A
18	WM	M	W	0,054	A	A	A	A
19	BF	F	B	0,074	A	A	A	P
20	BM	M	B	0,052	P	P	P	A
21	BM	M	B	0,073	A	P	P	A
22	WM	M	W	0,058	P	A	A	P

23	BF	F	B	0,050	A	A	P	A
24	WM	M	W	0,062	A	P	A	P
25	BM	M	B	0,066	A	A	P	A
26	WM	M	W	0,052	A	P	A	P